UNIVERSITÀ
DEGLI STUDI
FIRENZE

DOTTORATO DI RICERCA IN
Scienze della Terra

CICLO XXXI

COORDINATORE Prof. Lorella Francalanci

The Middle Jurassic – Lower Cretaceous paleodrainage evolution of the Central High Atlas (Morocco): implications for the development of the Moroccan Atlasic system.

Settore Scientifico Disciplinare GEO/02

Dottorando
Dott. Cavallina Chiara

Tutore
Prof. Benvenuti Marco

Coordinatore
Prof. Francalanci Lorella

Anni 2015/2018

Abstract – Cavallina

The High Atlas is an orogenic system resulting from the Cenozoic-Recent tectonic inversion of Triassic-Jurassic rift systems. Its present setting derives from a long and complex tectono-sedimentary evolution related to the Early Mesozoic opening of the Atlantic Ocean (pre-orogenic period) and, then, to the Cenozoic convergence between the African and European plates which led to a full tectonic inversion. The WSW-ENE trending chain is bounded by the North Atlas Fault to the north and the South Atlas Fault to the south, that represented the master faults of the rifted basins during the pre-orogenic period, then reactivated in inversion during the orogenic period. Early Jurassic syn-rift carbonate platforms, related to a marine ingression, were replaced in the Middle Jurassic-Late Cretaceous by post-rift fluvial and lacustrine environments. The related continental successions, regionally known as *Couches Rouges*, are not unanimously interpreted in the frame of the tectono-sedimentary evolution of the High Atlas. According to some authors they record localized early compressive-transpressive stages of deformation, others refer them to a period of tectonic quiescence.

This study illustrates a revised stratigraphy, facies analyses and paleodrainage reconstruction of the Guettioua (Bathonian) and Jbel Sidal Formations (Barremian), that represents the fluvial units of the *Couches Rouges,* outcropping at the core of several syncline basins throughout the Central High Atlas. The aim is to understand if there was a tectonic forcing on the development of the Middle Jurassic – Lower Cretaceous fluvial systems.

The sedimentological characters observed in the two fluvial formations suggest that they have been deposited by wide ephemeral fluvial systems, characterized by a high variable discharge. The reconstructed paleogeography, based on paleodrainage analysis, shows the fragmentation of the fluvial systems in several drainage basins, separated by local thresholds, uplifting during the sedimentation. Our reconstruction suggests that the post-rift fluvial systems were controlled by the presence of topographic highs in the area of the High Atlas of Marrakech, in the axial part of the chain and at its southern front, next to the South Atlas Fault. This conclusion, together with structural data and tectonic observations collected in some of the study areas, supports the idea that, from the Middle Jurassic, the Central High Atlas were affected by early compressive-transpressive stages of deformation.

INDICE

1. Introduction

The river drainage at different scales reflects the interplay of climate and tectonic movement, a condition making its changes on the long term a direct evidence of topographic changes (Waheed and Wells, 1990; Najman et al., 2003). The paleodrainage patterns represent a proxy of the uplift history of the orogenic belts, indicated by geomorphic and sedimentary lines of evidence, the latter providing important information about the mode and the timing of crustal deformation (Howard, 1967; Cox, 1989; Clark et al., 2004). Such record may be investigated through different methods ranging from facies and paleocurrent analyses (Haisheng et al., 2008; Ielpi and Ghinassi, 2014), petrographic and quantitative provenance analyses of sedimentary sequences (Vezzoli and Garzanti, 2009), to morphological drainage pattern analysis (Clark et al., 2004).

In this work, we approached the reconstruction of the paleocurrent patterns in the Middle Jurassic – Lower Cretaceous fluvial successions of the Central High Atlas (CHA, southern Morocco) from a sedimentary geology perspective, for checking the hypothesis of a predominant tectonic forcing on the development of fluvial systems at a regional scale.

The studied continental successions, indicated as *Couches Rouges* in the literature (Haddoumi et al., 2010 for a review), attest to a long Late Mesozoic regressive phase debated in the frame of the tectono-sedimentary evolution of the Central High Atlas. According to some authors, this continental stratigraphic interval records localized (Choubert and Faure Muret 1960-1962; Mattauer et al., 1977; Studer and Du Dresnay, 1980; Monbaron, 1982; Laville, 1985, 1988, 2002; Laville and Piqué, 1992; Piqué et al., 1998; Cavallina et al., 2017, 2018; Torres-López et al., 2018) to widespread (Benvenuti et al., 2017; Moratti et al., 2018) early compressive-transpressive stages of crustal deformation. Other authors refer these successions to a period of tectonic quiescence, during which the sedimentation was mainly controlled by sea-level variations (Beauchamp et al., 1999; Frizon de Lamotte et al., 2000, 2008, 2009; Teixell et al., 2003; Tesón and Teixell, 2008). Finally, crustal uplift and syn-depositional deformation during this span of time have been also referred to *halokinesis* related to the mobilization of the Triassic evaporites along pre-existing rift faults (Ettaki et al., 2007; Saura et al., 2014; Ibouh and Chafiki 2017; Moragas, 2017; Vergés et al., 2017; Moragas et al., 2018; Torres-López et al., 2018).

The main aims of the study are:

1) to revise the stratigraphic framework of the fluvial units of the *Couches Rouges* (Guettioua and Jbel Sidal Formations), based on standard sedimentary facies analysis method, recognition of Unconformity Bounded Stratigraphic Units (UBSU, Salvador 1994) and comparison with previous studies (Table 1, 2, 3, 4; Termier, 1941; Bourcart et al., 1942; Choubert et al., 1959; Hyndermeyer et al., 1977; Ferrandini and Le Marrec., 1982; Saadi et al., 1985; Milhi et al., 1993; Hadri et al., 2001; Zouibaa, 2003; Haddoumi et al., 2010)

2) to reconstruct the evolution of the paleo-drainage through time in relation to possible tectonic forcing associated with an incipient uplift and denudation of the Central High Atlas.

2. Geological Setting

2.1 Study Area

The study areas pertain to a wide territory in the central-southern part of Morocco, partially coincident with the CHA Mountains (Fig. 1). In detail, the study areas extend in a WSW-ENE direction, from the High Atlas of Marrakech to the West, to the towns of Errachidia and Tizi'n'Isly, respectively to the E and to the NE (Fig. 1).

The Middle Jurassic – Lower Cretaceous continental beds (*Couches Rouges*; Fig 1b*)* are largely exposed at the core of synclines located in the axial portion and at the northern front of the CHA (Jenny et al., 1981; Sohuel, 1987, 1996; Haddoumi et al., 2002, 2008, 2010; Charrière and Haddoumi, 2016, 2017), and recently recognized also along the southern front, facing the Ouarzazate Basin (Benvenuti et al., 2017; Cavallina et al. 2017, 2018; Moratti et al., 2018).

In this wide sector of the High Atlas chain, we have selected and studied 15 zones with excellent exposures of the *Couches Rouges*, grouped in four distinct sectors (Fig. 1b): 1) the High Atlas of Marrakech, to the west, including the syncline basins of Ait Ourir, Jbel Igoudlane and Adrar Aglagal; 2) the western sector of the Atlas of Beni Mellal, to the North-West, characterized by the Iouaridène, Guettioua, Ait Attab and Ouaouizaght synclines; 3) the eastern sector of the Atlas of Beni Mellal, to the North-East, with the Tilougguit, Tagleft, Tizi'n'Isli, Naour and Imilchil synclines; 4) the south-eastern front of the CHA including the synclines of Toundoute, M'semrir, the Dades Valley and the Goulmima anticline.

2.2 The Mesozoic tectono-stratigraphic evolution of the Central High Atlas

The Moroccan High Atlas is an orogenic system considered to be the result of the Cenozoic-Recent tectonic inversion of Triassic-Jurassic rift systems (Frizon de Lamotte et al., 2008). Its present structure derives from a long and complex tectono-sedimentary evolution related to the Mesozoic continental rifting of Pangea and subsequent opening of the Atlantic and NW Tethys oceans (*pre-orogenic period;* Mattauer et al., 1977; Giese and Jacobsagen, 1992; Laville and Piqué, 1992; Frizon de Lamotte et al., 2008, 2009) and, then, to the Cenozoic convergence between the Africa and Europe plates which led to a full tectonic inversion of the rifted basins (*orogenic period*; Mattauer et al., 1977; Frizon de Lamotte et al., 2008, 2009). The WSW-ENE trending chain is bounded by the North Atlas Fault to the north and the South Atlas Fault to the

south, referred to as the master faults of the rifted basins active during the *pre-orogenic period*, then accommodating the inversion during the *orogenic period* (Frizon de Lamotte et al., 2008, 2009). This intracontinental chain is subdivided in three domains: Western High Atlas, Eastern High Atlas, and Central High Atlas (CHA), the latter being the study area of the present work.

In the Moroccan Atlas system, located at the NW margin of the African craton, since the Late Permian (Fig. 2a), crustal extension gave rise to several rifted basins, filled during the Triassic-Earliest Jurassic (Fig. 2b) by continental clastic sediments, evaporites and basalts (El Arabi, 2007; Frizon de Lamotte et al., 2008). During the Early and the initial Middle Jurassic, regional marine ingressions (Fig. 2c) led to the development of syn-rift carbonate platforms (Frizon de Lamotte et al., 2000, 2008, 2009) followed, in the advanced Middle Jurassic (Fig. 2d), by post-rift fluvial and lacustrine environments (Choubert and Faure-Muret, 1960-1962; Haddoumi et al., 2002, 2008, 2010; Charrière et al., 2005; Charrière and Haddoumi 2016, 2017). Continental deposition, represented by the Guettioua, Iouaridène and Jbel Sidal formations, lasted up to the Lower Cretaceous, shortly interrupted by the Aptian marine transgression (Fig. 2e), testified by shelfal carbonates of the Ait Tafelft Formation (Haddoumi et al., 2002, 2008, 2010; Charrière et al., 2005) and apparently recorded only on the northern front of the CHA (Sohuel, 1987, 1996).

Continental-transitional settings reestablished during the Albian-Cenomanian (Fig. 2f) as indicated by fluvial-coastal deposits occurring all over the CHA, though referred to different formations. On the northern slopes of the CHA, the Ouaouizaght Formation consists of fluvial sandstones grading upward to sabhka gypsum and mudstones (Monbaron, 1981, 1982; Sohuel 1987). On the southern front, a fluvial complex widely exposed along the southern front of the CHA and regionally known as *Kem Kem beds* (Sereno et al., 1996; Ettachfini and Andreu, 2004; Cavin et al., 2010) includes the Ifezouane (fluvial sandstones) and the Aoufous (coastal mudstones and gypsum) Formations. The deposition regionally continued during the Late Cenomanian-Turonian in shallow carbonate ramps represented by the Akrabou Formation to the south and by the Ait Attab Formation to the north, hinting to a new transgressive stage affecting the CHA realm (Ettachfini and Andreu, 2004; Ettachfini et al., 2005).

Together with the sedimentary dynamic, the Moroccan Atlas domains were also affected by magmatic events around the Triassic-Jurassic transition (200-195 My), and the Middle Jurassic-Early Cretaceous (170-110 My; Westphal et al., 1979; Marzoli et al., 1999, 2004, 2011;

Martins et al., 2008, 2010; Verati et al., 2007; Frizon de Lamotte et al., 2009; Bensalah et al., 2013; Whalen et al., 2015; Moratti et al., 2018).

The first event was related to the evolution of the Central Atlantic Magmatic Province (CAMP), one of the largest igneous provinces on Earth, originated from mantle upwelling impinging at the base of the continental lithosphere of the Pangea at ca 200 Ma. This determined continental breakup and sea floor spreading leading to the formation of the Central Atlantic Ocean (Marzoli et al., 1999, 2004, 2011; Hames et al., 2000; McHone, 2003; Knight et al., 2004; Verati et al., 2007; Frizon de Lamotte et al., 2008; Martins et al., 2008; Merle et al., 2011; Blackburn et al., 2013). The CAMP is recorded in the CHA by basaltic lava flows, sills and dykes, interbedded between the Triassic evaporites and the Lower Jurassic limestone. The event is dated to 200-195 Ma (Marzoli et al., 1999; Verati et al., 2007).

The second event was likely related to the Peri-Atlantic Alkaline Pulse (PAAP) (Matton and Jébrak, 2009), following the CAMP magmatism, and consisting of transitional to alkaline magmas emplaced all around the Central and South Atlantic oceans. In the CHA it consists of basaltic lava flows, interbedded in the studied continental successions, and subvolcanic intrusive complexes. Old K-Ar datings (e.g., Hailwood and Mitchell, 1971; Smith and Pozzobon, 1979; Westphal et al., 1979) result in two groups of ages: 175-155 Ma and 135-110 Ma (Ibouh and Chafiki, 2017, for a review).

The lava flows associated with this second event may be particularly significant for the stratigraphic constraint of the *Couches Rouges.* Unfortunately, few $^{40}Ar/^{39}Ar$ new datings are available (Moratti et al., 2018, and references therein) and up to now datings have been referred to stratigraphic location of basaltic lava flows within the continental succession (Bensalah et al., 2013).

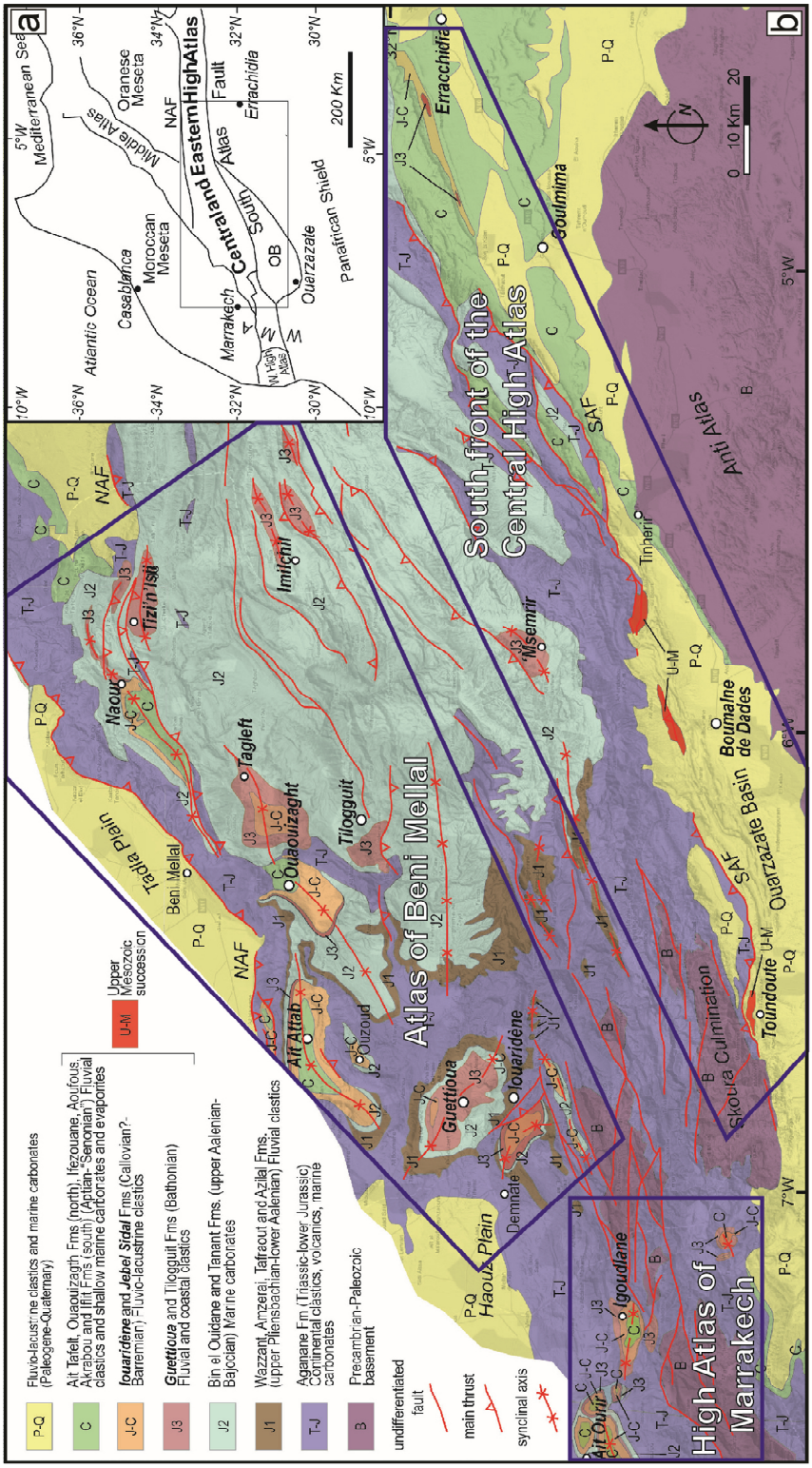

Fig. 1: a) Geographic location of the High Atlas chain and of the study area (black rectangle) b) Schematic geological map of the study area (modified from Carte Géologique du Maroc, 1985) reporting the Middle Jurassic – Lower Cretaceous units outcropping in the different basins. The blue sectors indicate the three regions selected in this study: the High Atlas of Marrakech, the Atlas of Beni Mellal and the south front of the Central High Atlas.

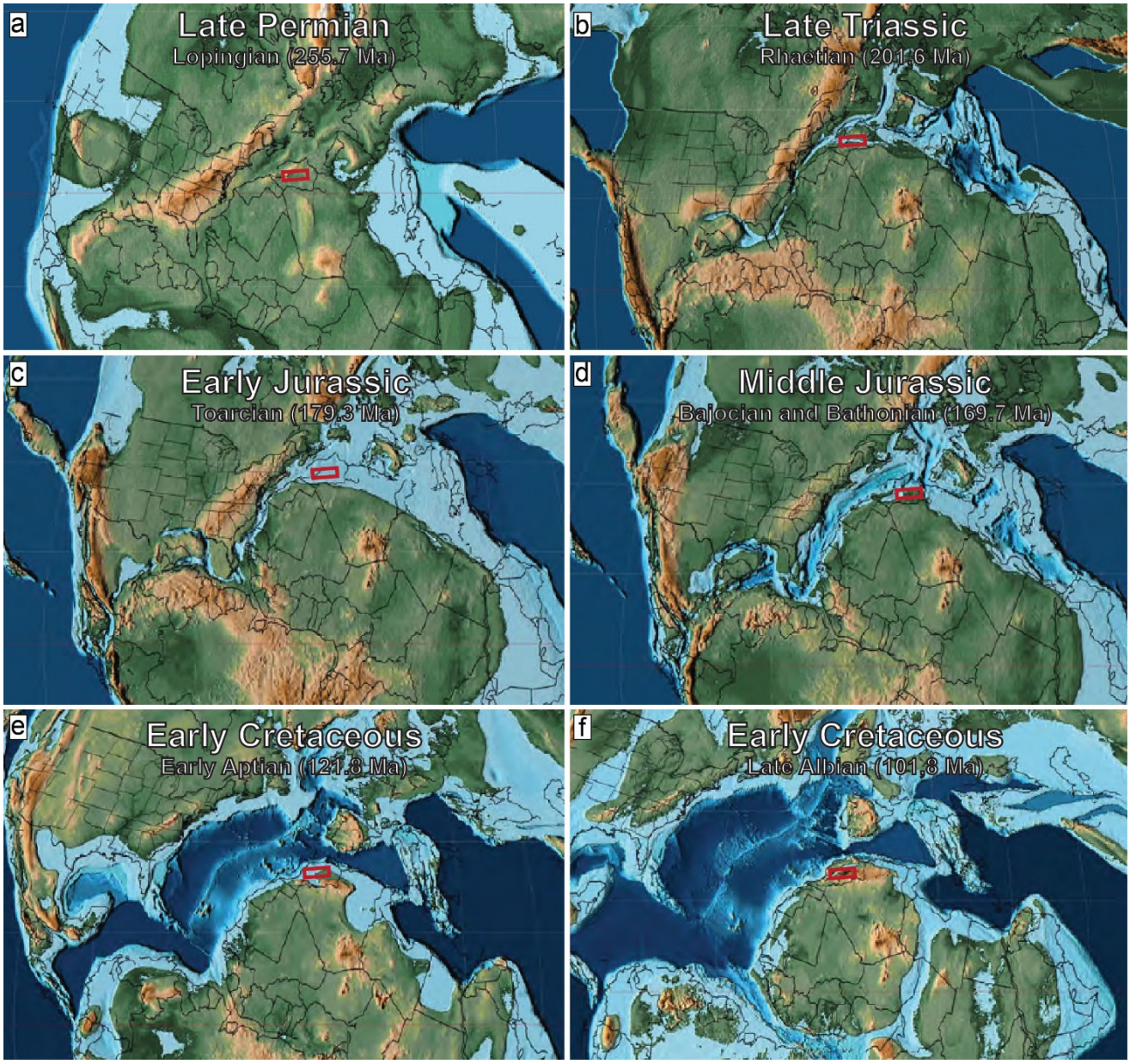

Fig. 2: Paleogeographic maps showing the paleogeography from the late Permian to the late Albian. The red rectangle approximately identifies the studied area. The maps are from volumes 2, 3 and 4 of the PALEOMAP PaleoAtlas for ArcGIS (Scotese, 2014a, b, c, d). Absolute age assignments are from Gradstein, Ogg & Smith (2008).

2.3 Stratigraphy and chronostratigraphic calibration of the *Couches Rouges*

The *Couches Rouges* include the coarse-grained, fluvial Guettioua and Jbel Sidal formations, separated by the fine-grained, lacustrine Iouaridène Formation (Fig.3). These continental red beds are well exposed on the axial zone and along the northern slopes of the CHA, at the core of wide syncline basins separated by narrow anticlines. On the southern front of the Central High Atlas, they outcrop along strongly deformed areas, close to the South Atlas Fault: the Toundoute area, the Dades Valley and the Goulmima anticline (Fig.1b).

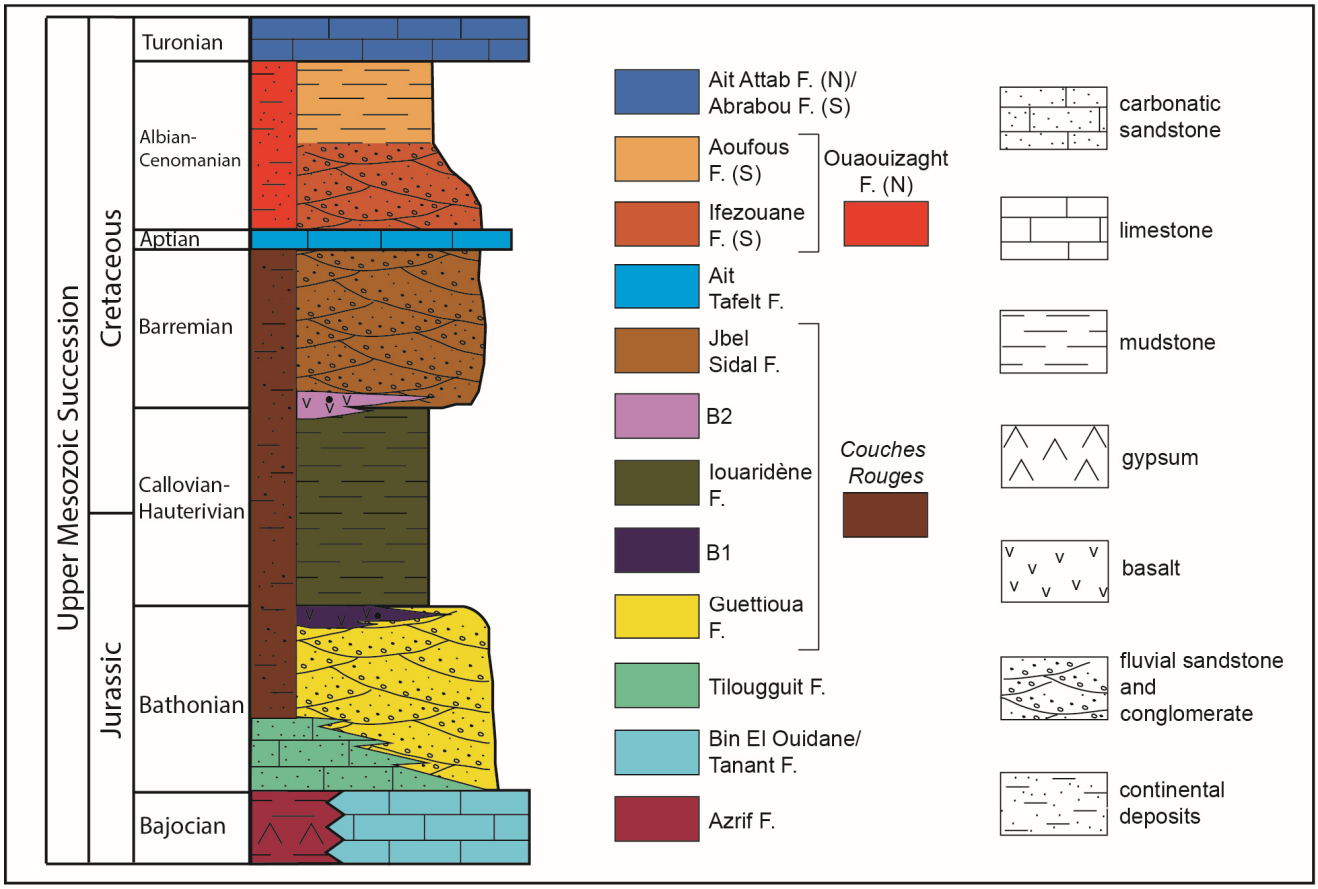

Fig. 3: Stratigraphic column synthetizing the Middle Jurassic – Upper Cretaceous successions of the Central High Atlas.

The paucity and/or lack of fossil remains having a biostratigraphic significance (Charrière and Haddoumi, 2017) makes a fine chronostratigraphic calibration of this succession difficult.

In general terms, the *Couches Rouges* rest over Lower Jurassic-Bajocian marine-transitional deposits and are sealed by the Aptian Ait Tafelt Formation at the northern front of the Central High Atlas, thus, the continental interval is limited between the Middle Jurassic and the Early Cretaceous (Fig.3).

Some microfossil taxa, mainly charophytes and ostracods, allow to approximately define the timing of the continental deposition. Bathonian-?Callovian microfossil assemblages have been recognized in the Guettioua Formation. The Upper Jurassic, mainly the Kimmeridgian, is recorded in the lower part of the Iouaridène Formation whereas the Barremian is documented by ostracod assemblages in the upper strata of this formation. The Barremian has been documented also in the overlying Jbel Sidal Formation (Haddoumi et al., 2002, 2008, 2010; Charrière et al., 2005; Charrière and Haddoumi 2016, 2017).

The top of the Guettioua Formation and the base of the Jbel Sidal Formation are locally marked by two basaltic units, named B1 and B2 (Haddoumi et al., 2002, 2010; Bensalah et al., 2013), erupted in the second stage of magmatic activity in the CHA recorded by transitional to alkaline magmas of the PAAP (Matton and Jébrak, 2009). The first one has been radiometrically dated to the Middle Jurassic, the second one is referred to the upper part of the Lower Cretaceous, according to the Barremian reference for the Jbel Sidal Formation exposed in the Ait Attab and Ouaouizaght synclines (Haddoumi 2002, 2010).

In Table 1-4, the rock-stratigraphy proposed in the present study for the *Couches Rouges* is compared with that established in existing geological maps and previous studies (Termier, 1941; Bourcart et al., 1942; Choubert et al., 1959; Hyndermeyer et al., 1977; Ferrandini et al., 1982; Saadi et al., 1985; Milhi et al., 1993; Hadri et al., 2001; Zouibaa, 2003; Haddoumi et al., 2010)

Table 1: Correlation panel for the area of the High Atlas of Marrakech, between the stratigraphy defined in this study and the stratigraphy defined in previous geological maps and other studies (G=Guettioua F.; I=Iouaridène F.; JS=Jbel Sidal F.).

Table 2: Correlation panel for the western sector of the High Atlas of Beni Mellal, between the stratigraphy defined in this study and the stratigraphy defined in previous geological maps (Til=Tilougguit F.; G=Guettioua F.; I=Iouaridène F.; JS=Jbel Sidal F.).

Table 3: Correlation panel for the eastern sector of the High Atlas of Beni Mellal, between the stratigraphy defined in this study and the stratigraphy defined in previous geological maps (Jmc=middle Jurassic continental deposits; G=Guettioua F.; I=Iouaridène F.; JS=Jbel Sidal F.).

Table 4: Correlation panel for the south front of the Central High Atlas, between the stratigraphy defined in this study and the stratigraphy defined in previous geological maps and other studies (G=Guettioua Formation; I=Iouaridène Formation; JS=Jbel Sidal Formation; Cim=Lower Cretaceous continental red beds; C4= Early Cenomanian – Infracenomanian continental deposits).

The following sections summarize the features of the *Couches Rouges* described in literature, such as the location of major outcrop, thicknesses, paleo-environmental reference, and the available chronostratigraphic calibration.

2.3.1 The Guettioua Formation

The Guettioua Formation, the lowest lithostratigraphic unit of the *Couches Rouges*, is composed of fluvial reddish-brownish, cross-stratified to massive, sandstone and conglomerate, alternated with massive and pedogenized mudstone. It is referred to an alluvial plain with gravelly-sandy paleo-channels and adjacent areas of flood expansion. The thickness of this unit varies in the region from a minimum of 10-20 meters in the Ait Ourir area to a maximum of 400 meters in the M'semrir syncline. The conglomerate fraction is characterized by clast compositions including carbonates derived from the denudation of the Early and Middle Jurassic marine limestone, forming the shoulders of the synclines. Mudstone bears paleo-soil horizons, dinosaur foot-prints and scattered skeletal remains (Monbaron, 1981, 1982; Monbaron et al., 1999; Montenat et al., 2005). In the Ait Attab, Ouaouizaght and Naour synclines, it is capped by basalt lava-flows ascribed to the B1 (Jenny et al., 1981; Saadi et al., 1985; Sohuel, 1987, 1996; Benvenuti 2009, 2010; Haddoumi et al., 2010; Charrière and Haddoumi, 2016).

This formation has been recognized by the authors in almost all the basins considered in the present study (except for the Tasgimouth syncline basin, in Ait Ourir, Pan.1), resting unconformably over Lower-Middle Jurassic continental to marine strata.

Chronostratigraphic calibration

The Guettioua Formation in the eastern sector of the CHA overlies the Tilougguit Formation, that bears a shallow marine molluscan fauna ascribed to the early Bathonian (Sohuel 1996, Charrière and Haddoumi, 2016). In the Iouaridène syncline the base of the homonym formation, overlying the Guettioua Formation, yielded charophytes dated to the Bathonian-Callovian transition (Sohuel, 1987, 1996; Haddoumi et al., 2010). These biostratigraphic data indicate a Bathonian age for the Guettioua Formation.

This Middle-Jurassic stratigraphic attribution is confirmed by K/Ar dating of B1 basalt, at the top of the formation in the Ait Attab and Ouaouizaght synclines. Two basaltic lavas were dated

to the Aalenian-Bajocian, respectively 173+/-4 and 169+/-9 My (Westphal et al., 1979; recently recalculated by Moratti et al., 2018, to 173 and 170 respectively, with the decay constants of ^{40}K reported in Steiger and Jäger, 1977). However, these datings are not consistent with the Bathonian age suggested by the biostratigraphic data. The inconsistency of the results could be due to the K/ Ar method, which uses model ages unable to correctly detect disturbances in the isotopic system (Moratti et al., 2018).

2.3.2 The Iouaridène Formation

This formation, in the mid portion of the *Couches Rouges,* is composed of lacustrine reddish to brownish-greenish mudstone, marls and evaporites subdivided in two lithological parts. The lower one is composed of reddish to orange mostly massive mudstone with subordinate marls and siltstone containing dinosaur foot prints, ripple marks and mud cracks; the upper part is made of massive dark brownish-greenish mudstone, subordinate siltstone and, locally at the top, evaporites (Jenny et al., 1981; Monbaron, 1981; Sohuel, 1987, 1996; Haddoumi et al., 2010).

It represents ephemeral, playa-like, lacustrine paleo-environments, characterized by periods of high evaporation with the deposition of gypsum layers and periods of desiccation, pointed out by the mud cracks and the dinosaur foot prints (Dutuit and Ouazzou, 1980; Ishigaki, 1989; Nouri et al., 2001; Boutakiout et al., 2008; Ishigaki and Matsumoto, 2009; Haddoumi et al., 2010; Charrière and Haddoumi, 2016). Its maximum thickness is several hundred-meters, exposed in the western sector of the High Atlas of Beni Mellal, while, in the westernmost outcrops (Ait Ourir and Jbel Igoudlane synclines), it forms thinner successions, up to 50-60 m.

This formation is apparently not recognized in some areas of the axial CHA such as in the Adrar Aglagal and in the eastern sector of the High Atlas of Beni Mellal (Haddoumi et al., 2010). Along the southern front of the CHA it is lacking or represented by lithologically different equivalents such as in the Dades River valley (Benvenuti et al., 2017). The Iouaridène Formation overlies the Guettioua Formation with the exception of the Tasgimouth syncline (in the Ait Ourir area, Tab.5) and the southern front of the Ait Attab syncline where it lies directly over the marine-transitional Lower to Middle Jurassic units.

Chronostratigraphic calibration

Ostracod and charophyte assemblages, collected in the western sector of the High Atlas of Beni Mellal (Charrière et al., 2005; Mojon et al., 2009; Haddoumi et al., 2010), suggest a time-transgressive onset of deposition: from the Bathonian-Callovian transition in the southernmost outcrops (Iouaridène and Guettioua synclines), to the Oxfordian?-Kimmeridgian in the Ouaouizaght syncline, to the Hauterivian?-Lower Barremian in the northernmost basins (Ait Attab syncline; Haddoumi et al., 2010; Haddoumi and Charrière, 2016). Furthermore, in the Ait Attab syncline, marine microfossils dated to the Lower-Upper Barremian, have been found at the top of the Iouaridène Formation (Haddoumi et al., 2010).

In the Dades Valley and in the Tagleft syncline, in a stratigraphic interval referable to the Iouaridène Formation for its stratigraphic position and for its sedimentological characters, have been found relics of plants. They are represented by an assemblage of ferns and microphyllous conifers (Benvenuti et al., 2017) comparable to fossil floras known from the Iberian Peninsula (Dieguez et al., 2010) and England (Seward 1894-1895) ascribed to the Early Cretaceous (i.e Berriasian-Albian).

2.3.3 The Jbel Sidal Formation

The Jbel Sidal Formation, at the top of the *Couches Rouges*, is composed by fluvial reddish-yellowish sandstone and mudstone with intervening conglomerate in lenticular beds and dolomites at the top, anticipating the marine marls and limestone of the overlaying Ait Tafelt Formation (Sohuel 1987; Sohuel, 1996; Haddoumi et al., 2010). Its thickness is variable between 100-200 meters and more than 500 meters.

It rests over the previous formations with high relief erosional surfaces and angular unconformities. In Ouaouizaght and Ait Attab synclines, the base is characterized by the presence of B2 basalts. The geographic distribution includes wide exposures in the High Atlas of Marrakech, over the Iouaridène Formation (Ait Ourir and Jbel Igoudlane synclines) or directly over the Guettioua Formation (Adrar Aglagal syncline). It crops out extensively in the western sector of the High Atlas of Beni Mellal (Iouaridène and Ouaouizaght synclines), lacking in the Guettioua syncline. It is not reported in previous studies in the eastern sector of the High Atlas of Beni Mellal.

Along the southern front of the CHA, it has been recognized in the Dades Valley (Benvenuti et al., 2017; Moratti et al., 2018) and, in this study, in the lower part of a fluvial succession previously referred to the Ifezouane Formation, cropping out at the core of the Goulmima anticline (Tab.4).

Chronostratigraphic calibration

An ostracofauna referred to the transition from early to late Barremian (Mojon et al., 2009; Haddoumi et al., 2010) has been found at the base of the Jbel Sidal Formation in the Ait Attab syncline. The Ait Tafelt Formation, representing the top of the unit in the northern outcrops, is the expression of the Aptian transgression (Andreu et al., 2003; Mojon et al., 2009; Haddoumi et al., 2010). The Jbel Sidal Formation is thus ascribed to the Barremian-Early Aptian.

This age is also confirmed by the K/Ar dating of the B2 basaltic lava flow at the base of this unit in the Ouzoud syncline, at the south of the Ait Attab syncline: 125+/-2 Ma (Westphal et al., 1979; recalculated to 128+/-2 Ma by Moratti et al., 2018), Barremian. A basaltic lava flow outcropping in the Jbel Istifane area (east to the Dades Valley) at the top of the Jbel Sidal Formation, has been recently dated through the $^{40}Ar/^{39}Ar$ method to 119.24+/-0.62 Ma (Aptian; Moratti et al., 2018), confirming a Barremian age for the Jbel Sidal Formation also at the southern front.

3. Facies Analysis of the upper Mesozoic continental formations of the Central High Atlas

13 facies have been defined and synthetized in table 5

3.1 Facies

3.1.1 Nodular gypsum (Facies G1)

Description

Nodular anydritic gypsum in thin tabular layers, up to 5-10 cm, occurring in specific intervals of the Adrar Aglagal continental succession

Interpretation

This facies attests to sulphate precipitation followed by subsequent diagenetic modification

3.1.2 Massive to laminated mudstone (Facies M1)

Description

Massive to planar laminated red to greenish mudstone. In places, mudstone is mottled and contains carbonate nodules (caliche), up to 2-3 cm in diameter. It is prevalently arranged in thick tabular beds ($M1_a$), forming lenses or drapes ($M1_b$) when found inside paleo-channels (Fig. 4a, c, e; 5e; Fig. 7a, b, c, d, e).

Interpretation

The massiveness of this facies suggests a bulk deposition from suspension settling whereas planar lamination hints to the traction by weak currents. By the fact, due to diagenetic transformations obliterating mostly through compaction the primary structures (Zavala et al., 2017), massive mudstones are normally referred to sediment settling in stagnant water. Nevertheless, sedimentologic studies on the marine mudstone fabric (Schieber, 2016), including graded and laminated structures (Lazar et al., 2015), demonstrated that mud deposition is commonly related to density currents such as hyperpycnal flows. This suggests that also in subaerial flow expansion areas, such as floodplains and floodbasin, a great amount of muds may be delivered by fluidal flows. Mottling and caliche nodules hint to modification due to soil development, marking prolonged periods of non-deposition. The deposition and

preservation of in-channel mud ($M1_b$) is due to rapid waning of high magnitude flood, a possible evidence of alluvial settings characterized by a variable regime of discharge (Williams, 1971; Abdullatif, 1989; Singh and Bhardway, 1991; Singh et al., 1993; North and Taylor, 1996; Shukla et al., 2001; Billi, 2007; Nichols and Fisher, 2007; Allen et al., 2011, 2014; Plink-Björklund and Birgenheier, 2013; Plink-Björklund et al., 2014; Plink-Björklund, 2015).

3.1.3 Massive marl and calcisiltite with plant remains (Facies Cs1)

Description

Yellowish to greenish marls to calcisiltites in dam-m lenticular beds. Normally structurelles, it could contain plant remains and coal (Fig. 4b).

Interpretation

Sediment settling from suspensions in small ephemeral ponds, developing in period of wet climate, favoring plant and coal accumulation.

3.1.4 Calcisiltite and calcareous sandstone with fossils (Facies Cs2)

Description

White to yellowish calcisiltite to calcareous sandstone in dam-m tabular beds, structureless, locally containing remains of shells (fragments of gastropods).

Interpretation

Sediment transport in high energy flows, in coastal paleo-environment

3.1.5 Massive siltstone (Facies S1)

Description

Massive, locally nodular, red-yellowish to greenish, siltstone to fine-grained sandstone in tabular ($S1_a$) to lenticular ($S1_b$) beds up to 20-30 cm. At the top of the beds, occasional mud cracks burrows and roots traces may be present. Locally, soft-sediment deformation structures

as convolute bedding with vertical or overturned limbs have been observed (Fig. 4c, d, e; 7a, b, c, d, e).

Interpretation

Deposition from sediment laden flows through massive settling due to high deposition rate (HDR). Occasional nodularity may indicate post-depositional modification due to bioturbation or pedogenic processes. Mud cracks and trace fossil record non-deposition and subaerial exposure. Commonly in terrestrial settings such traces affect flood plain mudstones (Hasiotis, 2004), but they could also occur in channels on accretion sets, indicating that the channels remained dry for relatively long periods between the floods (Uba et al., 2005; Saez et al., 2007; Plink-Björklund and Birgenheier, 2013; Plink-Björklund, 2015). The convolute bedding is a result of pore fluid expulsion generated during late flood stages (McKee et al, 1967; Tunbridge, 1981), or during rapid sediment loading (HDR) (Singh and Bhardwaj, 1991).

3.1.6 Rippled sandstone (Facies S2)

Description

Planar to trough-cross laminated well sorted fine to medium-grained sandstone, in centimeter-thick lamina-sets. Locally it shows a climbing attitude, with partial or total preservation of the stoss side of the bedforms (Fig. 4f, g).

Interpretation

Unidirectional flows in subcritical, or lower flow, regime (LFR) determining the formation of current ripples. The stoss side preservation, has been interpreted as the result of climbing ripples, forming when sediment fall-out rates exceed bedforms migration rates (HDR) (Allen, 1966, 1984).

3.1.7 Planar laminated sandstone (Facies S3)

Description

Planar to very low-angle (up to 5°) laminated red to yellowish medium to fine sandstone in decimeter to meter thick tabular beds. Locally, the base of the beds may present groove casts (Fig. 4h, i; 5d; 7b, c, d).

Interpretation

Upper plane beds in critical flow regime conditions. Experimental work shows that planar laminations can form due to very low-angle bedforms migration (McBride et al., 1975; Bridge, 1978; Bridge and Best, 1988; Cheel, 1990; Best and Bridge, 1992).

3.1.8 Graded sandstone (Facies S4)

Description

Grey siltstone to medium sandstone, organized in mm-cm composite layers with a light gray coarser portion at the base, grading upward in a dark grey finer portion to the top. The layers are horizontal to low angle inclined (Fig. 5a).

Interpretation

The composite layering is the result of flow bipartition (Fisher, 1983) due to the entering of a subaerial confined to poorly-confined flow in water. Passing from confined conditions to unconfined ones the sedimentary load settles down, similar to a turbidity current, with the coarser and heavy portion at the base.

3.1.9 Low angle cross stratified sandstone (Facies S5)

Description

Low angle (>5°, <25°) trough-cross stratified red to yellowish fine sandstone to pebbly sandstone in wide plane-concave beds up to 2-3 meters thick. Soft-sediment deformation structures such as overturned cross-strata are locally observed in this facies (Fig. 4g; 5b, c, d; 7d).

Interpretation

The facies is referred to 3D-dunes migration in channelized flows. The low angle lee-sides attest to bedform development under a flow regime intermediate between subcritical and supercritical (the washed-out dune stage, Simons and Richardson, 1963;; Coleman, 1969; Bronley, 1991; North and Taylor, 1996, Knighton, 1998; Brierley & Fryirs, 2005), in which the high velocity of the current in shallow channels joined to high sediment rate, prevents the formation of classic LFR bedforms. Overturned cross-strata point to partial liquefaction and deformation of water-saturated sediments under the influence of lateral shearing. The latter occur in association with rapid increases in bottom shear resulting from highly turbulent flow in transcritical flow conditions (Stear, 1985; Singh and Bhardwaj, 1991).

3.1.10 High angle cross stratified sandstone (Facies S6)

Description

High-angle (>25°) planar to trough-cross stratified medium sandstone to pebbly sandstone in plane-concave 50-150 cm thick beds (Fig. 5d; 7d).

Interpretation

Downstream migration of 2D and 3D dunes in channelized flows in subcritical regime. The development of planar or through-cross stratification depens on the flow velocity and give information on the shape of dune crests, linear in 2D dunes and sinuous in 3D dunes.

3.1.11 UFR sandstone (Facies S7)

Description

Brownish to yellowish fine sandstone to pebbly sandstone characterized by cross-bedding due to sinusoidal low-angle bedforms, scour and fill structures and sigmoidal cross strata (Fig. 5e; 6b; 7d).

Interpretation

The variety of sedimentary structures ascribed to this facies is referred to Froude transcritical and supercritical flow conditions. Scour and fill structures indicate initial erosion by water currents characterized by high velocities (UFR) followed by sediment aggradation and infilling of the scour features (HDR) (Kennedy, 1963; Leopold et al., 1966; Foley, 1978; Alexander et al., 2001; Cartigny et al., 2014; Plink-Björklund, 2015); The sinusoidal low-angle laminations, also referred to as antidunes, form at flow velocities and Froude numbers higher than that required for plane bed deposition, and migrate downstream, related to stationary waves, or migrate upstream, depending on flow velocities (Middleton, 1965; Simons et al., 1915; Allen, 1966, 1984; Middleton and Southard, 1984; Cheel, 1990; Alexander et al., 2001); the sigmoidal cross strata have been linked to the transition from dune to plane bed deposition, related to Froude numbers just below what is needed for UFR plane beds (Bridge, 1981; Bridge and Best, 1988) or to chute and pool migration (Cartigny et al., 2014).

3.1.12 Massive sandstone with scattered pebbles (Facies S8)

Description

Structureless or graded, moderately sorted, medium sandstone to pebbly sandstone characterized by the presence of scattered pebbles, mudclasts, and caliche clasts. It is found commonly at the bases of the channels and above minor internal erosion surfaces (Fig. 7d).

Interpretation

This facies has been interpreted as channel lag deposits. The pebbly fraction accumulated during the erosive, rising stage of floods, when large blocks of the river banks collapsed. The thick-soft sediment clast conglomerates is linked to UFR flow conditions and rapid lowering of water level during the waning stage of floods, where the banks are overlain by, or contain, muddy sediment and paleosols: when UFR conditions occur, the banks are undercut and develop shear cracks, whereby part of the bank slumps (Coleman, 1969; Gohan and Parkash, 1990; Singh et al., 1993; North and Taylor, 1996; Gibling and Tandon, 1997; Ghinassi et al, 2013; Björklund, 2015).

3.1.13 Graded conglomerate (Facies C1)

Description

Moderately sorted pebbly sandstone to conglomerate in dm-m thick tabular layers, characterized by rhythmic sorting and grain size. Very well sorted divisions, with open-work texture, are alternated to moderately sorted conglomerate and poorly sorted, matrix supported conglomerate or sandstone. The clasts are well-rounded to sub-rounded, up to 20-30 cm in diameter (Fig. 6a, c, d, e; 7d).

Interpretation

Transport and deposition by unconfined to poorly confined flows, intermediate between selective and mass flows (Benvenuti and Martini, 2001). The rhythmicity between matrix rich and well sorted or openwork beds is the result of alternance between UFR, LFR and HDR conditions. . According to some authors, this alternance develop in different depositional events: the openwork levels result from avalanches, along the slope of the bars, of sediments, previously selected by bedforms migrating on fluvial bars in UFR (Smith, 1972). The matrix rich levels are due to settling and infiltration of sands during low stage (LFR) or develop in HDR condition, that prevents the sorting (Smith, 1974; Steel and Thompson, 1983; Carling, 1990; Rust, 1984). Other authors refer therhythmic variations of texture to a dynamic sorting of bedload during single depositional events (Iseya and Ikeda, 1987) or to infiltration of sandstone in sorted gravel bedss, due to backflows in UFR, forming the matrix rich levels (Anketell and Rust, 1990).

G1	Nodular gypsum
M1	Massive to laminated mudstone
Cs1	Massive marls and calcisiltites with plant remains
Cs2	Calcisiltites and calcareous sandstone with fossils
S1	Massive siltstone
S2	Rippled sandstone
S3	Planar laminated sandstone
S4	Graded sandstone
S5	Low angle cross stratified sandstone
S6	High angle cross stratified sandstone
S7	UFR sandstone
S8	Massive sandstone with scattered pebbles
C1	Graded conglomerate

Table 5: facies names and short description

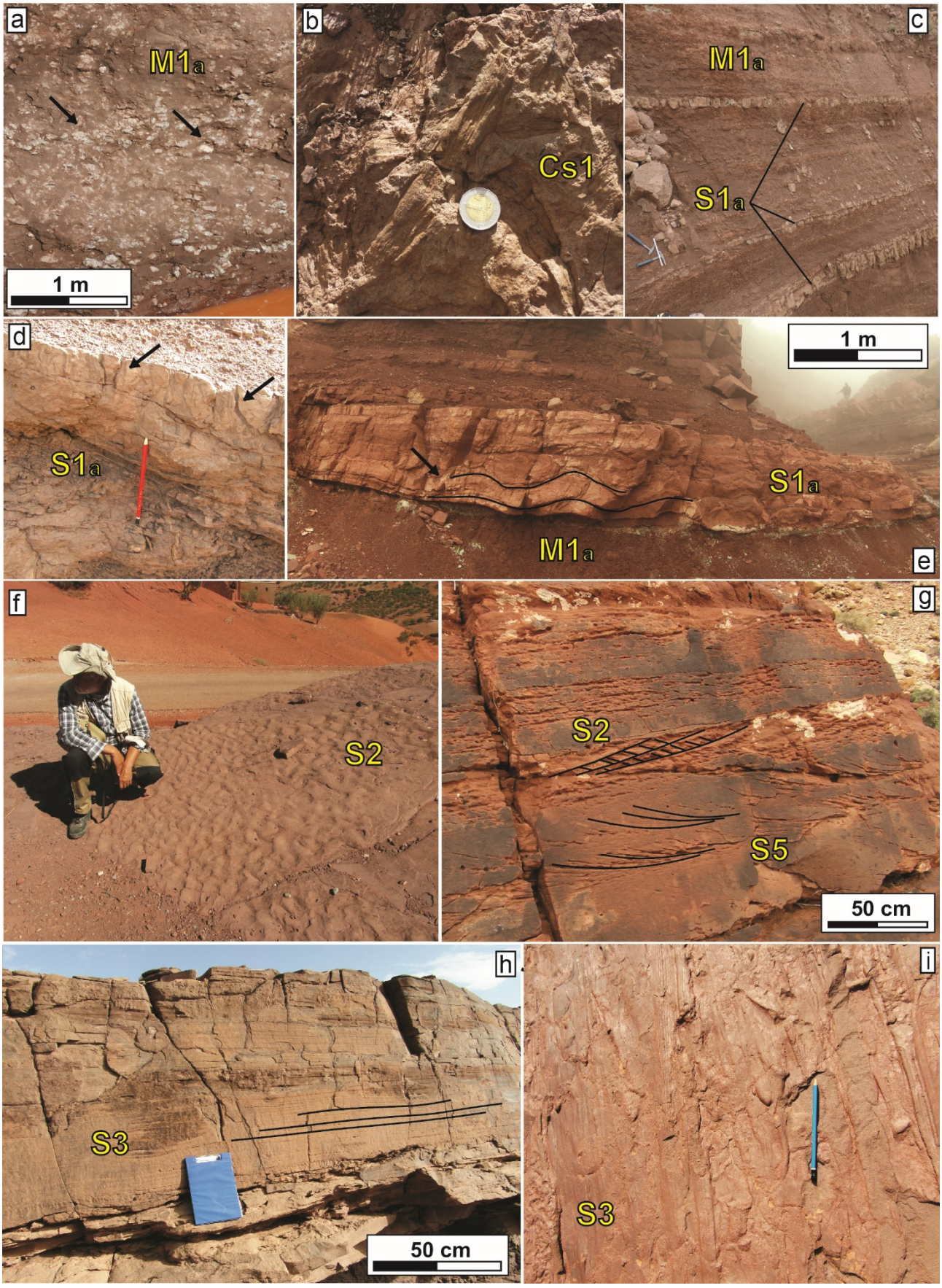
a
M1a
1 m
b
Cs1
c
M1a
S1a
d
S1a
1 m
S1a
M1a
e
f
S2
g
S2
S5
50 cm
h
S3
50 cm
i
S3

Fig. 4: a) Detail of facies $M1_a$, rich in carbonates nodules (caliches), indicated by the black arrows. Guettioua F. in Adrar Aglagal syncline b) Detail of facies Cs1, showing trace fossils of plants. Guettioua F. in 'Msemrir syncline c) Alternation between facies $S1_a$, in cm-dm tabular beds, and $M1_a$. Guettioua F. in Adrar Aglagal syncline d) Detail of facies S1 showing, at the top of the bed, abundant vertical terrestrial trace fossils, indicated by the black arrows. Jbel Sidal F. in Jbel Igoudlane syncline e) Facies S1 showing soft-sediment deformation, put in evidence by the black lines. Jbel Sidal F. in Jbel Igoudlane syncline f) Plan view of 3d ripples of facies S2. Jbel Sidal F. in Ouaouizaght syncline g) Alternation between facies S2 and facies S5, the latter one showing a climbing attitude. Some structures have been indicated with black lines. Jbel Sidal F. in Goulmima antycline h) plan-parallel lamination of facies S3. Guettioua F. in M'semrir syncline i) groove casts at the base of a bed of facies S3. Guettioua F. in Jbel Igoudlane syncline.

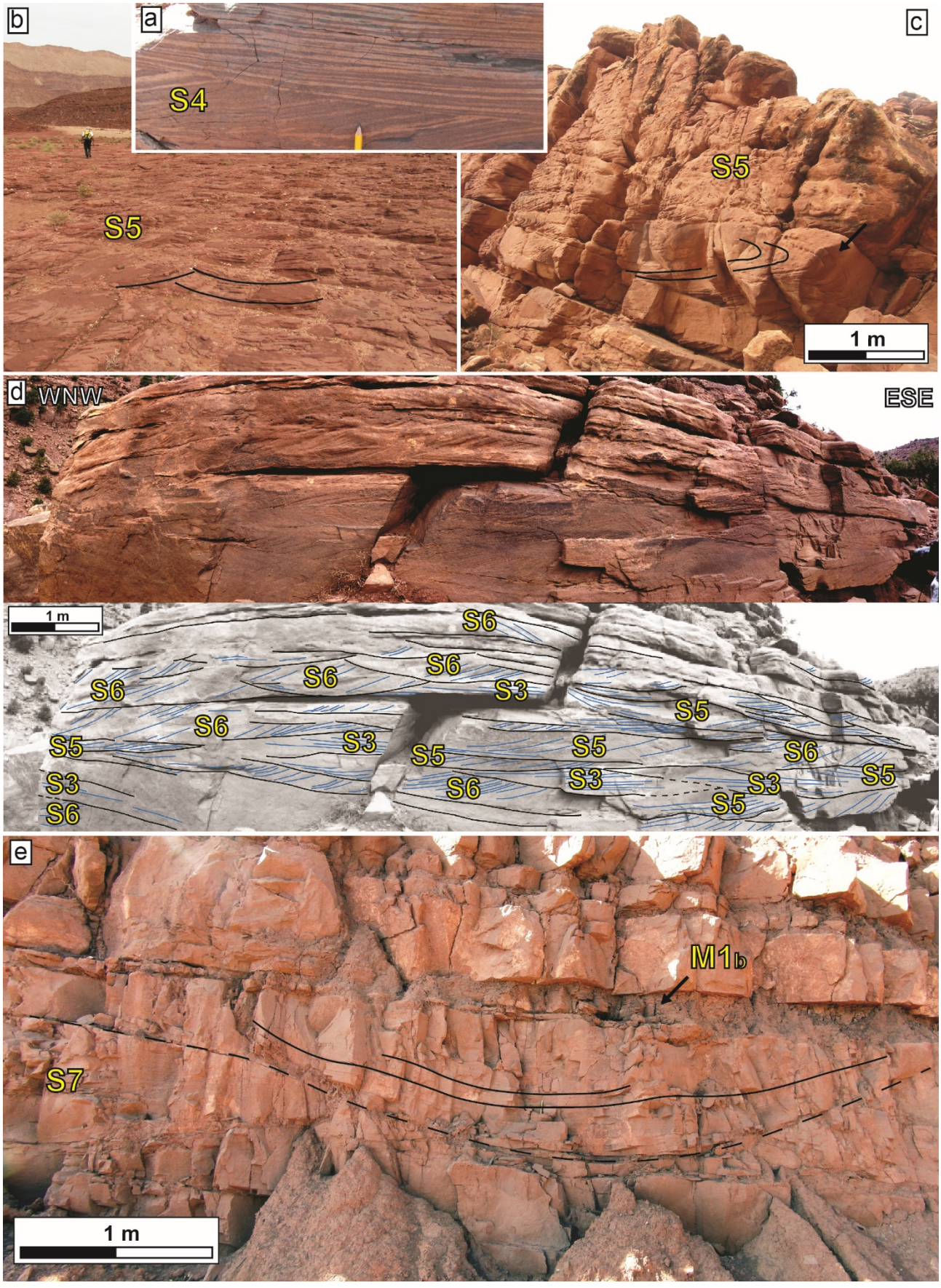
b
a
S4
S5
c
S5
1 m
d WNW
ESE
1 m
S6
S6
S6
S6
S3
S5
S6
S5
S3
S6
S3
S5
S5
S6
S3
S6
S3
S5
S3
S6
S5
e
M1b
S7
1 m

Fig. 5: a) detail of facies S4, showing rhythmicity between coarser and lighter sandstone and finer and darker one in low angle cross stratified beds. Gettioua F. in Tilouigguit syncline b) plan view of facies S5. Some structures have been put in evidence by black lines. Jbel Sidal. F. in Goulmima anticlyne c) facies S5, showing overturned cross-stratification, indicated by the black arrow. Jbel Sidal F. in Goulmima antycline d) amalgamated sandstone with alternating facies S3, S5 and S6. Black and blue lines put in evidence the sedimentary structures. Jbel Sidal F. in Adrar Aglagal e) Scour and fill structure (facies S7). The scour is indicated by the dashed line, the internal concentric lamination by the black lines. Jbel Sidal F. in Jbel Igoudlane.

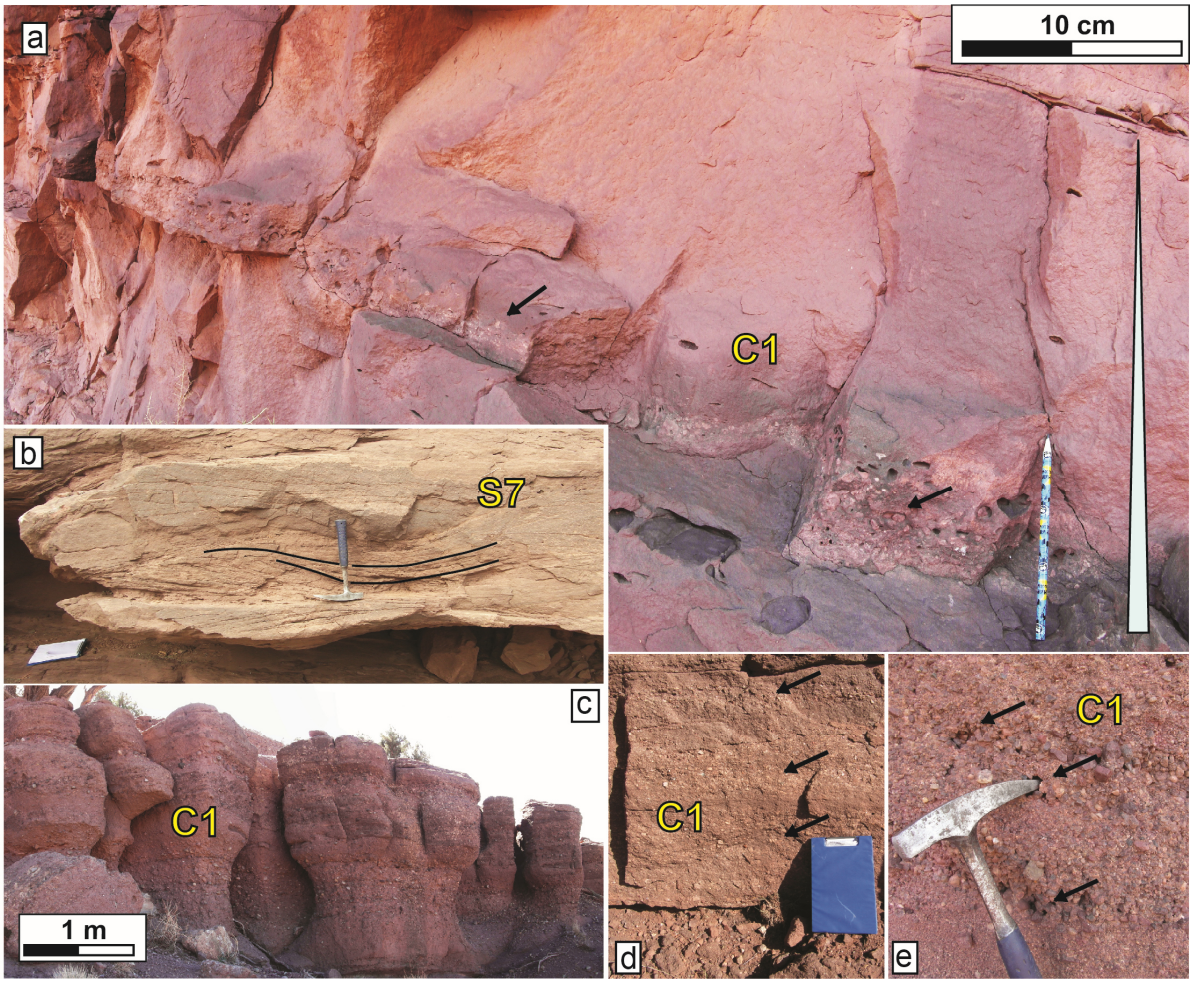

Fig. 6: a) Graded pebbly sandstone of facies C1. At the base of the bed, scattered pebbles and mud clasts are indicated by the black arrows. The light blu triangle symbolized the Fining Upward trend of the bed. Guettioua F. in Ouaouizaght syncline b) sigmoidal cross stratification (facies S7). Some lamina has been put in evidence with black lines. Guettioua F. in M'semrir syncline c) facies C1, showing rhythmicity in sorting and grain size. Jbel Sidal F. in Adrar Aglagal d) Facies C1: detail of the alternation between coarser and finer portions. The coarser ones are indicated by black arrows. Guettioua F. in Adrar Aglagal e) detail of openwork structures in facies C1, indicated by black arrows. Jbel Sidal F. in Adrar Aglagal.

3.2 Facies Associations

3.2.1 Facies Association 1 (FA1)

It is composed for the most part of the alternation of facies $M1_a$ and facies $S1_{a,}$ associating with subordinate S2, S3 and locally Cs1, Cs2 and S4, giving rise to three possible associations (Fig. 7a).

$FA1_a$: $M1_{a,}$ $S1_a$ associated with S2 and S3 stacked in tabular beds or in lenticular beds with a plan-convex geometry. It records an area of flood expansions in which Facies $M1_a$ represents the muddy background deposition occasionally interrupted by deposition from sandier overland flows, expressed by facies $S1_a$, S2 and S3. At the base of the Adrar Aglagal continental succession, this association also include the facies G, indicating sulphate precipitation in periods of high evaporation. The subaerial exposure in dry seasons allowed pedogenic modification outlined by mottling and caliche nodules common in facies $M1_a$.

$FA1_b$: $M1_{a,}$ $S1_a$ associated with Cs1, S2, S3 and S4 stacked in tabular beds or in channelized bodies (CS1 and S4). In this case the flood basin must have been affected by stagnation of water during wet periods, allowing the developing of ponds and ephemeral lakes.

$FA1_c$: $M1_{a,}$ $S1_a$ associated with Cs2, S2, S3 and in tabular beds. The presence of shells remains (Cs2) indicate the proximity of a more stable aquatic environment, as a lake or the sea.

3.2.2 Facies Association 2 (FA2)

FA2 is formed by facies M1, in alternation with facies S1, S2, S3 and subordinate S5, S6, S7, forming tabular beds at the outcrop scale, from decimeter to 5 m thick. The vertical stacking of muddy and sandy facies outlines three common patterns: ($FA2_a$) facies $M1_a$ and $S1_a$ alternate rhythmically; ($FA2_b$) sandy facies form coarsening and thickening upward (CU-TK) sequences (Fig. 7b); ($FA2_c$) sandy facies stack into fining and thinning upward (FU-TH) sequences (Fig. 7c). These patterns are interpreted as the record of distinct sub-environments of a floodplain where facies $M1_a$ is the background deposition from muddy overbank flows. Major floods from adjacent channel belts determined the development of crevasse complexes expanding over the floodplain. CU-TK sequences hint to crevasse lobe progradation whereas FU-TH is interpreted

as the filling of the channels feeding the lobes. Pedogenic features attest to periods of soil development related to reduced or absent sediment supply.

3.2.3 Facies Association 3 (FA3)

FA3 is composed of facies M1, S1, S8 and occasional S2, S3, S5, S6, S7 stacked in channelized bodies up to 5-10 m thick and several hundred meters wide (100<W/T<1000, Broad Sheets; Gibling, 2006) (Fig. 7d, e). The architecture of the channel fills outlines two common patterns:

$FA3_a$: M1, S1, S2, S3, S5, S6, S8 organized in horizontal, aggradational sets

$FA3_b$: 15-25° sloping beds of facies $M1_b$ in alternation with $S1_b$ and S8 forming heterolithic accretion sets (Fig. 7d, e).

These associated facies record broad and shallow fluvial channel fills. In channel fill type (b) the accretions sets are referred to bar forms; the presence of in-channel mudstones (facies $M1_b$), in places pedogenized, testifies the periodic deactivation of fluvial processes during dry periods.

3.2.4 Facies Association 4 (FA4)

FA4 is composed for the most part of the facies S5, locally presenting overturned cross-stratification, and subordinate facies $M1_b$ (forming etherolithic channel infill), S1 (occasionally forming convoluted beds), S2, S3, S6 and S7. These facies are stacked in horizontal, aggradational sets contained within plane-concave bodies up to 5-10 m thick and around 100 meters wide (15<W/T<100, narrow sheets; Gibling, 2006), (Fig. 7d). Single channel bodies are frequently amalgamated, forming thick sandstone bedsets up to 15-20 meters.

3.2.5 Facies Association 5 (FA5)

FA5 is composed of facies C1 and subordinate, S5 and S8 composing aggradational sets in lenticular, erosive, amalgamated bodies up to 10-20 m thick and around a hundred meters wide (15<W/T<100, narrow sheets; Gibling, 2006) (Fig. 7d), recording multistorey, broadly

channelized, fluvial channel bodies**.** The conglomerates or pebbly sandstones filling the channels testify to a short transport distance from the sediment source areas.

3.2.6 Facies Association 6 (FA6)

FA6 it is composed by the association of facies $M1_b$, $S1_b$, S8, and subordinate S2, S5 and S6. The sandstone facies are arranged in 20°-30° sloping accretion sets, contained in channelized bodies up to 10 m thick and around 50-100 meters wide (5<W/T<15, Broad Ribbons, Gibling, 2006). The sedimentary structures show paleocurrent directions diagonal to perpendicular to the axe of the paleo-channels, testifying the in-channel lateral to diagonal migration of accretion sets (Panels in attachment). This facies association is referred to the migration of lateral to diagonal bars in channels characterized by high-sinuosity.

3.2.7 Facies Association 7 (FA7)

FA7 consists of facies S6, in alternation with facies S5 and C1 and subordinate S2, S8 and S7, composing dm-m thick aggradational to very low angle (<10°) accretion sets, in plane-concave, erosive, amalgamated bodies up to 15-20 m thick and around 50-100 meters wide (5<W/T<15, Broad Ribbons; Gibling, 2006) (Fig. 7g). This facies association is referred to the development of multistore fluvial channel bodies.

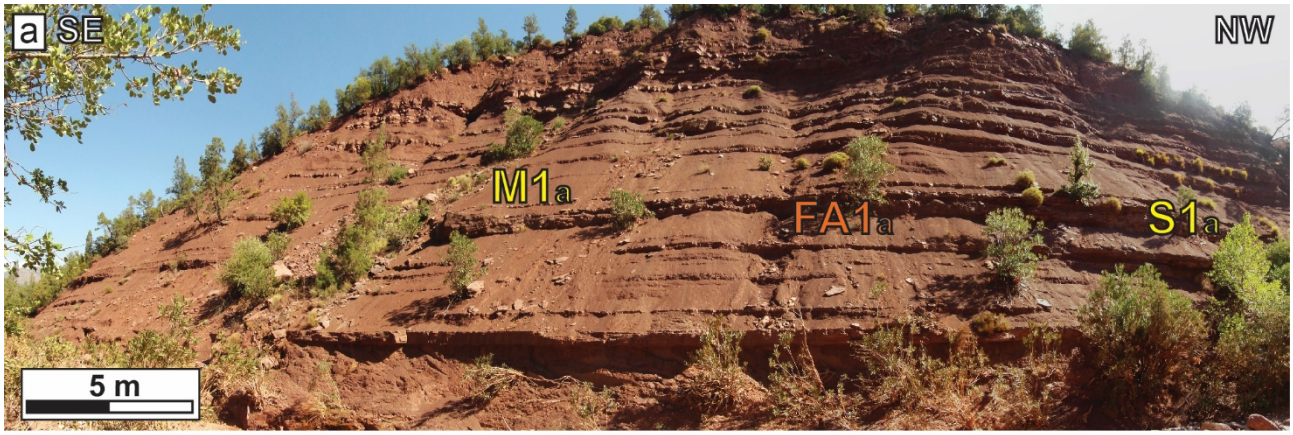
a
SE
NW
M1a
FA1a
S1a
5 m

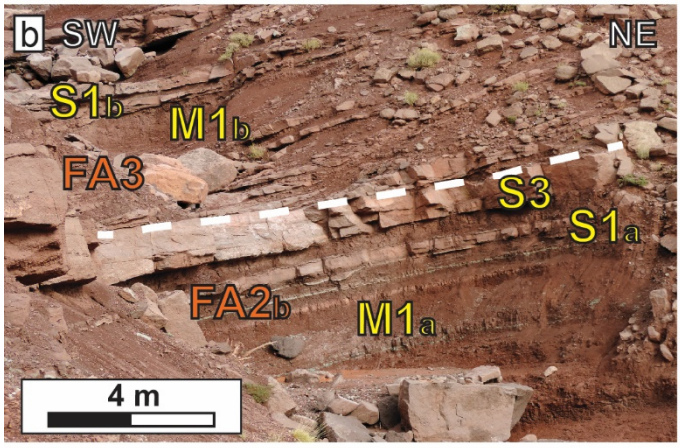
b
SW
NE
S1b
M1b
FA3
S3
S1a
FA2b
M1a
4 m

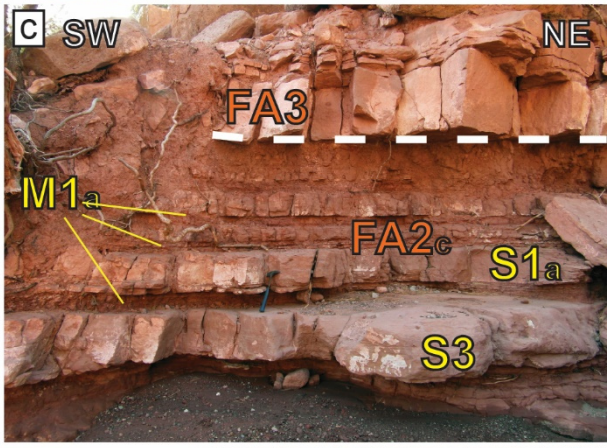
c
SW
NE
FA3
M1a
FA2c
S1a
S3

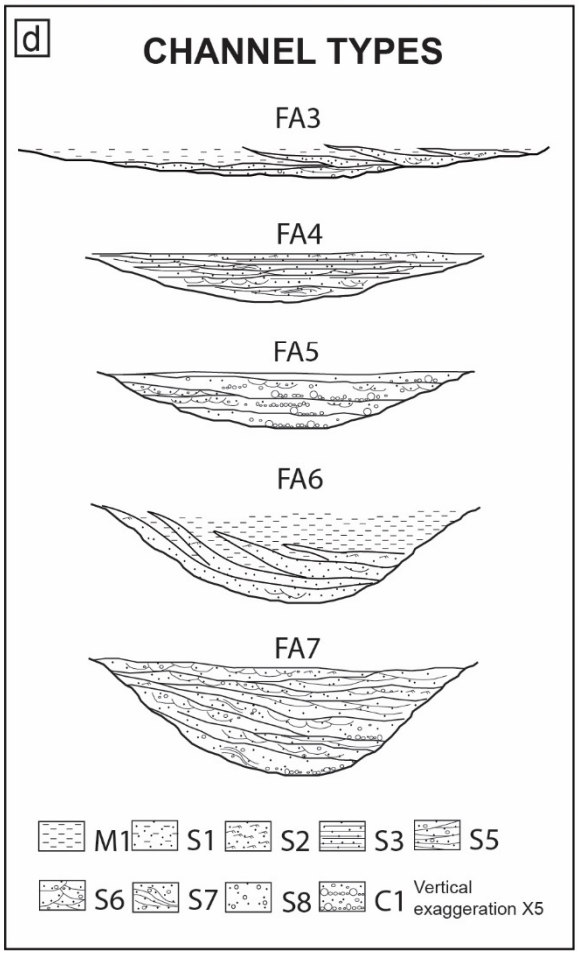
d
CHANNEL TYPES
FA3
FA4
FA5
FA6
FA7
M1
S1
S2
S3
S5
S6
S7
S8
C1
Vertical exaggeration X5


e
M1b
S1b
FA3b
10 m
FA2


f
FA6
5 m

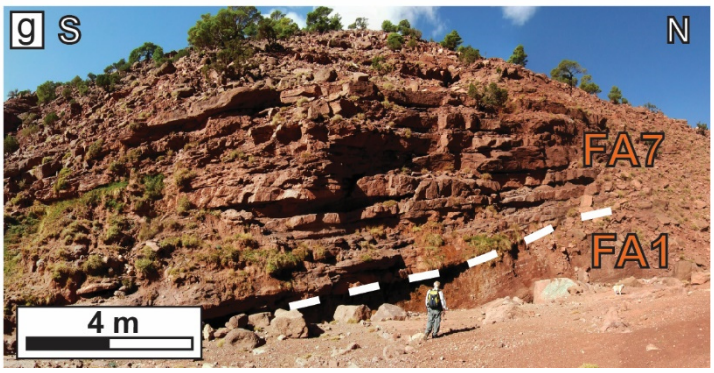
g
S
N
FA7
FA1
4 m

Fig. 7: a) Facies Association 1, composed by the alternation between facies $M1_a$ and $S1_a$. Jbel Sidal F. in Iouaridène syncline b) Pattern b of the Facies Association 2: Facies $M1_a$, $S1_a$ and S3 are stacked in a coarcening and thickening upward sequence. Guettioua F. in Adrar Aglagal syncline c) Pattern c of the Facies Association 2, overlain by Facies Association 3. Facies $M1_a$, $S1_a$ and S3 arranged in a fining and thinning upward sequence. Jbel Sidal F. in Adrar Aglagal syncline d) Sketch of the Facies Associations 3 to 7, expressing the different types of channel, geometry and infill e) Pattern b of the Facies Association 3, composed by the alternation of the facies $M1_b$ and $S1_b$ in low angle accretion sets. *Guettioua F. in Adrar Aglagal f) Facies Association 6, showing high angle accretion sets. Guettioua F. in Guettioua syncline g) Facies Association 7 showing sandstone facies in amalgamation, forming a channel complex. Guettioua F. in Adrar Aglagal.*

4. A case Study: the paleodrainage record of the Upper Mesozoic fluvial succession in the Adrar Aglagal syncline and its implication in the tectono-sedimentary evolution of the Central Atlasic System.

This chapter illustrates the results of a stratigraphic, sedimentologic and structural study of the continental succession exposed at the core of the Adrar Aglagal syncline, located in the southern part of the High Atlas of Marrakech (Fig. 1).

The studied succession, composed by fluvial conglomerates, sandstones and mudstones, is the local expression of the Upper Mesozoic continental complex, comprising the fluvial units of the *Couches Rouges* (the Guettioua and Jbel Sidal formations) and a fluvial Cretaceous succession interpreted as the local equivalent of the Ouaouizaght/*Kem Kem beds* (Ifezouane and Aoufus Formations) (Fig. 8). These red beds attest to a Middle Jurassic-Early Cretaceous regressive phase debated in the frame of the tectono-sedimentary evolution of the Central High Atlas. Indeed, the significance of this long phase of continental deposition is relevant to discussions on the stages of build-up of the Atlas Mountains.

The main aims of this study are: 1) to revise the stratigraphic framework of the Adrar Aglagal continental succession, based on standard sedimentary facies analysis method and recognition of Unconformity Bounded Stratigraphic Units (UBSU; Salvador, 1994); and 2) to restore the evolution of paleo-drainage patterns through time to understand if there is a tectonic forcing in the organization of the fluvial systems.

The sedimentological and stratigraphic analysis, integrated with high-resolution field mapping of the area, is exploited for reconstructing the tectono-stratigraphic evolution of this portion of the Central High Atlas. Despite the limited extension of the study area, its evolution in terms of successive steps of drainage development may have wider implications.

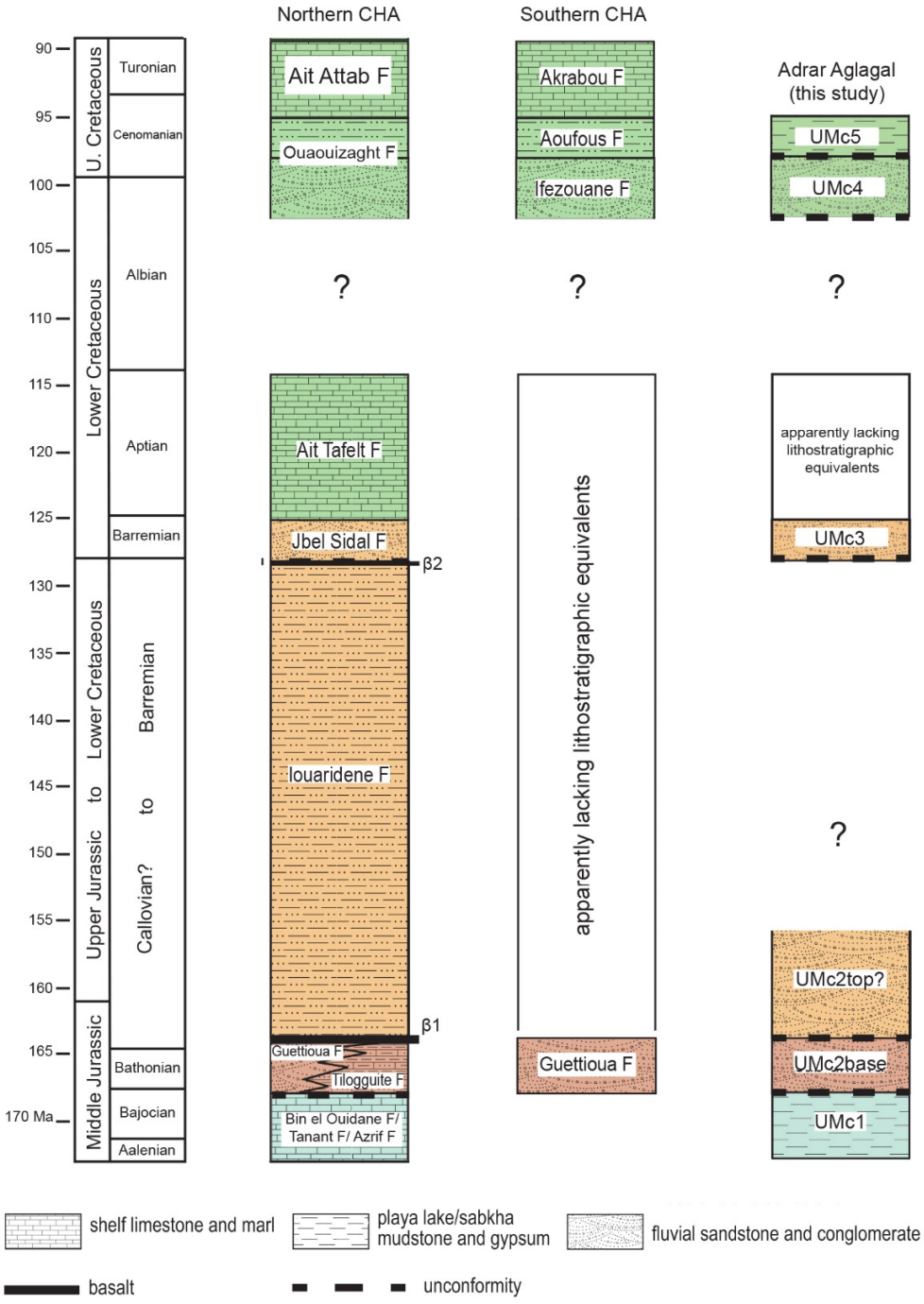

Fig. 8: Stratigraphic scheme comparing the Late Mesozoic successions of the northern and southern front of the Central High Atlas (CHA) with the units defined in the Adrar Aglagal area. UMc = Upper Mesozoic continental succession. Data for the section relative to the northern front of CHA are from: Jenny et al. (1981), Sohuel (1987), Jenny (1988), Charrière et al. (2005), Ettachfini et al. (2005), Haddoumi et al. (2010). Data for the section relative to the southern CHA are from: Jenny et al. (1981), Hindermeyer et al. (1977), Ettachfini and Andreu (2004), Cavin et al. (2010). Modified from Benvenuti et al. (2017).

4.1 Study area

The Adrar Aglagal syncline is located at the southern front of the Central High Atlas, about 150 km southeast from Marrakech (Fig. 9). This area is characterized by a Lower Jurassic – Lower Cretaceous marine-continental succession, detached over Triassic deposits (e.g., Saadi et al., 1985) (Fig. 9d). Marine-transitional limestones, dolomites and gypsum (here named Lower Jurassic marine-transitional succession, LJm), outlining a regressive trend (Courtinat and Algouti, 1985), form the limbs of the syncline. The continental clastic, mostly fluvial, sediments (here named Upper Mesozoic continental succession, UMc) crop out at its core (Figs. 9c, 10a). This succession, previously referred to the Early and Middle Jurassic (Saadi et al., 1985) or to the early Jurassic-late Cretaceous (Termier, 1941; Choubert, 1959), has been revised through a high-resolution field mapping on a surface of about 60 km^2. The resulting map and two geological sections have been synthesized in Fig. 10.

We subdivided the succession by means of Unconformity Bounded Stratigraphic Units (UBSU; Salvador, 1994), defined on the base of the recognition of erosional and angular unconformities at the base of each unit. The studied succession, 500-600 m thick, consists of five stratigraphic units (UMC1-UMC5), with distinctive sedimentological features interpreted for their paleoenvironment meaning. Three stratigraphic sections have been measured, covering all the succession, to describe in detail the defined units. Other stratigraphic and sedimentological data have been taken throughout the Adrar Aglagal relief and its surrounding.

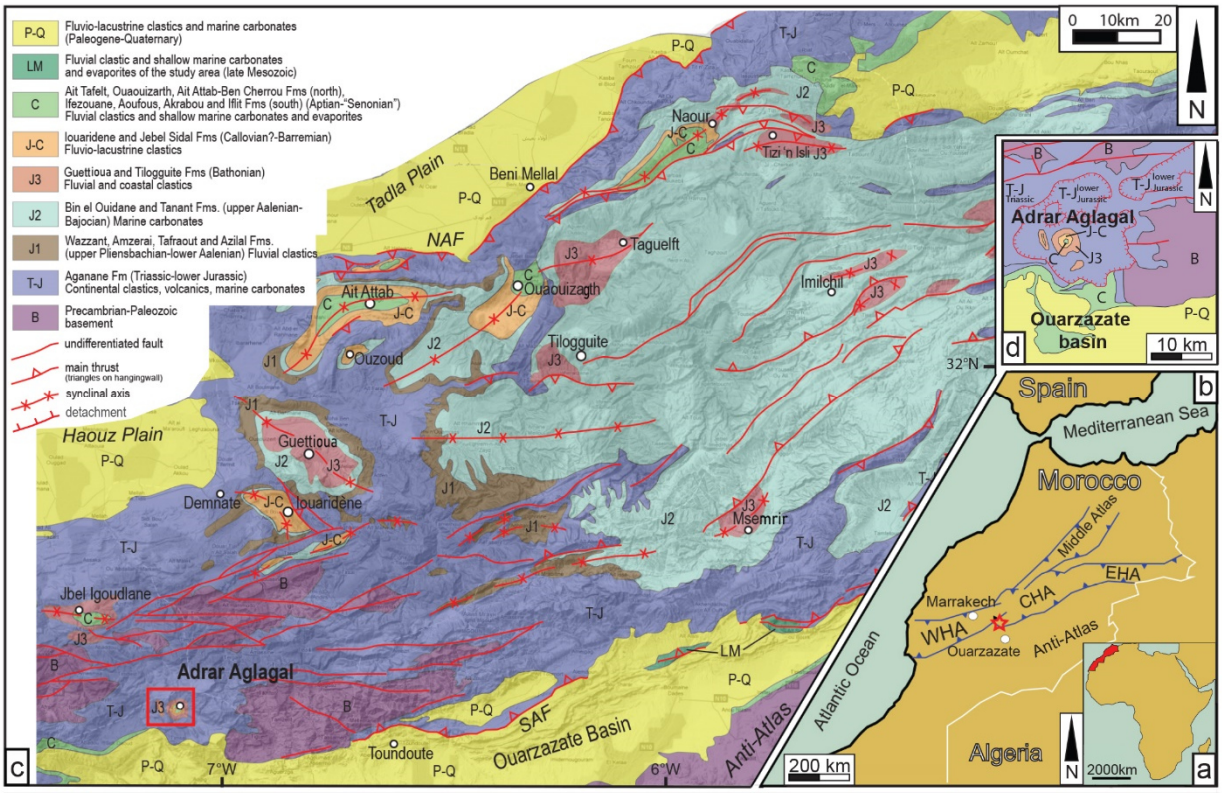

Fig. 9 a) Geographic location of Morocco (in red) b) Schematic map of northern Morocco showing the location of the studied area (red star). WHA = Western High Atlas, CHA = Central High Atlas, EHA = Eastern High Atlas c) Schematic geological map of the Central High Atlas (modified from Saadi et al., 1985) with location of the Adrar Aglagal syncline (red rectangle). The main synclines filled with late Mesozoic continental Red Beds (J1, J3, C) are indicated. NAF = North Atlas Fault, SAF = South Atlas Fault d) Detail of the studied area and its surroundings, showing the main detachment at the base of the Adrar Aglagal Lower Jurassic – Lower Cretaceous succession onto the Triassic basement. See Fig. 9c for the legend (modified from Saadi et al., 1985).

4.2 Stratigraphy of the Adrar Aglagal Upper Mesozoic continental succession

4.2.1 UMc1

This unit is up to 200 m thick, well exposed in the Ounila and Ouwawriykt river valleys (Fig. 10a) where it rests above a low angle unconformity over the Lower Jurassic gypsum and mudstone (Fig. 11a).

Composed exclusively of $FA1_a$ (Fig. 7), this unit formed in a flood basin, dominated by terrigenous sedimentation, with periods of bottom exposure and soil development. Common mottling suggests alternating arid periods, with the oxidation of iron minerals, and humid periods, causing reduction (and the green color) of the sediments. Gypsum layers are present in two intervals within this unit, hinting to sulphate precipitation in periods of high evaporation and reduction of terrigenous supply. This was possibly due to pulses of aridity and/or tectonic subsidence, determining high accommodation in the basin and sediment starving. The gypsum was possibly sourced by dissolution of the underlying gypsum at the top of the Lower Jurassic marine transitional succession. This is also supported by the common occurrence of satin-spar gypsum veins in the background mudstone. At the top, a deep paleosol, characterized by intense mottling and caliche nodules, testifies to a long period of decreased sediment supply and subaerial exposure.

This unit shows significant lithological similarities with the Azrif Formation of the Jbel Igoudlane syncline (Jenny et al., 1981), located 30 km to the north-northwest of the study area, on the northern front of the Central High Atlas (Fig. 9c). The Azrif Formation is referred to as the continental equivalent of the Bajocian carbonate platforms, outcropping more to the east (Jenny et al., 1981; Frizon de Lamotte et al., 2000, 2008, 2009).

4.2.2 UMc2

This unit, up to 100 m thick, rests above a high relief erosional surface, deep up to 20 m, on the previous unit, outlining an ENE-WSW trending paleo-valley, visible in the Ouwawriykt river valley.

This unit is composed of FA2, FA3, FA4 and FA7 (Fig. 7), stacked in three fining and thinning upward sequences (Figs. 11b, 12). At the top of each sequence, intense mottling and caliche nodules mark pedogenic modifications, recording periods of subaerial exposure.

The first sequence is composed by FA7 passing laterally to FA2, indicating multistore channels and the related floodplain. The second sequence results from the alternation of FA2 and FA3, representing wide channels and their overbank deposits. The third sequence is mainly composed by FA4 passing vertically to FA2 recording the progressive switching off of a poorly-confined fluvial system.

The clast composition (observed in conglomerate facies) shows significant variations in this unit. Carbonate and dolomite clasts, derived from the Lower Jurassic units, are abundant in the first sequence and become rare at the top of the unit. Here, red sandstones and basalt clasts from Triassic deposits and metamorphic clasts from Paleozoic basement are dominant (Fig. 12).

This unit shows lithological similarities with the Guettioua Formation, that represents the first fluvial system of the *Couches Rouges* and includes carbonate clasts derived from the denudation of Lower and Middle Jurassic marine limestones (Jenny et al., 1981). In this area, an equivalent of the Iouaridène lacustrine formation has not been found, but it cannot be excluded that a fluvial equivalent could be represented by the upper part of UMc2 (Fig. 8).

4.2.3 UMc3

UMc3 is up to 300 m thick and it has an angular unconformity on UMc1 and UMc2 (Fig. 11c, d). In the southeastern part of the area it directly overlies the Lower Jurassic marine-transitional succession (Fig. 10). It is exposed all over the study area, forming the top of the topographic highs in the southeastern and western sectors of the syncline.

The unit consists of FA2, FA3 and FA4 (Fig. 7) and is subdivided into three (UMc3a-c) fining upward sequences (Fig. 12).

$UMc3_a$ is made of FA4, outlining wide paleochannels filled by very coarse conglomerates (up to 40-50 cm diameter in the southernmost part of the area). FA4 passes upwards to FA2 that outlines the progressive switching off of the channels and the predominance of unconfined flows to the top. $UMc3_b$ consists of FA3 stacked in thick amalgamated sand bodies, alternated to FA2, testifying the reactivation of fluvial sedimentation in an alluvial plain dominated by poorly-confined flows. To the top, FA2 dominates hinting to frequent avulsion processes.

$UMc3_c$ is composed by an alternation of FA2, FA3 and FA4, testifying the migration of broad and shallow channels in an alluvial plain.

The clast composition of the conglomerates of this unit shows the gradual decrease of the Lower Jurassic carbonate and dolomite clasts (still present in the first sequence) and the concurrent increase of clasts from the Triassic basalts, the Triassic red sandstones, and Paleozoic basement (Fig. 12).

This unit is referred to as the local equivalent of the Jbel Sidal Formation, the second fluvial unit of the *Couches Rouges* (Andreu et al., 2003; Mojon et al., 2009) (Fig. 8).

4.2.4 UMc4

This unit is 50 m thick and crops out at the top of the Adrar Aglagal relief, resting on UMc3 with an erosional surface, and outlining 10 meters deep, E-W trending, paleo-valley.

This unit is formed by the vertical stacking of FA4 (Fig. 7), recording the infill of the paleo-valley by poorly-confined gravel-rich flows (Fig. 12). This unit represents the reactivation of fluvial-alluvial deposition, starting with the incision of a paleo-valley and successive infill by coarse sediments, indicating the proximality of the source of sediment supply.

The clast composition shows the dominance of Paleozoic and Triassic clasts, whilst the Jurassic carbonates are missing (Fig. 12).

This unit, for its stratigraphic position and its sedimentological features, could be a local equivalent of the Albian-Cenomanian Ifezouane Formation (Fig. 8).

4.2.5 UMc5

UMc5 is 35 m thick being the topmost deposit of the studied succession exposed at the summit of the Adrar Aglagal and erosively overlying UMc4 (Fig. 11e).

This unit is composed by FA5 and FA2 (Fig. 7), the latter one dominating at the top. This unit testifies for the development of fluvial systems characterized by wide and poorly-confined paleochannels, filled by sandy deposits, passing upwards to a muddy alluvial plain.

This unit is tentatively referred to the Cenomanian (cf., Termier, 1941; Choubert, 1959), representing a possible equivalent of the Aoufous Formation, farther to the east recording the fining of a sedimentary complex characterized at the base by the fluvial sandstones of the Ifezouane Formation (Cavin et al., 2010) (Fig. 8).

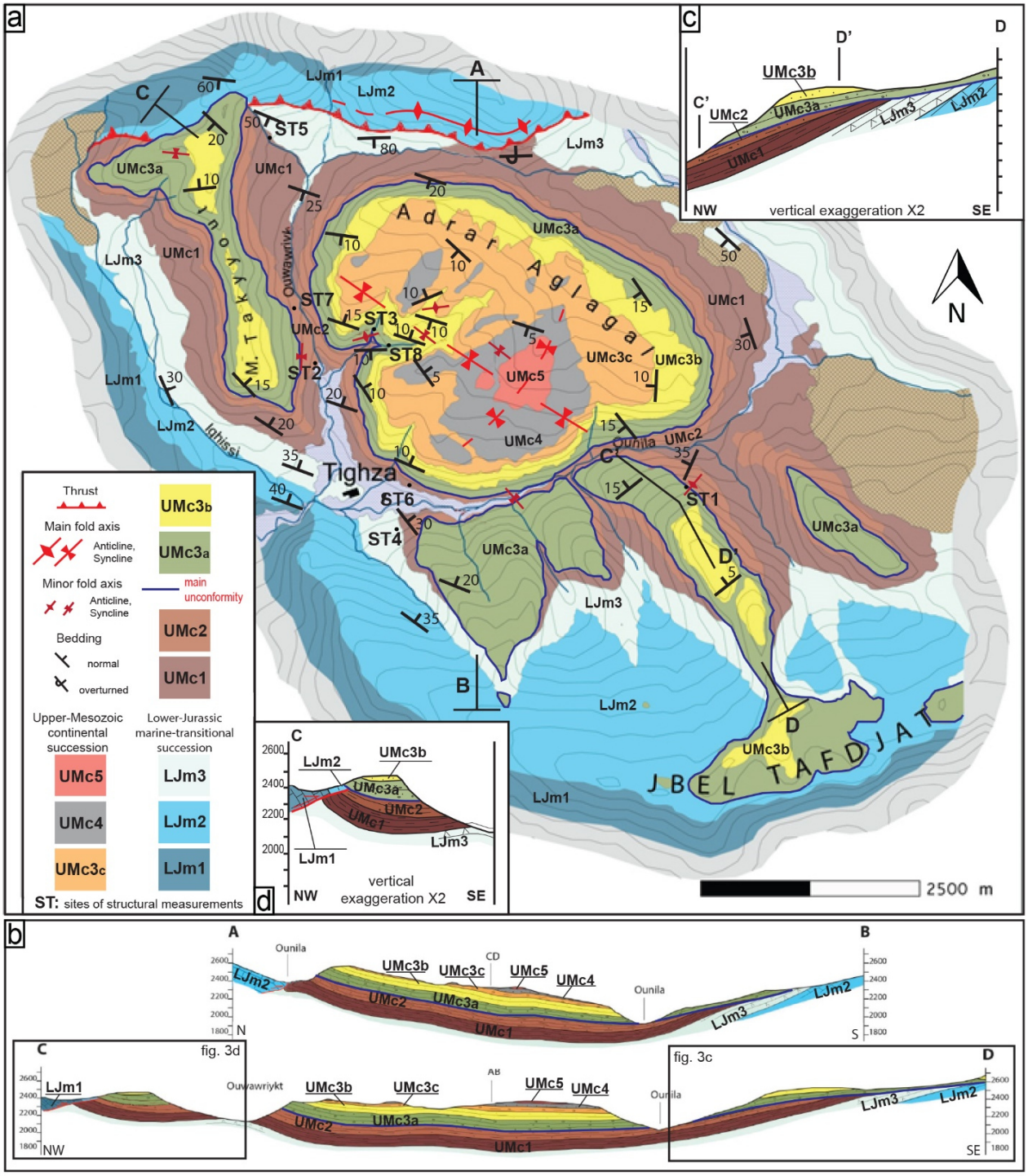

Fig. 10: a) Geological map of the Adrar Aglagal syncline b) Geological cross-sections (AB and CD) c) Detail of the southeastern part of the CD geological section, showing the progressive unconformities affecting the studied successions and the basal angular unconformity of UMc3 (vertical exaggeration X2) d) Detail of the northwestern part of the CD geological section, showing the sealing of the thrust (vertical exaggeration X2).

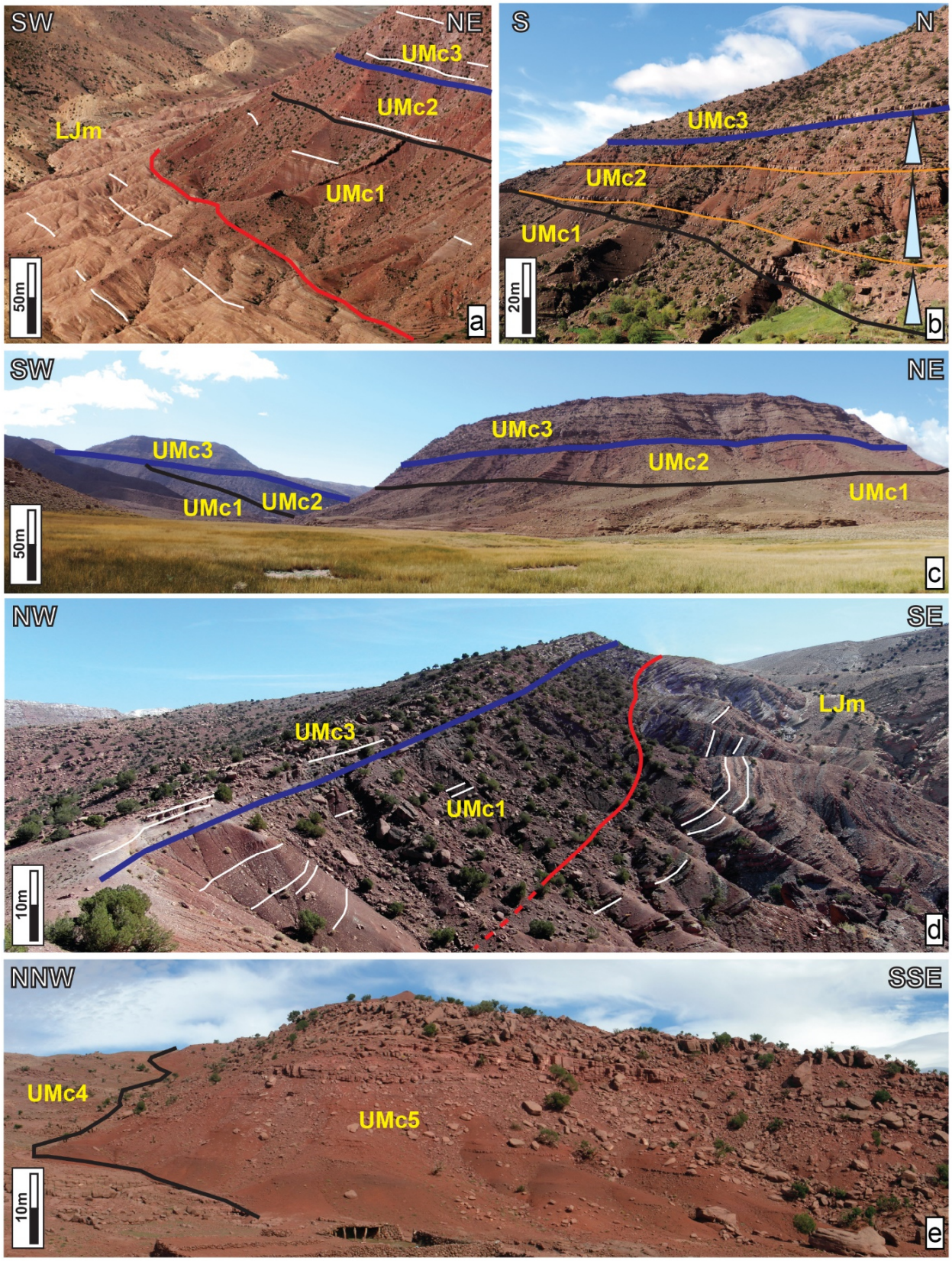
SW
NE
UMc3
UMc2
LJm
UMc1
50m
a
S
N
UMc3
UMc2
UMc1
20m
b
SW
NE
UMc3
UMc3
UMc2
UMc1
UMc2
UMc1
50m
c
NW
SE
LJm
UMc3
UMc1
10m
d
NNW
SSE
UMc4
UMc5
10m
e

Fig. 11 a) Panoramic view of the syntectonic progressive unconformities between the upper part of the Lower Jurassic marine-transitional succession, UMc1 and UMc2. The blue line outlines the unconformity at the base of UMc3; the white lines identify the bedding attitude b) Panoramic view of the low-relief erosional surface at the base of UMc2 (black line) and its internal subdivision (orange lines) in three FU sequences (light blue triangle). The blue line represents the unconformity at the base of UMc3 c) The northern limb of the Adrar Aglagal syncline, showing on the left UMc3 unconformably on UMc1 and UMc2 (blue line) d) Panoramic view of the southern portion of the studied area, showing the main unconformity (blue line) between UMc3 and the underlying units. The white lines identify the bedding attitude e) View of the top of the Adrar Aglagal mountain showing UMc5 over UMc4.

4.3 Paleocurrent analysis

The axes of the paleochannels, together with the paleoflow directions measured in the in-channel deposits of unit UMc2, point to an ENE direction in the first sequence, gradually passing to a NNE directed paleo-drainage towards the third sequence (Fig.12). This feature hints to a quite well confined fluvial system that during this stage flowed to depocentres located northward.

Unit UMc3 shows a variation throughout its stratigraphic architecture. In the first sequence the paleochannel orientation and the paleoflow indicators, together with the grain-size fining from south to north, testify to a still persistent NNE flow direction. In the second and third sequences, although the paleochannels develop in a north-south direction, the paleocurrent pattern is more dispersed with paleoflow directions towards the north, and some towards west and southwest (Fig. 12), hinting to a less confined fluvial system.

Unit UMc4 records a return to more confined fluvial transport as indicated by a persistent WNW direction (Fig. 12) attested by the channel orientation and the paleoflow indicators.

Finally, unit UMc5 marks a return to a predominant NNE-SSW direction of the paleochannels apparently not confirmed by paleocurrents measured on the in-channel structures, pointing to a westward flow direction (Fig. 12). In this case the discrepancy of the paleocurrent indicators may indicate dispersion within broad channels by bedforms migrating diagonally in respect with the predominant channel orientation.

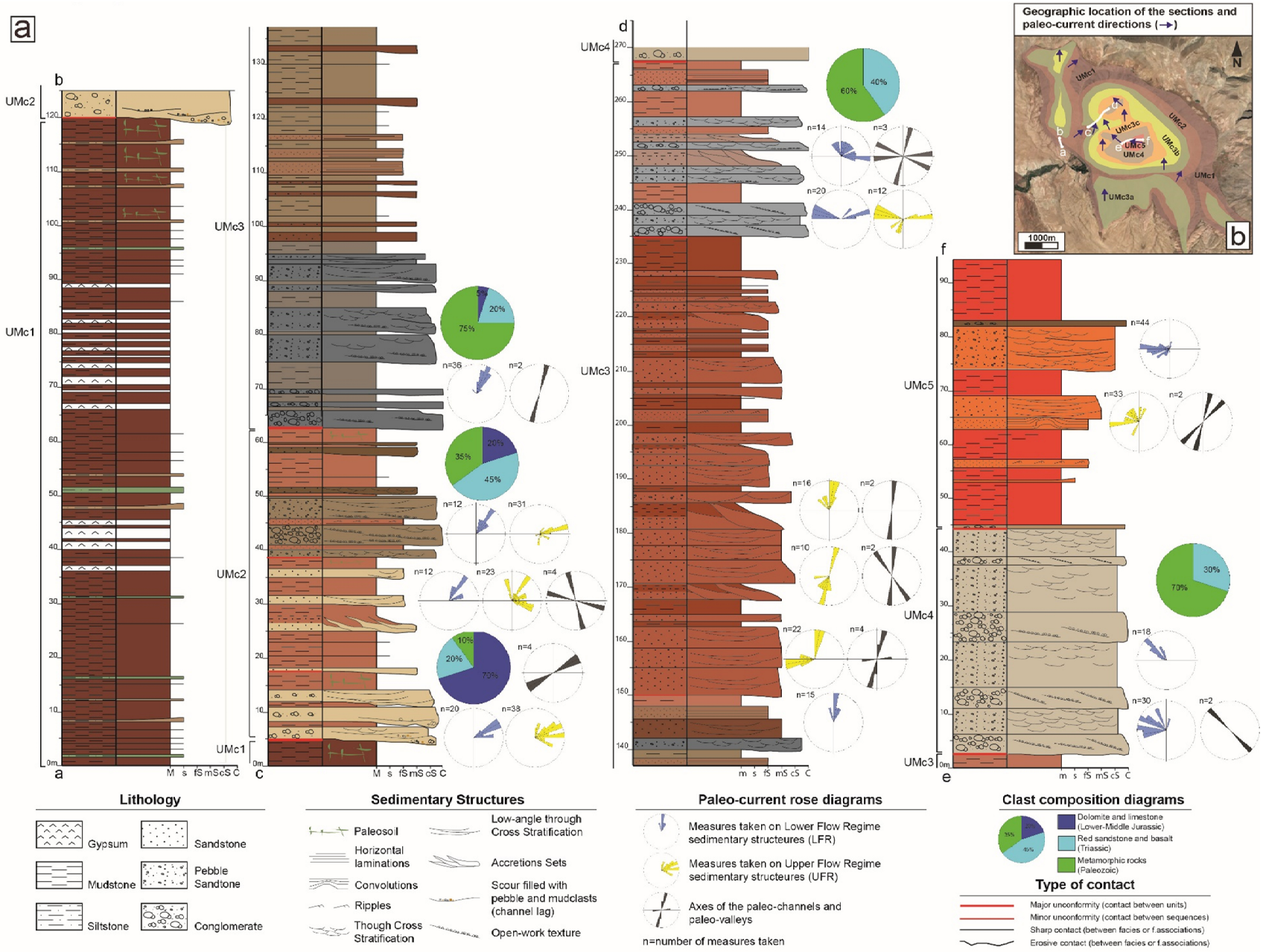
a
b
UMc2
UMc1
UMc3
UMc2
UMc1
a
c
d
UMc4
UMc3
e
f
UMc5
UMc4
UMc3
Geographic location of the sections and paleo-current directions (→)
N
UMc1
UMc3c
UMc2
UMc3b
UMc5
UMc4
UMc1
UMc3a
1000m
b
Lithology
Gypsum
Sandstone
Mudstone
Pebble Sandstone
Siltstone
Conglomerate
Sedimentary Structures
Paleosoil
Horizontal laminations
Convolutions
Ripples
Though Cross Stratification
Low-angle through Cross Stratification
Accretions Sets
Scour filled with pebble and mudclasts (channel lag)
Open-work texture
Paleo-current rose diagrams
Measures taken on Lower Flow Regime sedimentary structeures (LFR)
Measures taken on Upper Flow Regime sedimentary structeures (UFR)
Axes of the paleo-channels and paleo-valleys
n=number of measures taken
Clast composition diagrams
Dolomite and limestone (Lower-Middle Jurassic)
Red sandstone and basalt (Triassic)
Metamorphic rocks (Paleozoic)
Type of contact
Major unconformity (contact between units)
Minor unconformity (contact between sequences)
Sharp contact (between facies or f.associations)
Erosive contact (between facies or f.associations)

Fig. 12. a) Stratigraphic sections of the Upper Mesozoic continental succession in the Adrar Aglagal Syncline. Rose diagrams represent the paleo-currents taken from: 1) lower flow regime (LFR) sedimentary structures (in blue), 2) critical to transcritical or upper flow regime (UFR) sedimentary structures (in yellow), 3) axes of paleochannels and paleovalleys. Compositional diagrams show the variations of sediment source in the development of the succession. b) Location of the stratigraphic sections (a-b, c-d and e-f) and the average trend of the measured paleocurrents (modified from Google Earth).

4.4 Structural features

The syncline is an open double-plunging fold, whose flanks show syntectonic progressive unconformities outlined by the wedging of strata of the LJm2-3, UMc1 and UMc2 with dips decreasing from the oldest to the youngest unit towards the core of the syncline (Figs. 10, 11a, d). This architecture is sealed by the angular unconformity at the base of UMc3 (Figs. 10, 11a, c, d), well exposed in the northwestern and southeastern portion of the studied area, where UMc3 lies on all the previous units (Figs. 10, 11c, d). A progressive synsedimentary deformation thus happened before deposition of UMc3 and was possibly tied to a folding of the syncline along a NE-SW axis. In the SE-NW direction syntectonic progressive unconformities develop until UMc4, that forms a large fold with a NW-SE axis at the core of the syncline (Fig. 10).

The northern limb of the syncline is affected by a SSE-verging thrust, compatible with a σ_1 oriented NNW-SSE. This structure brings a thrust anticline made of Jurassic carbonates (LJm1 and LJm2) directly over LJm3 and UMc1. LJm3 evaporites are intensely deformed by folds and reverse faults, and UMc1 presents sub-vertical to overturned beds (Figs. 10, 13c, 14c). To the west, the thrust is sealed by UMc3 (Figs. 10a, b, d; 13a, b, d), testifying that it was active before its deposition. Just south of the thrust, UMc3a deposits are affected by open WSW-ENE-trending folds, that point to a reactivation of the NNW-SSE shortening direction, though the thrust remained blind (Figs. 10, 13).

Open symmetric folds, observed at the cartographic scale, affect the studied succession and the intervening unconformities (Fig. 10, map and cross-sections). The collected data have been reported in stereographic projections, subdivided according to the affected unit (Fig. 14a). They identify two main axes (NE-SW and NW-SE, hinting to σ_1 directed NW-SE and NE-SW respectively), recurrent in the whole succession up to UMc3, and sub-parallel to the major axes

of the syncline. Folds with NW-SE axis affect the uppermost unit, Umc4, in the core of the syncline (Figs. 10a, 14a), testifying the activity of the NE-SW shortening direction. The NE-SW σ_1 also led to the slight refolding of the previous axis of the syncline (Fig. 10a).

Some mesoscopic folds and faults also affect the succession. Mesoscopic folds have been detected at three sites of measurements (Fig. 10a). At Site 1 folds with axes oriented NE-SW and a vergence to the NW, affect UMc2 and UMc3 and the intervening unconformity (Fig. 14a, b). At Site 2, minor open symmetric folds with axes oriented N-S affect UMc2 (Fig. 14a). At Site 3, UMc3 is slightly deformed, by open symmetric folds with axes oriented ENE-WSW (Fig. 14a). The lower part of the studied succession, up to the first sequence of UMc3, is also affected by mesoscopic reverse faults, some of which showing evidence of synsedimentary deformation. This evidence consists of faults whose throws tend to reduce or disappear upsection, or, in other cases, faults are sealed by overlying sediments. At site 8, ENE-WSW-trending reverse faults in UMc3a dislocate alternated fine sandstone-mudstone levels by 20 cm. Towards the top the dislocation tends to reduce and is sealed by the overlying deposits (Fig. 14d). Structural data on mesoscopic faults have been collected at 5 sites of measurements (Sites 4-8, Fig. 10a) and reported on stereographic projections (Fig. 14a). Kinematic indicators consist of frictional-wear striae created during the differential sliding between fault blocks along the fault zone. No clear indication of synsedimentary striation was found. Fault slip data that allowed calculating the paleo-stress direction are present only at sites 7 and 8. In the other cases we have considered the detected faults as pure reverse faults to approximate the paleo-stress. The data collected at the mesoscopic scale evidence two main stresses, oriented NW-SE and NE-SW (Fig. 14a), responsible for the observed structures and the main folds of the syncline basin.

The presence of macro and mesostrucures, namely the about E-W fold south of the main thrust, the N-W verging folds at site 1, and the buried fault at site 8 (Figs. 10a, 14b,d), at the base of UMc3, whose axis is compatible with a NW-SE shortening direction, could be explained in a context of continuous synsedimentary tectonic activity. The deformation was not entire at the time of deposition of UMc3, but it still affected the sedimentary processes during the deposition of the basal portion of this unit.

The time of activation of the NE-SW oriented σ_1 is debatable, but the bedding attitude of units UMc1-UMc4 in the E-W direction and the large fold with NW-SE axis affecting UMc4 at the core of the syncline point to activity during its deposition.

We also notice that the oldest unit (UMc1) has suffered the strongest deformation, being affected by folds and faults pointing to both main paleo-stresses. A certain amount of this deformation could be due to decollement by the weak gypsum layers of LJm3. Nevertheless, strongly deformed gypsum levels are confined to this unit only in correspondence to the thrust affecting the syncline to the north (Fig. 9a, c). In the other areas of outcrop, deformation of LJm3 deposits is framed in a coherent pattern with the lower and upper units, where we did not observe any flow or decollement structure.

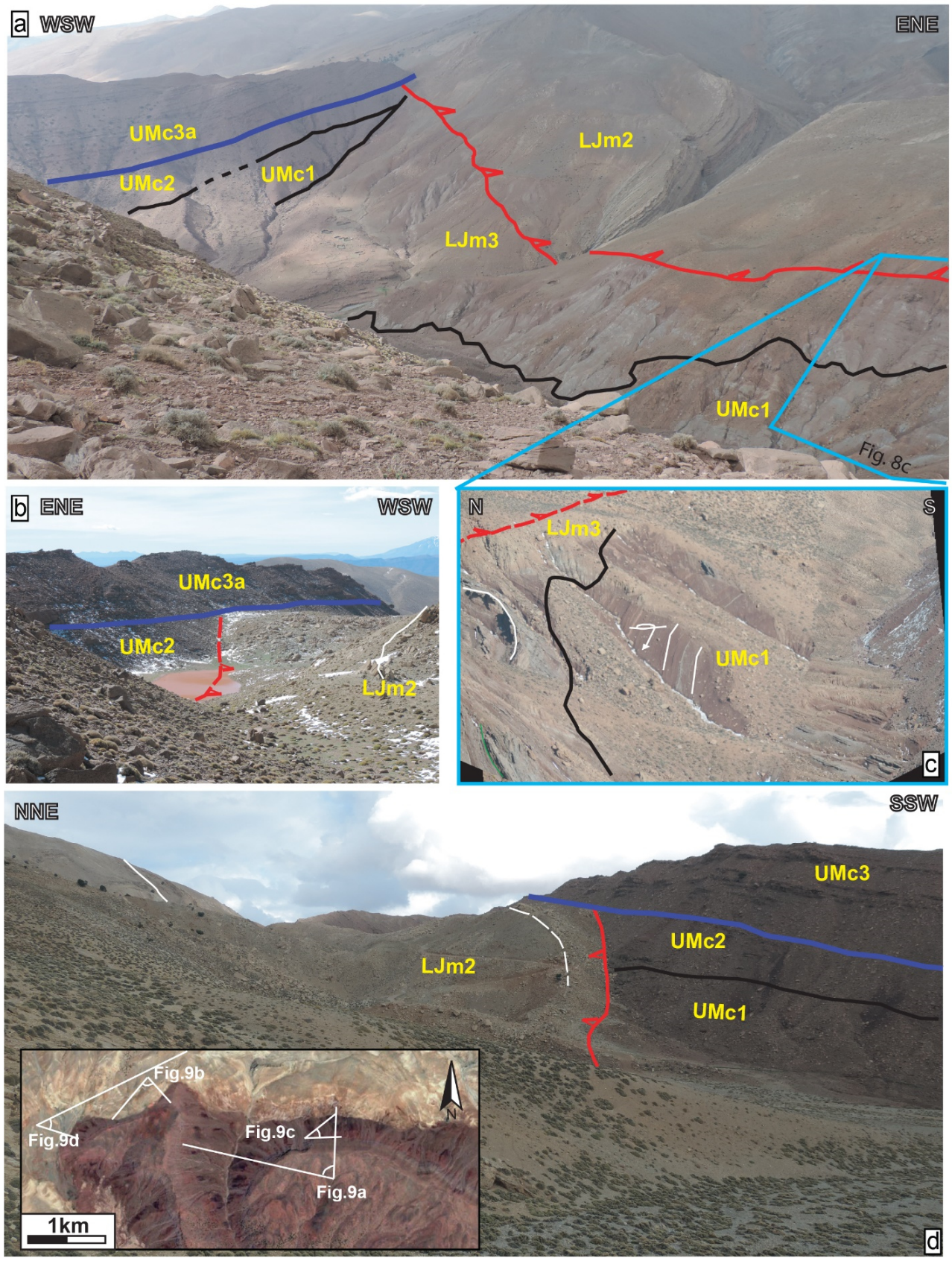
a WSW
ENE
UMc3a
UMc2
UMc1
LJm2
LJm3
UMc1
Fig. 8c
b ENE
WSW
UMc3a
UMc2
LJm2
N
S
LJm3
UMc1
c
NNE
SSW
UMc3
UMc2
LJm2
UMc1
Fig.9b
Fig.9d
Fig.9c
Fig.9a
N
1km
d

Fig. 13: Panoramic views of the northwestern part of the studied area, showing the thrust affecting LJm2-UMc2 units, sealed by UMc3. a) View of the thrust from the east (31°19'43" N, 7°06'43" W). b) View from north (31°20'39'' N, 7°08'30'' W) of the western sector of the thrust. c) detail of Fig. 9a showing the folded and steepened bedding of LJm3 and overturned bedding of UMc1 (31°20'07'' N, 7°07'01'' W). d) View from west (31°20'15'' N, 7°09'36'' W) of the western part of the thrust. e) Geographic location of the panoramic views (modified from Google Earth). Black lines: stratigraphic contacts; Blue line: main unconformity at the base of UMc3; Red line: thrust (triangles on the hangingwall); white lines: bedding.

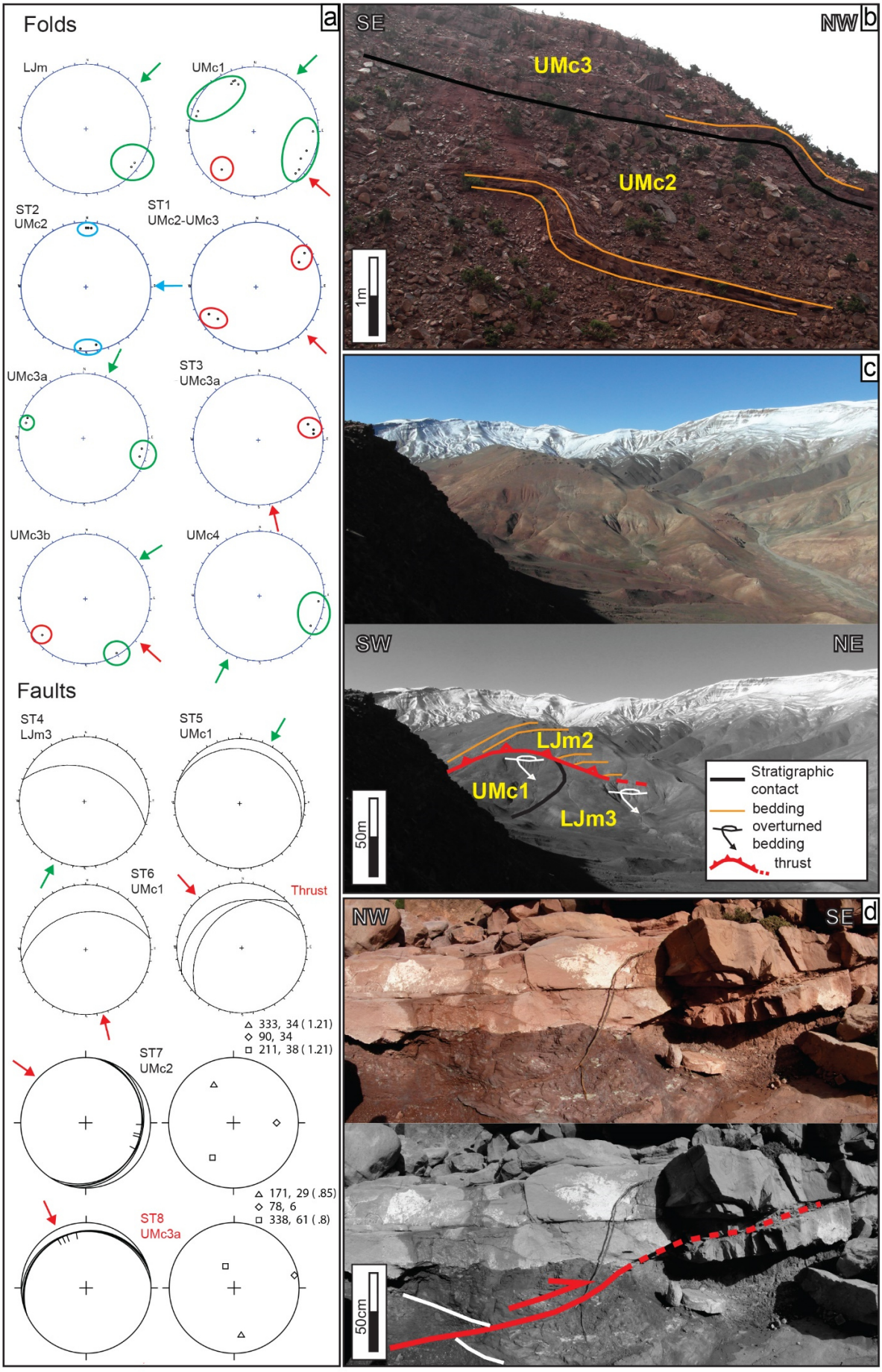
Folds
a
LJm
UMc1
ST2
UMc2
ST1
UMc2-UMc3
UMc3a
ST3
UMc3a
UMc3b
UMc4
Faults
ST4
LJm3
ST5
UMc1
ST6
UMc1
Thrust
△ 333, 34 (1.21)
◇ 90, 34
□ 211, 38 (1.21)
ST7
UMc2
△ 171, 29 (.85)
◇ 78, 6
□ 338, 61 (.8)
ST8
UMc3a
SE
NW
b
UMc3
UMc2
1m
c
SW
NE
LJm2
UMc1
LJm3
50m
Stratigraphic contact
bedding
overturned bedding
thrust
NW
SE
d
50cm

Fig. 14: a) Stereographic projections (lower hemisphere, Schmidt net) reporting the axis of megascopic folds on LJm, UMc1, UMc3 and UMc4, the axis orientation of the mesoscopic folds and the fault planes taken at sites 1 to 8 (location in Fig. 10a). The arrows indicate the paleo-stresses that caused the deformations: same colors are used for similar stress orientations. In red the sites in which sealed structures have been detected. Points indicate orientation of fold axes; ciclographic lines indicate fault planes (small lines indicate the pitch measured on the fault plane); triangle, diamond and square respectively indicate the orientation of σ_1, σ_2 and σ_3 calculated through the inversion method of Angelier and Mechler (1977). b) Mesoscopic fold affecting UMc2, UMc3 and the intervening unconformity at site ST1 (black line). c) Panoramic view of the northern part of the study area, the CHA axial zone in the background, annotated for the thrust bringing LJm2 over the younger units. d) Mesoscopic reverse fault affecting the upper part of UMc3a at site ST8. The throw along the fault diminishes toward the top, where younger beds seal the fault. (Thick orange line: stratigraphic contact; thin orange lines: bedding; red line: reverse fault; red arrow indicates movement of the hangingwall).

4.5 Discussion

The presented data suggests a syn-depositional development of the syncline hinting to active tectonics during the late Mesozoic. The following points illustrate the lines of evidence for a discussion on this aspect.

4.5.1 The paleocurrent pattern

The fluvial systems succeeded in the development of the succession record an overall paleo-drainage sourcing from the southern and attracted to the northern quadrants (Figs. 12b, 15). A correlation between the successive paleovalley axes and the syncline trends, suggests a tectonic control on the fluvial orientation and sediment dispersion, in the lower part of the succession, also supported by structural data. The dispersion of paleocurrent directions indicative of the variable confinement of the system, represents a further datum for assessing the changing rates of the syndepositional deformation.

In this perspective:

a) During the deposition of UMc2 the paleo-drainage is parallel to the NE-SW trending syncline axis hinting to a paleo-valley funneled along the structural trend. In this stage a NW-

SE σ_1 affected the area controlling the fold growth and consequently the fluvial valley orientation and its filling.

b) The following UMc3 initially records a paleodrainage still confined, directed to the NNE ($UMc3_a$) and positively associated to a low dispersion of the paleocurrent pattern suggesting that the NW-SE σ_1 was still active. The paleo-current pattern in $UMc3_{b-c}$ characterized by high dispersion, is referred to an acme of the tectonic subsidence that favored a fining of the sediment supply and the final filling of the paleo-valley.

c) In the upper part of the succession, a confined river in a NW-SE trending valley (UMc4) that evolves in less confined systems (UMc5) suggests a dynamic similar to the one described for UMc3. The NW-SE trend of the UMc4 valley fits exactly with the second axis of the syncline, supporting the hypothesis of a NE-SW σ_1 active during this stage. Deformation may have reached its maximum intensity with the deposition of UMc5, characterized by high dispersion rate in the paleocurrent pattern together with the absence of well-developed fluvial incisions

4.5.2 The composition of sediment supply

The clast composition of the conglomerates shows the progressive decrease of carbonate clasts coming from the Lower and Middle Jurassic formations and the concurrent increase of clasts deriving from the Triassic and Paleozoic successions (Figs. 12, 15a). Such a clast-compositional trend, firstly, points to exposure of the Lower and Middle Jurassic carbonates since the deposition of UMc2 and, secondly, indicates that progressively deeper crustal levels were eroded within an ongoing crustal uplift as coherently supported by the structural and paleo-drainage data. During the development of UMc2, such an actively uplifting sediment source may be identified in the Marrakech High Atlas, considered to have been uplifted and exposed in several inversion phases, starting from the Middle/Late Jurassic (Leprêtre et al., 2018, and references therein). This would also fit to a more north-northwestern location of the studied area, since the Adrar Aglagal syncline is part of the Mesozoic inlier detached to the south (Jenny et al., 1981; Saadi et al., 1985) and overthrust onto the Subatlas zone and the Ouarzazate Basin during the Cenozoic compressional phases tied to Africa-Europe convergence (e.g., Frizon de Lamotte et al., 2008).

4.5.3 Tectono-stratigraphic evolution of the Adrar Aglagal Syncline

The presented data allow to reconstruct a tectono-stratigraphic evolution of the succession summarized in three main stages (Fig. 15b):

1) The first stage (Bathonian to Hauterivian?) includes the tectono-depositional events that resulted in the deposition of UMc1 and UMc2, controlled by crustal shortening along a σ_1 oriented NW-SE. The deposition of UMc1 attests to the progressive development of a continental basin anticipated by the restricted setting recorded by the underlying LJm3 evaporite-bearing unit. The mud-dominated deposition of UMc1 suggests high rates of tectonic subsidence culminating in folding of the related deposits. The successive deep incision of UMc1 in a period of reduced tectonic activity led to the formation of a NE-SW trending paleo-valley filled with the UMc2 deposits under renewed growth of the syncline. NW-SE σ_1, at the end of deposition of UMc2, culminated with activation of the thrust in the northwestern sector of the area, that led to overlap of the LJm succession over UMc1 and UMc2. The erosional truncation of the uplifted and inclined UMc2 strata indicates tectonic quiescence before deposition of the overlying UMc3.

2) The second stage (Barremian), includes the tectono-depositional events recorded in unit UMc3. After valley incision within UMc2 deposits, the early confined filling represented by $UMc3_a$ is referred to renewed shortening with σ_1 oriented NW-SE that continued to be active until the deposition of the fan-related $UMc3_{b-c}$ units. The following tectonic quiescence allowed the renewed fluvial incision of this unit before deposition of UMc4.

3) The third stage (Albian-Cenomanian), resulted in deposition of UMc4 and UMc5, controlled by crustal shortening where σ_1 rotated to a NE-SW direction. Similar to previous stages, UMc4 filled a relatively confined paleovalley parallel to the rotated axis of the syncline being replaced by fan deposits of UMc5.

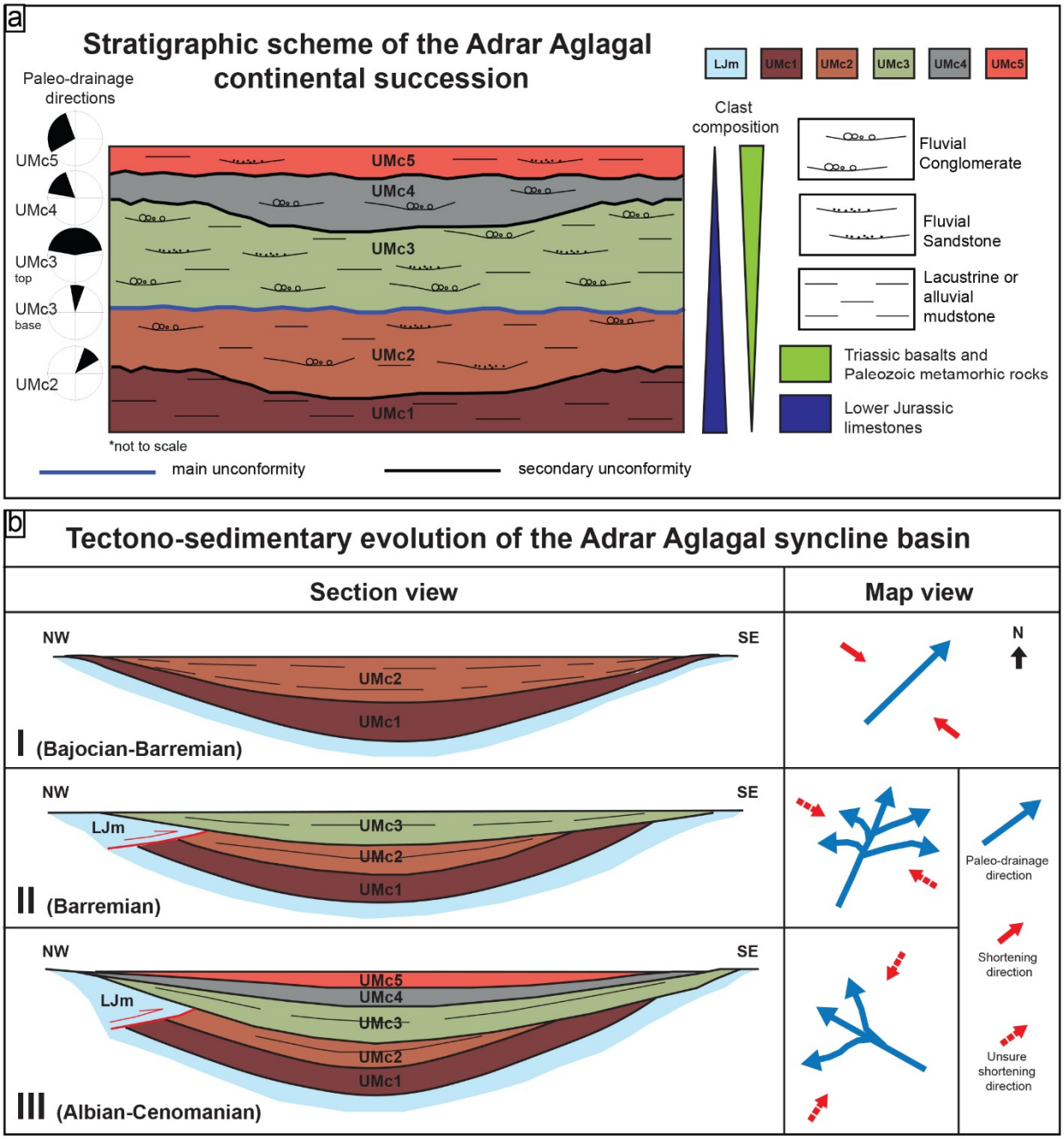

Fig.15: a) Stratigraphic scheme of the Adrar Aglagal continental succession: the paleo-drainage and clast composition variation from the base to the top of the succession is shown b) Tectono-sedimentary model of the Adrar Aglagal syncline basin showing the section view and the planview of the syncline during three evolution stages. The red arrows indicate the main active stress (continuous line = certain data; dashed line = uncertain data), the blue arrows indicate the main axes of the paleo-drainage.

4.5.4 Regional implications

The tectono-stratigraphic evolution reconstructed in the study area bears a significance beyond the case of localized relief uplift and denudation. It extends to a portion of the Central High Atlas axial zone the evidence of crustal uplift active during the late Mesozoic recognized in earlier studies (Choubert and Faure-Muret, 1960-1962; Mattauer et al., 1977; Studer and du Dresnay, 1980; Laville, 1988, 2002; Laville and Piqué, 1992) and being presently reconsidered across the Moroccan Atlasic domain (Gouiza, 2011; Bertotti and Gouiza, 2012; Saura et al., 2014; Benvenuti et al., 2017; Vergés et al., 2017; Fekkak et al., 2018; Moratti et al., 2018). The Moroccan Atlas system thus resulted from both Mesozoic (pre-collisional) and Cenozoic (collisional) stages of mountain building. The Mesozoic geodynamic setting including the northern margin of the Africa plate, though not prone to orogenic processes, favored diffuse uplift associated with contractional structures. Such deformation was a consequence of the opening and successive spreading of the Central Atlantic and of the NW Tethys oceans following continental rifting of Pangea, with convergent intraplate stresses propagation in the intervening African margin (Benvenuti et al., 2017; Moratti et al., 2018). This caused incipient inversion of the rifting structures, relief formation and development of a dynamic regional drainage pattern during the late Mesozoic. Renewed tectonic inversion induced by the Africa-Europa plates collision during the Cenozoic was superimposed on the previously formed structural setting.

5. The Guettioua and Jbel Sidal Synthems in the Central High Atlas: stratigraphy and paleodrainage analysis

The following is a regional synthesis along a W-E transect, at the CHA northern and southern front respectively, of the stratigraphic and sedimentological features of the Guettioua and Jbel Sidal Formations, beeing the lower and the upper fluvial units of the *Couches Rouges.* The two formations have been redefined as synthemes through the recognition of Unconformity Bounded Stratigraphic Units (UBSU, Salvador 1994).

The stratigraphic sections, the paleocurrent measurements and the revised geological maps have been reported in panels 1, 2, 3 and 4 (in attachment). The stratigraphic and sedimentological features have been sythetized in Tables 6 and 7.

5.1 The Guettioua Synthem

5.1.1 The lower boundary

In the High Atlas of Marrakech region and from north to south, this synthem rests angularly over different units. In the Ait Ourir synclines, it overlies Lower Jurassic limestone, mudstones and gypsum (LJm), referred to a supra-tidal to intertidal coastal paleo-environment (Ferrandini et al., 1982; Bah, 1993; Hadach et al., 2015). In the Igoudlane syncline it rests unconformably on a succession including Lower Jurassic marine and lacustrine limestone, marl, gypsum, siltstone (Sinemurian Aït Ras and Imi-n-Ifri Fs, Pliensbachian – Toarcian Aït Chitachen F.) and Middle Jurassic coastal mudstone, siltstone and, subordinate, sandstone (Bajocian Azrif F; Fig. 16a; Jenny et al., 1981; Saadi et al., 1985). In the Adrar Aglagal syncline it rests unconformably over a Lower Jurassic succession (LJm) composed by limestone, marl and gypsum, also ending with the Bajocian Azrif Formation (Jenny et al., 1981; Courtinat and Algouti, 1985; Cavallina et al., 2018).

In the western sector of the Atlas of Beni Mellal this synthem is reported to be over the Bajocian marine limestones. In the Ouaouizaght syncline it rests on the marine-transitional mudstones, dolomites and sandstones of the lower Bathonian Tilougguit Formation (Bourcart et al., 1942;Sohuel, 1996; Haddoumi, 2010) recording coastal intertidal and subtidal paleo-environments (Jenny et al., 1981). In the High Atlas of Beni Mellal region from west to east this synthem is unconformably over Lower-Middle (Bajocian) Jurassic marine carbonates of

the Bin El Ouidane-Tanant formations (Jenny et al., 1981; Monbaron, 1982; Jenny, 1985, 1988) in the Iouaridène syncline, and apparently also in the Ait Attab and Guettioua synclines, as reported in previous studies (Saadi et al., 1985). The revision done in this study suggests that in these two synclines the synthem is erosively over the Lower Bathonian Tilougguit Formation made of lacustrine-coastal mudstone, sandstone and limestone (Souhel, 1987; Fig. 16b). Also in the Ouaouizaght syncline and in the eastern sector of the High Atlas of Beni Mellal (Tilougguit, Tagleft, Tizi'n'Isly, Naour and Imilchil synclines) the Tilougguit Formation represents the base over which the Guettioua synthem deposited (Saadi et al., 1985; Zouibaa et al., 2003).

Along the southern front of the CHA, from west to east, the Guettioua synthem is directly or partially over the Tilogguite-equivalent deposits basing on the following considerations. In the structurally complex Tondout area, a revision (Benvenuti, 2010, Panel 4) of the Mesozoic successions ascribed to the Triassic-Early Jurassic in previous studies (Allain et al., 2008) suggests that the Guettioua-equivalent deposits rest over an alternance of limestone, mudstone and sandstone lithologically equivalent to the Tilougguit Formation. In the Dades River valley a similar revision (Benvenuti et al., 2017; Moratti et al., 2018) of a continental succession ascribed to the Late Cretaceous (Hyndermayer et al., 1977) indicated that Guettioua-equivalent deposits rest partially over uppermost Lower Jurassic coastal limestone and mudstone (Toarcian-Aalenian Tafraout Formation) and over a Tilougguit-equivalent succession. Farther to the east, in the wide Goulmima anticline, the synthem again overlies a lateral equivalent of the Tilougguit F (Oued Ziz Formation; Hadri, 2001).

5.1.2 The upper boundary

Along the same geographic gradient, the Guettioua synthem is angularly overlain by the ?Upper Jurassic-Lower Cretaceous lacustrine Iouaridène Formation in the Ait Ourir, Igoudlane, Iouaridène, Guettioua, Ait Attab and Ouaouizaght synclines (Saadi et al., 1985; Andreu et al., 2003; Haddoumi et al., 2010). Elsewhere, the capping deposits are ascribed to different units. In the Adrar Aglagal (Cavallina et al., 2018) and Goulmima (Papini et al., in prep.) synclines the Guettioua synthem is overlain by fluvial deposits referred to as the Jbel Sidal Synthem. In the Tondoute area, Dades River valley and Tagleft syncline, the capping deposits are floodplain-lacustrine brownish mudstone possibly representing a local equivalent of the Iouaridène Formation (Benvenuti, 2010; Benvenuti et al., 2017; Moratti et al., 2018). In the

Tilougguit, Tizi'n'Isli, Imilchil and M'semrir synclines, capping deposits are missing due to erosion or non-deposition (Saadi et al., 1985; Milhi et al., 1993; Zouibaa et al., 2003), whereas, in the Naour syncline, the Guettioua synthem is overlain by the Aptian marine limestone of the Ait Tafelft Formation, attesting to a quite large hiatus (Zouibaa et al., 2003).

5.1.3 Stratigraphic and sedimentological features

In the High Atlas of Marrakech (Pan. 1), the Guettioua Synthem presents variable thick successions (from 10 to 110 m), showing an internal organization in three sequences. From north to south:

Ait Ourir.

10 to 50 m thick successions. The coarse facies show a polygenic composition with carbonate clasts coming from the Lower Jurassic limestones, basaltic and red sandstone clasts coming from the Triassic units.

- $G_{AO}1$: composed by floodplain facies associations (FA2). Mudstone dominated, with a coarse vs fine-grained ratio (C/F) around 25/75, the sandstone fraction is stacked in thin tabular to plane-concave beds.

- $G_{AO}2$: composed by broad multistory channels (FA5), amalgamated in beds up to 5 m, and, subordinate, FA2. The coarse portion is dominating (C/F ratio around 80/20).

- $G_{AO}3$: composed by broad sheets (FA3), amalgamated in beds up to 2-3 m, and floodplain (FA2) deposits in alternation (C/F ratio around 40/60).

This tripartition, showing a CU passing upward to a FU trend, has been observed only in the Adenndim syncline (pan.1a, section C_1-C_2), interpreted as the axial part of the system. The other observed areas (pan.1a, sections A_1-A_2 and B_1-B_2) show only $G_{AO}2$ and record only few meters of the entire succession.

Jbel Igoudlane.

110 m succession, showing a FU, passing upward to a CU trend (Pan.1b, section K_1-K_2). The coarse facies show a high percentage of carbonate clasts.

- $G_{JI}1$: composed by the alternation of floodplain (FA2) deposits and sandstone narrow sheets (FA4) in amalgamated beds up to 5-8 m. Mudstone is dominating over sandstone (C/F around 35/65).

- $G_{JI}2$: composed by the alternation of floodplain deposits (FA2) and broad sheets (FA3), the latter amalgamated in bed up to 5 m. C/F ratio around 50/50.

- $G_{JI}3$: composed by the alternation of floodplain (FA2) deposits and conglomerate narrow sheets (FA5), amalgamated in beds up to 3 m. C/F ratio still around 50/50.

Adrar Aglagal

40-60 m successions, showing a FU, passing upward to a CU trend (Pan.1c, sections M_1-M_2 and M_3-M_4). At the top of each sequence, intense mottling and caliche nodules mark pedogenic modifications, recording periods of bottom exposure. The coarse facies show a high percentage of carbonatic clasts at the base passing upward to a high percentage of Triassic and methamorphic clasts.

- $G_{AA}1$: composed by multistorey broad ribbons (FA7), up to 10-15 m, passing laterally to floodplain deposits (FA2). The C/F ratio is around 80/20 in the axial part (section M_1-M_2), laterally decreasing (50/50 in section M_3-M_4).

- $G_{AA}2$: composed by the alternation of floodplain deposits (FA2) and broad sheets (FA3), amalgamated in beds up to 3-5m. The C/F ratio is around 35/65.

- $G_{AA}3$: only preserved in the axial section (section M_1-M_2) is mainly composed by broad multistorey channels (FA5), up to 5 m, passing vertically to floodplain deposits (FA2). C/F ratio is around 65/35.

In the western sector of the High Atlas of Beni Mellal, the Synthem presents quite thick successions, with variable thickness (from a minimum of 70 m in the Ait Attab syncline to a maximum of 500 m in the Guettioua syncline). The successions show an internal tripartition in three FU sequences with an overall CU trend, except for the Ait Attab succession, where it shows a low thick succession with a FU trend (Pan. 2).

Iouaridène:

100 m succession, showing a CU trend (Pan. 2a, section O_1-O_2). The coarse facies show a high percentage of carbonatic clasts:

- G_I1: mudstone dominated (C/F ratio 75/25), composed by floodplain deposits (FA2), dominant at the base, in alternation with occasional broad sheets ($FA3_a$), up to 3-5 m, in the upper part.

- G_I2: is composed by the alternation of sandstone narrow sheets (FA4), amalgamated in beds up to 6-8 m, and floodplain deposits (FA2). It is coarse dominated (C/S ratio 65/35).

- G_I3: is composed by multistorey broad ribbons (FA7), up to 8-10 m, passing laterally to floodplain deposits (FA2). C/F ratio 80/20.

Guettioua:

500 m succession, showing a CU trend (Pan. 2b, section Q_1-Q_2). The coarse facies show a high percentage of carbonatic clasts:

- G_G1: is composed by floodplain deposits (FA2) with C/F ratio around 50/50. The sandstone are stacked in tabular beds, up to 5 m.

- G_G2 is composed by sandstone narrow sheets (FA4), in amalgamated beds up to 5 m dominating at the base, and isolated broad sheets ($FA3_b$) in alternation with floodplain facies (FA2) to the top.

- G_G3 is composed by low sinuosity broad ribbons (FA6), up to 10 m, grading upward to isolated broad sheets ($FA3_b$) and floodplain deposits (FA2) in alternance. The C/F ratio is around 50/50.

Ait Attab

The succession shows a variable thickness: 80 m at the northern flank, diminishing to the south until it completely disappears at the southern flank.

It is composed by the alternation of floodplain deposits (FA2) and broad sheets (FA3), amalgamated in beds up to 3-5 m, in a FU trend. It is mudstone dominated (C/F ratio 30/70) (Pan. 2c, section R_1-R_2).

Ouaouizaght:

The succession shows a variable thickness: up to 180 m on the western flank, its thickness diminishes to the east until it disappears completely.

It is composed by the alternation between floodplain (FA2) and broad sheets (FA3), in amalgamated beds up to 10-20 m at the top of the succession, showing a CU trend. C/F ratio around 50/50 (Pan. 2d).

In the eastern sector of the High Atlas of Beni Mellal, the Synthem presents thick successions, with constant thickness (150-200 m). The successions show an overall CU trend, subdivided in three FU sequences in the Tilougguit syncline (Pan. 3).

Tilougguit

150-200 m succession, showing an internal tripartition in three sequences, showing an overall CU trend (Pan. 3a, section U_1-U_2)

- G_T1: it is composed by terminal fan deposits ($FA1_a$) only, showing a FU trend. Mudstone dominated (C/F ratio around 15/85), the sandstone is stacked in dm-m tabular beds.

- G_T2: it is composed by terminal fan deposits ($FA1_b$) only, showing a FU trend. Mudstone dominated (C/F ratio around 20/80), the sandstones are stacked in very wide lenticular beds, isolated to amalgamated (at the base) up to 4-5 m thick.

- G_T3: it is composed by broad sheets (FA3), amalgamated in beds up to 6-8 m, and subordinate floodplain deposits (FA2). Sandstone dominated (C/F ratio around 60/40).

Tagleft

150 m thick succession, composed by terminal fan deposits ($FA1_a$ and $FA1_b$) at the base (C/F around 20/80) passing upward to broad sheets (FA3) and sandstone narrow sheets (FA4; Fig 15c), amalgamated in sandstone bodies up to 3-4 m, in alternation with floodplan deposits (FA2) (Pan. 3b).

Imilchil

200 m succession, mudstone dominated (C/F around 10/90), composed by terminal fan deposits (FA1) at the base, alternating to the top with floodplain deposits (FA2), with tabular sandstone

bodies up to 1-2 m thick and rare, small, paleo-channels filled with mudstone to fine sandstone (Fig. 16d; Pan. 3c).

Naour

Up to 150-200 m, mudstone dominated (C/F ratio around 20/80) succession, composed by terminal fan deposits (FA1), passing upward to, rare, sandstone narrow sheets (FA4), in amalgamated beds up to 5 m, alternating with floodplain deposits (FA2) (Pan. 3d).

Tizi'n'Isly

Mudstone dominated (C/F ratio around 10/90) succession, up to 150-200 m, composed by the alternation of terminal fan deposits (FA1) and floodplain deposits (FA2), with tabular sandstone bodies up to 1 m thick (Pan.3d).

In the southeastern front of the Central High Atlas, the Guettioua Synthem presents successions variable for thickness and stratigraphic features (Pan. 4)

M'semrir:

Up to 450-500 m succession, internally subdivided in 4 sequences, showing an overall CU trend (Pan. 4a, sections W_1-W_2 and W_3-W_4). The lithological composition of these deposits is carbonatic.

- G_M1 is composed by terminal fan deposits ($FA1_b$) only, mudstone dominated (C/F ratio 10/90), showing a CU trend.

- G_M2 is composed by broad sheets (FA3) at the base, stacked in beds up to 10m, passing upward to terminal fan deposits ($FA1_b$) showing a FU trend. It is mudstone dominated (C/F ratio around 30/70). In the southern section, the paleo-channels are filled by fine to medium sandstone or even mudstone (W_1-W_2), while in the northern section, in the channel fill, we have also found pebble sandstone to microconglomerate (W_3-W_4).

- G_M3 is composed of floodplain deposits (FA2) and broad sheets (FA3) in alternation, showing a FU trend, ending in the southern section with terminal fan deposits ($FA1_b$). It is mudstone dominated (C/F is around 30/70 in the southern section W_1-W_2 and 40/60 in the northern one W_3-W_4).

- G_M4 outcrops only at the core of the syncline, resting unconformably over G_M3 (Fig. 16e). It is composed by floodplain deposits (FA2) and broad sheets (FA3), in amalgamated beds up to 5-10 m. C/F ratio around 55/45.

Goulmima:

Around 80 m thick succession, subdivided in two FU sequences. The coarse facies present a high percentage of carbonatic clasts (Pan.4b, sections X_1-X_2 and X_3-X_4).

- G_G1: composed by broad sheets (FA3), in amalgamated beds up to 10 m, grading upward to floodplain deposits FA2. The succession is coarse dominated (C/F ratio 65/35) and shows a FU trend.

- G_G2: composed by broad ribbons (FA3), in amalgamated beds up to 10-15 m, grading upward to floodplain deposits (FA2). The succession is coarse dominated (C/F ratio 70/30) and shows a FU trend.

Toundoute:

The succession, up to 150-200 m, shows a FU trend. The coarse facies present conglomerate and sandstone derived mostly from volcanic and crystalline rocks and subordinately from dolomite and limestone.

It is composed by conglomerate narrow sheets (FA5), at the base, and broad sheets (FA3) at the top, amalgamated in beds up to 5 m, in alternation with flood plain deposits (FA2). It presents a C/F ratio around 40/60 (Pan. 4c).

Dades Valley:

Thick succession (up to 250 m), showing a general FU trend. The coarse facies present conglomerate and sandstone derived mostly from volcanic and crystalline rocks and subordinately from dolomite and limestone.

It is composed by conglomerate narrow sheets (FA5) at the base and broad sheets (FA3) at the top, amalgamated in thick beds up to 10-15 m, in alternation with flood plain deposits (FA2). It presents a C/F ratio around 45/55 (Pan. 4c).

5.1.4 Paleodrainage

In the High Atlas of Marrakech, the Guettioua synthem shows paleodrainage directions towards N, in Ait Ourir, and NE, in Jbel Igoudlane and Adrar Aglagal, with low to high dispersion in the paleo-current direction (Pan. 1; Tab. 6)

- Ait Ourir: $G_{AO}1$- no detected; $G_{AO}2$- NNW, high dispersion; $G_{AO}3$- N, moderate dispersion (Pan. 1a).

- Jbel igoudlane: $G_{JI}1$- NE, moderate dispersion; $G_{JI}2$- ENE low dispersion; $G_{JI}2$- NNE, low dispersion (Pan. 1b)

- Adrar Aglagal: $G_{AA}1$- NE, low dispersion; $G_{AA}2$: NE, high dispersion; $G_{AA}3$: NE, low dispersion (Pan. 1c).

In the western sector of the High Atlas of Beni Mellal it shows NE and ENE directed paleodrainage, presenting low to very high dispersion (Tab. 6; Pan2).

- Iouaridène: G_I1- NNE, High dispersion. G_I2: ENE, moderate dispersion. G_I3: ENE, moderate dispersion (Pan. 2a)

- Guettioua: G_G1- no detected; G_G2- ENE, very high dispersion; G_G3- NE, high dispersion (Pan. 2b).

- Ait Attab: because of the rareness of the sedimentary structures it was not possible to measure paleo-current directions in this section. The axes of the paleo-channels record a paleo-drainage along a NE-SW axe (Pan. 2c).

- Ouaouizaght: ENE, very high dispersion (Pan.2d)

In the eastern sector of the High Atlas of Beni Mellal, it presents a paleodrainage still directed to NE, presenting a high to very high dispersion (Tab. 6; Pan.3).

- Tilougguit: G_T1- NE, very high dispersion; G_T2: NE, high dispersion; G_T3: NE, low dispersion (Pan. 3a).

- Tagleft: ENE, very high dispersion rate (Pan. 3b).

- Imilchil: NE, high dispersion (Pan. 3c).
- Naour: NNE, high dispersion (Pan. 3d).
- Tizi'n'Isli: NE, high dispersion (Pan.3d).

At the southern front of the Central High Atlas the paleodrainage presents variable directions, with low to high dispersion (Tab. 6; Pan.4).

- M'semrir: G_M1- NNW high dispersion; G_M2- NW on the southern flank of the syncline, NE on the northern flank, high dispersion; G_M3- NNW on the southern front, ENE at the northern front, high dispersion; G_M4 NE, moderate dispersion (Pan. 4a).
- Goulmima: G_G1- NNW, low dispersion; G_G2: NNW, low dispersion (Pan.4b).
- Toundouet: NNE, low dispersion (Pan.4c)
- Dades Valley: SSE, low dispersion (Pan.4c)

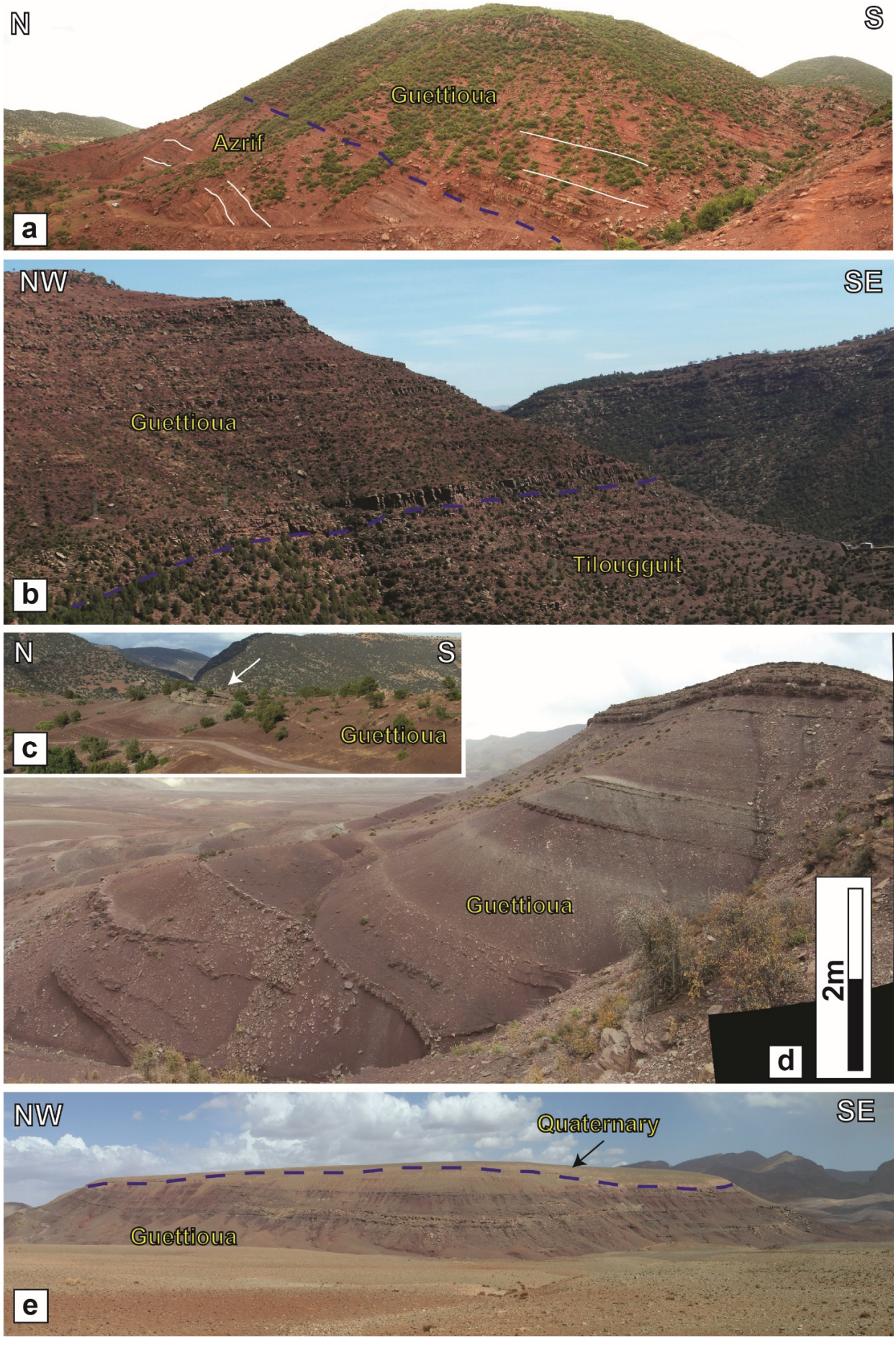
N
S
Guettioua
Azrif
a
NW
SE
Guettioua
Tilougguit
b
N
S
c
Guettioua
Guettioua
2m
d
NW
SE
Quaternary
Guettioua
e

Fig. 16: panoramic view of the Guettioua Synthem in the Central High Atlas. a) The Guettioua Synthem unconformably overlying the Azrif F. in the Jbel Igoudlane area. Base of the section K_1-K_2 (Pan. 1) b) The Guettioua Synthem unconformably overlying the Tilougguit Formation in the Guettioua Syncline c) The Guettioua Synthem in the Tagleft syncline, the white arrow indicates an isolated paleo-channel (narrow sheet, FA4) d) The Guettioua Synthem in the Imilchil syncline, composed by terminal fan deposits (FA1) only e) G_M4 filling an erosive paleo-channel eroded in the overlied G_M3, at the top of the M'semrir succession. To the top, Quaternary alluvial fan deposits.

Stratigraphic and sedimentary features of the Guettioua F. in the Central High Atlas

Area	Internal subdivisions	Presence of paleo-valleys	Thickness	C/F ratio	Grade of amalgamation/ thickness of the sandstone	Geometry of the paleo-channels	Grain of the channel infill	Dispersion degree of the paleo-currents	Zone
Ait Ourir	GAo1	no	10 to 50 m	low: 25/75	very low: 1m	no paleo-channels	no paleo-channels	no detected	Distal
	GAo2	yes		high: 80/20	medium: 5-8 m	narrow sheets	coarse: C to cS	High: 90°-180°	Proximal
	GAo3	no		medium: 40/60	low: 3m	broad sheets	medium to coarse: mS to cS	Moderate: ≥90°	Proximal-Medial
Jbel Igoudlane	GJ1	yes	110 m	low: 35/65	medium: 5-8 m	narrow sheets to broad sheets	medium: cS to mS	Moderate: ≥90°	Proximal/Proximal-Medial
	GJ2	no		medium: 50/50	medium: 5 m	broad sheets	medium: mS	Low: <90°	Proximal-Medial
	GJ3	no		medium: 50/50	low: 3m	narrow sheets	coarse: C to cS	Low: ≥90°	Proximal/Proximal-Medial
Adrar Aglagal	GAA1	yes	40 to 60 m	high: 80/20	very high: 10-15 m	broad ribbons	coarse: C to cS	Low: <90°	Proximal
	GAA2	no		low: 35/65	medium: 5 m	broad sheets	fine: M to mS	High: 90°-180°	Medial-Distal
	GAA3	no		medium: 65/35	medium: 5 m	narrow sheets	coarse: C to cS	Low: <90°	Proximal-Medial
Iouaridène	Gi1	no	100 m	high: 75/25	medium: 3-5 m	broad sheets	medium: cS to fS	High: 90°-180°	Proximal-Medial/Medial-Distal
	Gi2	no		medium: 65/35	medium: 6-8 m	narrow sheets	medium: cS to fS	Moderate: ≥90°	Proximal-Medial
	Gi3	yes		high: 80/20	high: 8-10 m	broad ribbons	coarse: cS	Moderate: ≥90°	Proximal/Proximal-Medial
Guettioua	GG1	no	150-200 m	medium: 50/50	medium: 5 m	no paleo-channels	no paleo-channels	no detected	Medial-Distal
	GG2	no		medium: 50/50	medium: 5 m	broad to narrow sheets	medium: cS to mS	Very High: ≥180°	Medial-Distal/Proximal-Medial
	GG3	no		medium: 50/50	high: 10 m	broad ribbons to broad sheets	medium: cS to mS	High: 90°-180°	Proximal-Medial
Ait Attab		no	70 m	low: 30/70	medium: 3-5 m	broad sheets	medium: mS	Low: <90°	Proximal-Medial/Medial-Distal
Ouaouizaght		no	130 m	medium: 50/50	very high: 10-20 m	broad sheets	medium: mS	Very High: ≥180°	Proximal-Medial
Tagleft		no	150 m	low: 30/70	medium: 3-5 m	narrow sheets to broad sheets	fine: M to mS	Very High: ≥180°	Medial-Distal
Tilougguit	GT1	no	150-200 m	very low: 15/85	very low: 1m	no paleo-channels	no paleo-channels	Very High: ≥180°	Distal
	GT2	no		very low: 20/80	medium: 3-5 m	no paleo-channels	no paleo-channels	High: 90°-180°	Distal/Medial Distal
	GT3	no		medium: 40/60	medium: 6-8 m	broad sheets	fine: M to fS	Low: <90°	Medial-Distal
Naour		no	150-200 m	very low: 20/80	very low: 1m to medium: 5 m	broad sheets	fine: M to fS	High: 90°-180°	Distal
Tizi'n Isli		no	150-200 m	very low: 10/90	very low: 1m	no paleo-channels	no paleo-channels	High: 90°-180°	Distal
Imilchil		no	150-200 m	very low: 10/90	very low: 1m	no paleo-channels	no paleo-channels	High: 90°-180°	Distal
Toundout		no	150-200 m	medium: 45/55	medium: 5 m	narrow sheets to broad sheets	coarse: C to cS	Low: <90°	Proximal-Medial
Dades Valley		yes	250 m	medium: 45/55	very high: 10-15 m	narrow sheets to broad sheets	coarse: C to cS	Low: <90°	Proximal-Medial
M'semrir	GM1	no	500 m	very low: 10/90	very low: 1m	no paleo-channels	no paleo-channels	High: 90°-180°	Distal
	GM2	no		low: 30/70	medium: 6-8 m	broad sheets	fine: M to fS	High: 90°-180°	Medial-Distal
	GM3	no		low: 30/70	medium: 6-8 m	broad sheets	medium: cS to mS	High: 90°-180°	Medial-Distal/Proximal-Medial
	GM4	yes		medium: 55/45	high: 10 m	broad sheets	medium: cS to mS	Moderate: ≥90°	Medial-Distal/Proximal-Medial
Goulmima	GG1	no	80 m	medium: 65/35	high: 10 m	broad sheets	coarse: C to cS	Low: <90°	Proximal-Medial
	GG2	no		high: 70/30	very high: 10-15 m	broad sheets	coarse: C to cS	Low: <90°	Proximal-Medial

Tab. 6: stratigraphic and sedimentological features of the Guettioua Synthem in all the studied outcrops.

5.2 The Jbel Sidal Synthem

5.2.1 The lower boundary

In the High Atlas of Marrakech, from north to south: in the Ait Ourir area it rests unconformably over a mudstone dominated succession (up to 50 m), recognized in this study as the local expression of the Iouaridène Formation and previously generically referred to as "Dogger" (Ferrandini et al., 1982; Hadach et al., 2015, 2018); in the Jbel Igoudlane it rests unconformably over a thick succession of the Iouaridène Formation (Saadi et al., 1985); in the Adrar Aglagal syncline it rests directly over the Guettioua F. at the core of the syncline, over the Azrif F. and the below formations (LJm) in the southeastern front of the structure, while in the northwestern part of the area it seals a thrust that brings the Lower Jurassic carbonates over the Azrif F., outlining a strong angular unconformity and a huge stratigraphic hiatus (Cavallina et al., 2018).

In the western sector of the High Atlas of Beni Mellal, in the Iouaridène, Ait Attab and Ouaouizaght synclines, it unconformably overlies the Iouaridène F, presenting in this area very thick successions, up to several hundred meters thick (Saadi et al., 1985). The synthem is lacking in the Guettioua Syncline, due to erosion or non-deposition.

In the southern front it rests over a local equivalent of the Iouaridène lacustrine formation in the Dades River Valley (Benvenuti, 2010; Benvenuti et al., 2017; Moratti et al., 2018), while in the Goulmima anticline it overlies in unconformity the deposits of the Guettioua Synthem (Papini et al., in prep.). Apparently lacking in the Toundoute area and in M'semrir syncline.

5.2.2 The Upper Boundary

To the top it sharply passes to the Aptian-Albian marls, dolomites and limestone of the Ait Tafelt Formation in the northern outcrops (Ait Ourir, Jbel Igoudlane, Ait Attab and Ouaouizaght; Ferrandini et al., 1982; Saadi et al., 1985), except for the Iouaridène syncline where the capping is missing, due to erosion or nondepostition.

At the southern front (Adrar Aglagal and Dades Valley), it is overlied in unconformity by fluvial successions referred to the Albian-Cenomanian, Ifezouane and Aoufous Formations (Benvenuti et al., 2017; Cavallina et al., 2018); in the Goulmima anticline it is overlied by a

mudstone-gypsum succession, possibly representing a continental equivalent of the Ait Tafelt F. (Papini et al., in prep.).

5.2.3 Stratigraphic and sedimentological features

In the High Atlas of Marrakech, the Jbel Sidal Synthem presents successions variable for thickness and stratigraphic features (Pan. 1)

Ait Ourir:

The successions show variable thickness, from a maximum of 180 m in the Adenndim syncline to a minimum of 100 meters in the other synclines.

It is composed by alternating floodplain deposits (FA2) and paleochannels (FA3, FA4 and FA7) forming a FU sequence (Tab.1a). The base is coarse-grain dominated (60/40 to 75/25 C/F ratio), with broad ribbons (FA7), forming amalgamated sandstone beds up to 10-15 m. To the top the mudstone becomes dominant (40/60 to 20/80 C/F ratio) and the coarse-grain facies are organized in narrow sheets to broas sheets (FA4 and FA3), up to 3-5 m, or in tabular beds (FA2) (Pan. 1a; Tab. 7).

Jbel Igoudlane:

Very thick succession, up to 500 m, composed by sandstone narrow sheets (FA4), in amalgamated beds up to 5-15 m (Fig. 17a), and floodplain deposits (FA2) in alternation, it is sandstone dominated at the base (C/F ratio around 55/40), mudstone dominated to the top (C/F ratio around 40/60), presenting an overall FU trend (Pan. 1b; Tab.7).

Adrar Aglagal:

Up to 300 m, it is subdivided in three FU sequences (Pan.1c; Tab.7).

- $JS_{AA}1$: conglomerate narrow sheets (FA5), in 5-8 m thick amalgamated beds dominant at the base (C/F ratio around 80/20), passing upward to floodplain deposits (FA2; C/F ratio 30/70).

- $JS_{AA}2$: conglomerate narrow sheets (FA5) at the base and broad sheets at the top (FA3), in alternation with floodplain deposits (FA2). C/F ratio 85/15. The coarse-grain facies are stacked in amalgamated bodies up to 5-10m).

- $JS_{AA}3$: Similarly to the previous sequence it shows a FU trend with FA5 dominating at the base grading upward to FA3 and then FA2. C/F ratio 85/15

In the western sector of the High Atlas of Beni Mellal, the Jbel Sidal Synthem presents successions variable for thickness and stratigraphic features (Pan. 2)

Iouaridène:

Up to 400 m, the succession is mudstone dominated (C/F ratio around 80/20), composed by terminal fan deposits ($FA1_a$ passing upward to $FA1_c$) and subordinate broad sheets ($FA3_a$, composed only by the finest facies: M1 and S1) and floodplain deposits (FA2), filling a NE-SW oriented paleo-valley. It shows a FU trend: the base is composed by FA2 and rare FA3, passing upward to a succession completely composed by the repetition of $FA1_a$ ending at the top with $FA1_c$ (Pan. 2a; Tab.7).

Ait Attab:

100-200 m succession, composed by floodplain deposits (FA2) in alternation with sandstone narrow sheets (FA4), in amalgamated beds up to 10-20 m. It shows a fining upward trend (Pan.2c): it is sandstone dominated at the base (C/F around 60/40) and mudstone dominated at the top (C/F around 30/70) (Tab.7).

Ouaouizaght:

The Jbel Sidal succession is up to 300 m in the axial part of the syncline, around 200 at the western front. It shows an overall FU trend, internally subdivided in two FU sequences (Pan.2d; Tab.7).

- $JS_{OU}1$, outcropping only on the western front, is sandstone dominated (C/F 75:25), composed by the alternation of sandstone narrow sheets (FA4), composing thick amalgamated beds up to 10 meters, and floodplain deposits (FA2).

- $JS_{OU}2$, outcropping both on the axial and in lateral portion of the structure, presents a variable thickness: 100 m to the west, 200 m along the axis of the syncline. It is mudstione dominated (C/F 35/65), composed by floodplain deposits (FA2) and narrow sheets (FA4) forming amalgamated sandstone bodies up to 5-8 m (Fig. 17b). To the top $FA1_c$ is also present, testifying a transgressive trend that continues up to the Ait Tafelt Formation.

In the southern front of the CHA, the Jbel Sidal Synthem presents successions variable for thickness and stratigraphic features (Pan. 4)

Goulmima:

The thickness varies from south to north from around 50 m to more than 100 m. It is composed by the sandstone narrow sheets (FA4), in amalgamated bed up to 15-20m (Fig. 17c), and, subordinate, floodplain daposits (FA2), forming an overall FU sequences (Pan.4c). The succession is sandstone dominated (C/F ratio 95/5) (Pan. 4b; Tab. 7).

Dades Valley:

Up to 100 m succession composed by two FU cycles, showing conglomerate narrow sheets at the base (FA5) passing upward to sandstone narrow sheets (FA4) alternating with floodplain deposits (FA2). C/F ratio around 50/50. The sheets are amalgamated in beds up to 5-10 m thick (Tab.7).

5.2.4 Paleodrainage

In the High Atlas of Marrakech the Jbel Sidal Formation shows paleodrainage direction towards S and W, in Ait Ourir, and NNE, in Jbel Igoudlane and Adrar Aglagal, with low to very high dispersion in the paleo-current direction (Pan. 1; Tab. 7)

- Ait Ourir: WNW in tha Ouanina syncline, SSE in the Tasgimouth syncline, SSW in the Tafilelt and Adenndim synclines, WSW in the Jbel Sour. High dispersion (Pan. 1a).
- Jbel Igoudlane: NNE. Very high dispersion (Pan. 1b)
- Adrar Aglagal: N. Low to very high dispersion (Pan. 1c)

In the High Atlas of Beni Mellal it presents direction toward SSW (in Ait Attab and Ouaouizaght synclines) and NW (in the upper part of the Ouaouizaght succession). The dispersion is low to very high (Pan 2; Tab. 7).

- Iouaridène: NE-SW (axis of the paleovalley), direction not detected (Pan. 2a)
- Ait Attab: SSW. Low dispersion (Pan. 2c).

- Ouaouizaght: lower portion- WSW, high dispersion; upper portion – WNW, very high dispersion (Pan. 2d).

In the southern front of the CHA, the paleodrainage presents variable directions with low to very high dispersion.

- Goulmima: N. Very high dispersion (Pan. 4b).
- Dades Valley: SSE. Low dispersion (Pan. 4c).

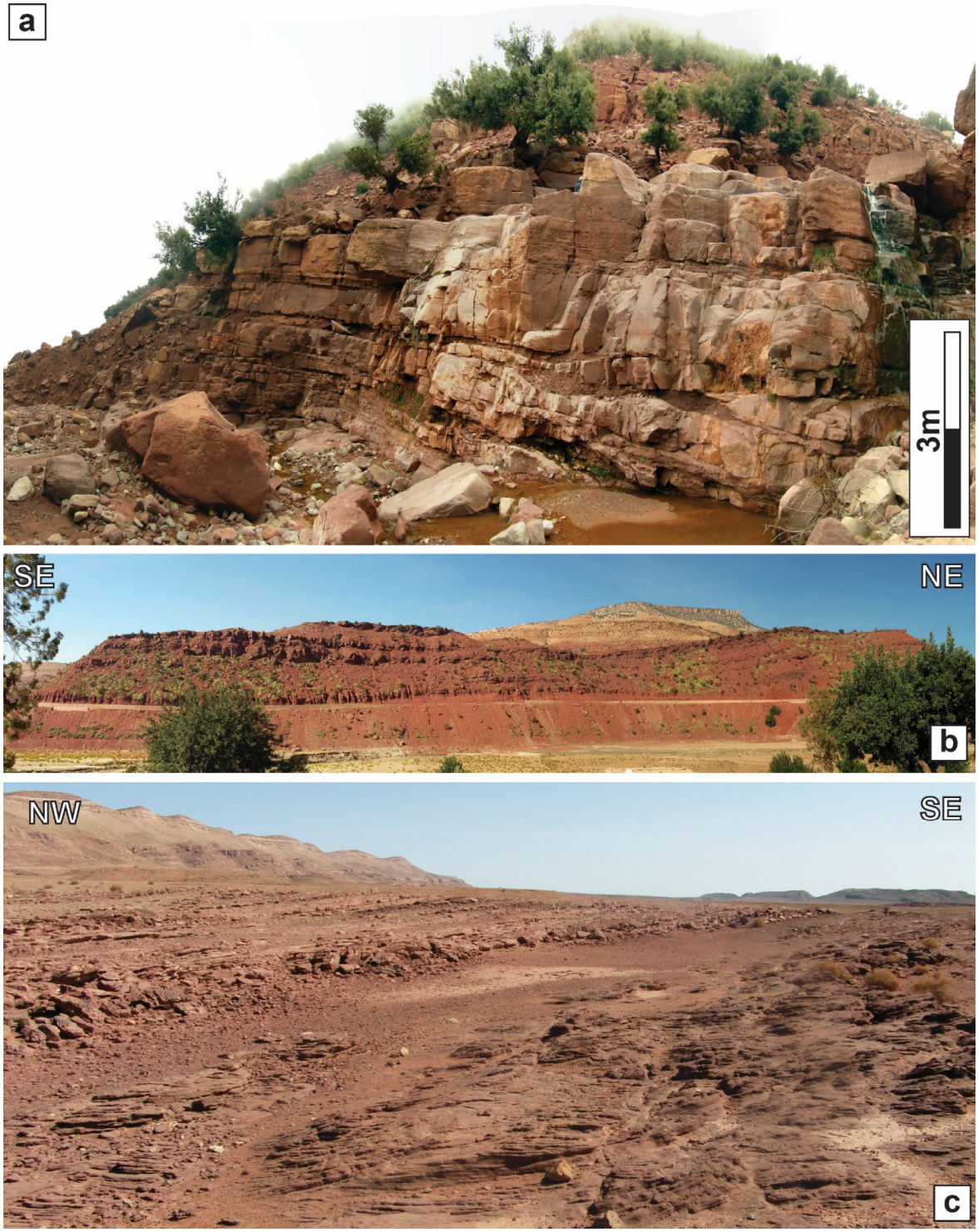

Fig. 17: panoramic view of the Jbel Sidal Synthem in the Central High Atlas a) outcrops of the upper portion of the synthem in the Jbel Igoudlane syncline, showing sandstone narrow sheets (FA4) in a thick amalgamated body b) the lower part of the synthem in the Ouaouizaght syncline, showing the alternance between sandstone narrow sheets (FA4) and floodplain mudstone (FA2) c) the Jbel Sidal synthem at the core of the Goulmima anticline, showing sandstone narrow sheets (FA4) in amalgamated beds.

Stratigraphic and sedimentary features of the Jbel Sidal F. in the Central High Atlas								
Area	**Internal subdivisions**	**Presence of paleo-valleys**	**Thickness**	**C/F ratio**	**Grade of amalgamation/ thickness of the sandstone**	**Geometry of the paleo-channels**	**Grain of the channel infill**	**Dispersion degree of the paleo-currents**	**Zone**
Ait Ourir	JS_{BASE}	no	100 to 180 m	high: 70/30	very high: 10-15 m	broad ribbons to narrow sheets	coarse to medium: C to mS	High: 90°-180°	Proximal/Proximal-Medial
	JS_{TOP}	no		low: 30/70	medium: 3-5m	narrow sheets to broad sheets	medium: cS to fS	High: 90°-180°	Proximal-Medial
Jbel Igoudlane		no	500 m	medium: 55/45	very high: 10-15 m	narrow sheets	medium: cS to mS	Very High: ≥180°	Proximal-Medial
Adrar Aglegal	$JS_{AA1base}$	no	300 m	high: 80/20	high: 5-8 m	narrow sheets	coarse: C to cS	Low: <90°	Proximal/Proximal-Medial
	JS_{AA1top}	no		low: 30/70	low: 2-3m	no paleo-channels	no paleo-channels	no detected	Distal
	JS_{AA2}	no		high: 85/15	high: 5-10 m	broad sheets	medium: mS to fS	High: 90°-180°	Proximal-Medial
	JS_{AA3}	no		high: 85/15	high: 5-8 m	narrow sheets to broad sheets	coarse to mecium: C to mS	Very High: ≥180°	Proximal-Medial
Iouaridène		yes	400 m	high: 80/20	low: 2-3m	no paleo-channels	no paleo-channels	no detected	Distal
Ait Attab	BASE	no	50 to 150 m	medium: 60/40	very high: 10-20 m	narrow sheets	medium: mS to fS	Low: <90°	Proximal-Medial
	TOP	no		low: 30/70	low: 2-3m	no paleo-channels	no paleo-channels	no detected	Distal
Ouaouizaght	JS_{OU1}	no	200-300 m	high: 75/25	high: 10 m	narrow sheets	medium: mS to fS	High: 90°-180°	Proximal-Medial
	JS_{OU2}	yes		high: 35/65	high: 5-8 m	narrow sheets	medium: mS to fS	Very High: ≥180°	Proximal-Medial/Medial-Distal
Dades Valley		yes	100 m	Medium: 50/50	high: 5-10 m	narrow sheets	coarse to medium: C to mS	Low: <90°	Proximal-Medial
Goulmima		no	50 to 100 m	Very high: 95/5	very high: 15-20 m	narrow sheets	medium: mS to fS	Very High: ≥180°	Proximal-Medial

Tab.7: Stratigraphic and sedimentological features of the Jbel Sidal Synthem in all the studied outcrops.

6. Discussion

The presented data open to a range of aspects stimulating a potentially wide discussion that we limited to two main points.

1) Since the research has been aimed at recovering information on the regional dynamics of fluvial systems from the sedimentary record, a first point deals with the depositional model for the fluvial dispersal suggested by the facies analysis.

2) The second point stresses the occurrence of a dynamic relief between the Middle Jurassic and the Early Cretaceous in the CHA, suggested by two lines of evidence.

- The first concerns the topographic picture that emerges from tracing at a regional scale the unconformities delimiting the Guettioua and the Jbel Sidal synthems.

- The second relies on the reconstruction of the paleo-drainage patterns obtained by the paleocurrent dataset.

Both these points support the hypothesis of diffuse vertical movements in the CHA reasonably related to crustal deformation active during the Middle Jurassic-Lower Cretaceous. A discussion on the mechanisms forcing such a deformation goes beyond the aim of this study.

6.1 Depositional model of the fluvial systems

The late Mesozoic fluvial successions of the CHA, including the Guettioua and Jbel Sidal synthems, have been generically referred in the literature to deposition in meandering and braided rivers (Jenny et al., 1981; Souhel 1987, 1996; Haddoumi et al., 2002, 2008, 2010; Charrière et al., 2005; Charrière and Haddoumi, 2016, 2017). Nevertheless, facies analysis carried out in the present study suggests that the studied successions escape the classical facies models established for braided and meandering fluvial systems (Miall, 1978, 2010).

Arguments supporting this conclusion are briefly summarized as follows:

1) The relatively abundance of sedimentary structures diagnostic of high flow velocities (UFR) and high deposition rate (HDR), compared to the paucity of structures related to subcritical flow conditions (LFR), suggests transport and deposition mostly by flood pulses heavily charged with sediment.

2) Most of the paleo-channels bearing the described facies, are characterized by a stratal architecture dominated by very low angle-to aggradational accretion sets (FA3-FA4-FA5), rather than by the classic cross-stratified barforms which typify the braided and meandering channels (Miall, 1978, 2010; Lunt et al., 2004; Ghinassi et al., 2013). The high flow velocities and deposition rates, suggested by the described facies and their associations, prevented the formation of high angle accretion sets commonly recognized in meandering and braided channel fills.

3) Excluding FA6 and FA7, hinting to relatively deep channels not much represented in the studied successions, the dominant geometry of the paleochannels is expressed by a high W/T ratio (FA3-FA5) indicative of shallow and poorly-confined flows.

4) The infill of the paleochannels commonly presents in-channel mud layers and heterolytic infill, consisting of alternating sandstone and mudstone or, even, in-channel paleosols, indicating significant breaks of the fluvial activity.

5) The high amount of muddy and sandy floodplain deposits (FA1 and FA2) in alternation to the channel fills (FA3-FA7) contrasts with the typical architecture of braided systems characterized by thick amalgamated conglomerate/sandstone bodies. In the studied cases, deposition outside the channels related to crevassing occurred at frequency comparable to that of in-channel aggradation.

These features depict ephemeral fluvial systems characterized by a variable discharge analogous to the seasonal rivers presently occurring in a wide range of geomorphic settings (Plink-Björklund, 2015). The rivers recorded by the studied successions were active only during wet periods, when large sediment-laden flood flows favor the development of the depositional features described above. During dry periods, a low base flow with limited or null sediment transport brings to an almost total deactivation of the channels undergoing pedogenetic modification of their sediment infill.

These rivers, characterized by discontinuous discharge, frequent avulsions and high sedimentary rates, are frequently associated to areas of flood expansions giving rise to fan shaped planforms. The latter may find convergence with alluvial depositional systems in the literature termed as: fluvial fans (Ventra and Clarke, 2019), megafans (Leyer et al., 2005) and distributary fluvial systems (DFS, Nichols and Fisher, 2007). Actively subsiding basins may represent a setting for the occurrence of these systems (Ventra and Clarke, 2019).

Our facies reconstruction emphasizes the sedimentological features of the proximal fluvial feeder of DFS, not described in the existing models (Nichols & Fisher, 2007), and represented by channel fills confined in paleo-valleys. The geographic distribution of the proximal valley tracts outlines quite well a paleo-topography with thresholds separating distinct catchments opening into medial and distal zones where fluvial fans developed.

In fig. 18 we propose a schematic model for the studied fluvial systems, that combines the fluvial distributary system model, elaborated by Nichols and Fisher (2007), with the proximal fluvial feeder described in the studied succession. The reconstructed fluvial model is subdivided in four areas, each one with typical features such as the occurrence of paleo-valleys, the thickness of the deposits, the coarse-grain/fine-grain ratio, the grade of strata amalgamation, the geometry of the channels, the grain-size of the channel-fill, the dispersion of the paleocurrent directions (Tab. 6, 7, 8).

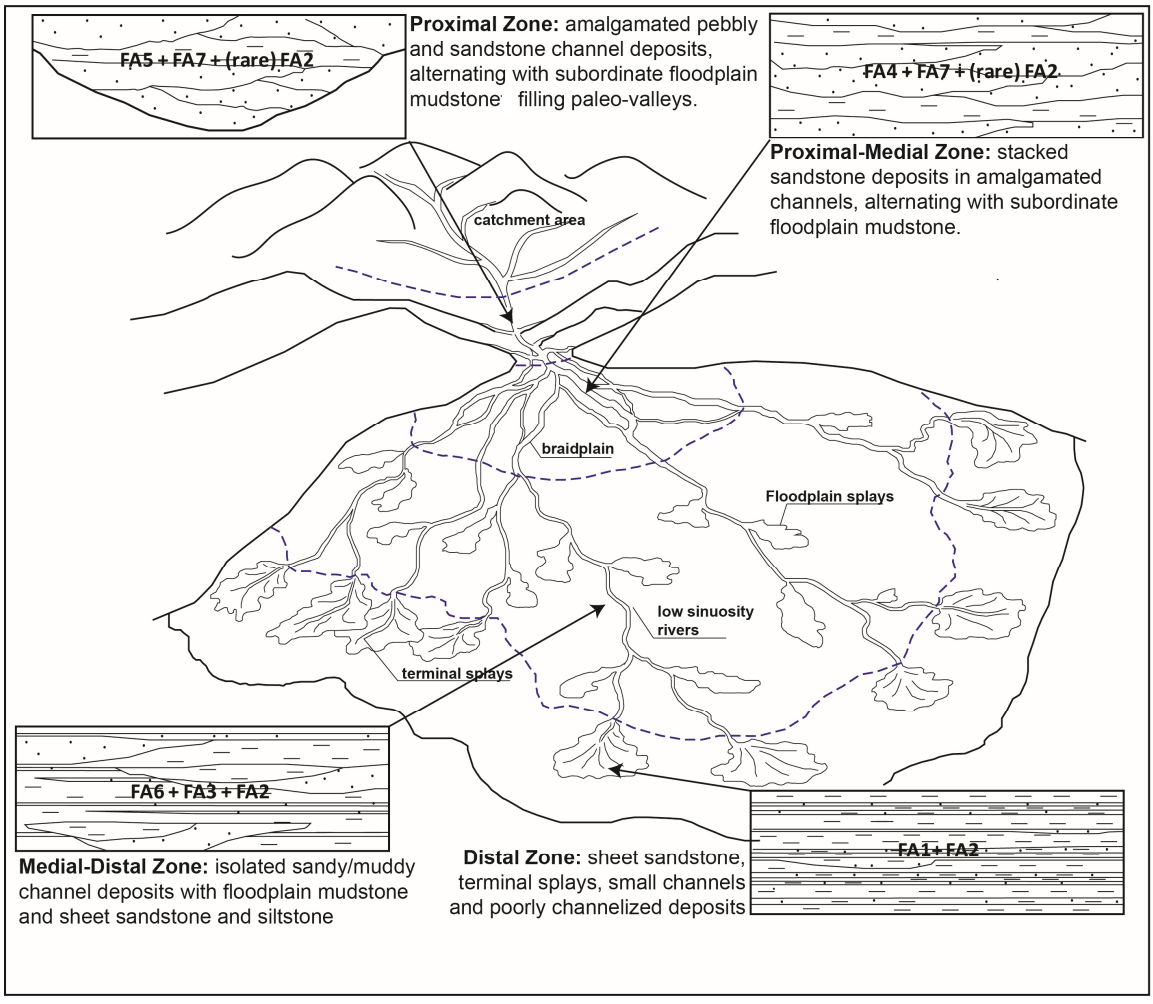

Fig. 18 Model for the fluvial systems represented by the CHA fluvial successions. Modified from Nichols and Fisher, 2007.

Proximal zone	Successions related to paleo-valley fills, variable thickness, medium to high C/F ratio, medium to very high amalgamation of the sandstone bodies, broad ribbons to narrow sheets, coarse grain channel-fill (conglomerate to pebbly sandstone), low to high dispersion in the paleo-current directions.
Proximal-medial zone	Lacking paleo-valleys, medium thickness of the successions, high to medium C/F ratio, medium to very high amalgamation of the sandstone bodies, broad ribbons to broad sheets, paleo-channels filled with fine to coarse sandstone, low to very high dispersion rate. This portion is quite similar to a braid plain.
Medial-distal zone	Lacking paleo-valleys, medium to thick successions, low C/F ratio, low to medium amalgamation of the sandstone bodies, narrow sheets to broad sheets, paleo-channels filled with mudstone to medium sandstone, high to very high dispersion rate. This portion is similar to a meandering or anostomozing fluvial system.
Distal zone (terminal fan)	Lacking paleo-valleys, very thick successions, low to very low C/F ratio, low to very low sandstone amalgamation, narrow sheets to broad sheets (or absence of paleo-channels), mudstone to fine sandstone infill of the paleo-channel (where they are present), high to very high dispersion rate.

Tab. 8. Sedimentological and stratigraphic features, from proximal to distal zone, of the reconstructed fluvial model.

6.2 Evidence of a dynamic relief in the Middle Jurassic-Early Cretaceous CHA domain

6.2.1 The unconformable contacts of the Guettioua and Jbel Sidal synthems

When traced from the western to the eastern sectors of the CHA, the lower unconformity bounding the Guettioua synthem clearly illustrates an overall topographic gradient with the more elevated areas located in the High Atlas of Marrakech, where the synthem rests over Lower Jurassic limestone, and more depressed areas progressively moving toward east. Along

this direction the Guettioua synthem is unconformably over the Bajocian limestones and then over the lower Bathonian coastal deposits (Tilougguit Formation) pointing to an attraction of the drainage toward coastal and possibly marine areas eastward. From west to east along the southern front of the CHA, the Guettioua-equivalent deposits, differentiated in the Upper Mesozoic continental successions through recent stratigraphic revisions (Benvenuti, 2010; Benvenuti et al., 2017; Moratti et al., 2018; Papini et al., in prep.), rest over mixed carbonate-clastic strata ascribed to the lower Bathonian Tilougguit Formation. In this reconstruction the Guettioua fluvial setting developed over pre-existing coastal environments established in the present southern foreland of the CHA. This conclusion suggests that a depressed area flooded by marine ingressions, already existed between the Anti-Atlas and an embryonic CHA during the late Mesozoic.

Through the tracing of its lower bounding unconformity, the Jbel Sidal synthem outlines a significantly different paleogeographic scenario. This unit rests unconformably over the Iouaridène Formation at the northern front (Ait Ourir, Jbel Igoudlane, Iouaridène, Ait Attab, Ouaouizaght), documenting the fluvial occupation of previously subsiding areas that accommodated thick lacustrine successions. At the southern front of the chain, Jbel Sidal-equivalent deposits directly overlay the Guettioua-equivalent strata, (Adrar Aglagal and Goulmima; Cavallina et al., 2018; Papini et al., in prep.) or rest over Iouaridène-equivalent fluvio-lacustrine facies (Dades; Benvenuti et al., 2017), outlining an articulated topography with irregularly distributed highs and lows on this side of the chain.

6.2.2 The paleodrainage evolution (Figs. 19, 20)

The Guettioua Synthem (Bathonian):

The paleodrainage pattern reconstructed for the Guettioua synthem. shows an overall WSW-ENE direction, subparallel to the CHA trend, in agreement with the land-sea gradient and the facies distribution (tab. 6 and 7) discussed above. Nevertheless, some of the studied successions records N-S paleo-drainage directions that are transversal to the CHA trend that, joined to the facies features and distribution, attest to the fragmentation of the coeval drainage system in different hydrographic basins, separated by topographic highs and thresholds.

The Atlas of Marrakech was a topographic high, possibly inherited from the West Moroccan Arch referred to as a relief already emerged in the Early Jurassic (Jabour et al., 2004; Frizon de Lamotte et al., 2008).

To the north the Ait Ourir sections record a drainage trend from south to north within the cyclic stack of the Guettioua strata. The terminal fan, represented by $G_{AO}1$ sequence (tab. 6), is unconformably overlain by the paleovalley facies of the $G_{AO}2$ sequence, documented in all the Ait Ourir synclines. The uppermost $G_{AO}3$ sequence composed of proximal-distal facies confirms that the fluvial system flowed transversally to the CHA trend, towards N, possibly opening beyond the North Atlas Fault towards a depressed area. Within a relatively constant drainage orientation the facies architecture reflects pulses of DFS progradation and backstepping forced by relative base-level and /or sediment supply variations.
In the Adrar Aglagal and Jbel Igoudlane the Guettioua strata record a NE-trending drainage documented by the infill of two symmetric paleo-valleys. The facies architecture suggests an early retrogradation of the system ($G_{AA}1$ – proximal zone – to $G_{AA}2$ – medial distal- and $G_{JI}1$ – proximal/proximal medial – to $G_{JI}2$ – proximal medial) and then a progradation ($G_{AA}3$ – proximal medial – and $G_{JI}3$ – proximal/proximal medial).

Along the High Atlas of Beni Mellal the Guettioua synthem records the medial (Iouaridène, Guettioua, Ait Attab and Ouaouizaght) to distal (Tilougguit, Tagleft, Naour, Tizi'n'Isli and Imilchil) zones of the DFS sourcing in the High Atlas of Marrakech. The facies architecture, showing an internal tripartition with a general CU trend, testifies the progressive progradation of the fluvial system (tab. 6; Fig. 19).

At the southern front the fluvial systems show even more evidence of a fragmentation in separated paleodrainage basins:
- In the Toundoute and Dades River valley, the Guettioua synthem represents the proximal-medial zone of a fluvial fan, flowing respectiveley, to the NE in the Toundout area and to the SSE in the Dades River Valley, possibly responding to early activation in the South Atlas Fault area.
- In the 'Msemrir area, the Guettioua Synthem presents two different paleo-drainage directions, recording two different systems: a terminal fan, flowing northward, is progressively attracted in a fluvial fan directed to the ENE. This latter becomes dominant in the upper part of the succession, possibly responding to the coeval uplift of a topographic high located to the

northwest. The synsedimentary character of this uplift is also testified by the progressively coarser grain of the fluvial in-fill (CU trend) in the upper part of the succession.

- In the Goulmima anticline the Guettioua Synthem represents the proximal to medial portion of a fluvial fan, flowing northward, possibly responding to the early reactivation of the South Atlas Fault.

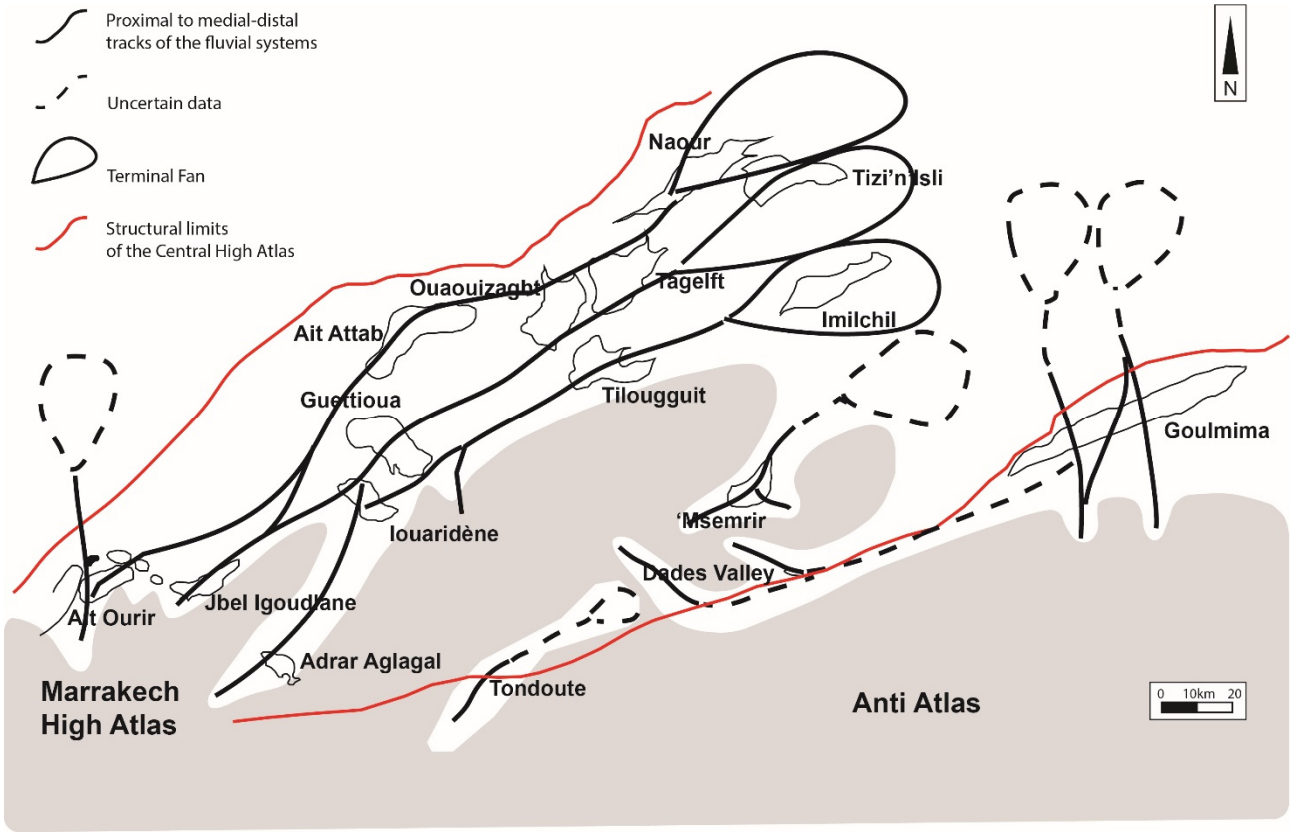

Fig. 19 Paleogeographic reconstruction of the CHA during the Bathonian, based on paleodrainage record. In grey the area characterized by a higher elevation. In black the synclines in which the Guettioua Synthem is not recorded.

The Jbel Sidal Synthem (Barremian)

The paleocurrent dataset allows to reconstruct a drainage pattern, during the Barremian, showing high variability along the CHA and significant modifications in respect with the scenario recorded by the Guettioua Synthem.

Along the west-east gradient the paleocurrent data point to a WSW-directed paleodrainage in the Ait Ourir area represented by facies indicative of DFS proximal to proximal-medial zone (Tab. 7). This system should have been fed by a topographic high separating this area from the

adjacent Jbel Igoudlane. In the latter, as well as in the southern Adrar Aglagal, the related deposits recording the deposition in a DFS proximal to distal zone, show a paleodrainage directed to NNE. These two systems, probably coalescent, may have converged in the Iouaridène syncline feeding a terminal fan (Tab. 7). Basing on the paleocurrent pattern the Iouaridène syncline attracted also the Jbel Sidal rivers sourcing to NE, represented by facies typical of DFS proximal-medial to medial-distal zones and crossing the Ait Attab and the Ouaouizaght areas (Tab. 7). In the Ouaouizaght syncline the SW-directed system is overlain by a NW-directed one recorded by facies of the DFS medial-distal zone (cf Sohuel, 1997). This younger system records an apparently local but significant change of the paleo-hydrography during the Barremian, suggesting uplift to the SE due to a possible tectonic pulse. All the Jbel Sidal successions on the northern front of the CHA present a FU trend, representing a transgressive trend, causing the backstepping of the fluvial systems and culminating with the overlying marls and limestone of the Ait Tafelt Formation.

Finally, to the south, in the Goulmima anticline and in the Dades River valley, the Jbel Sidal Synthem, similarly to the Guettioua Synthem, represents the proximal-medial zone (Tab. 7) of fluvial fans with paleodrainage directed perpendicular to the axis of the Atlas system (North directed in the Goulmima anticline; South directed in the Dades Valley). To the top, the continental sedimentation continues with the Ifezouane and Aoufous F., testifying that this sector of the chain was not affected by the Aptian marine ingression recorded at the northern front, possibly because of higher elevation on the sea level.

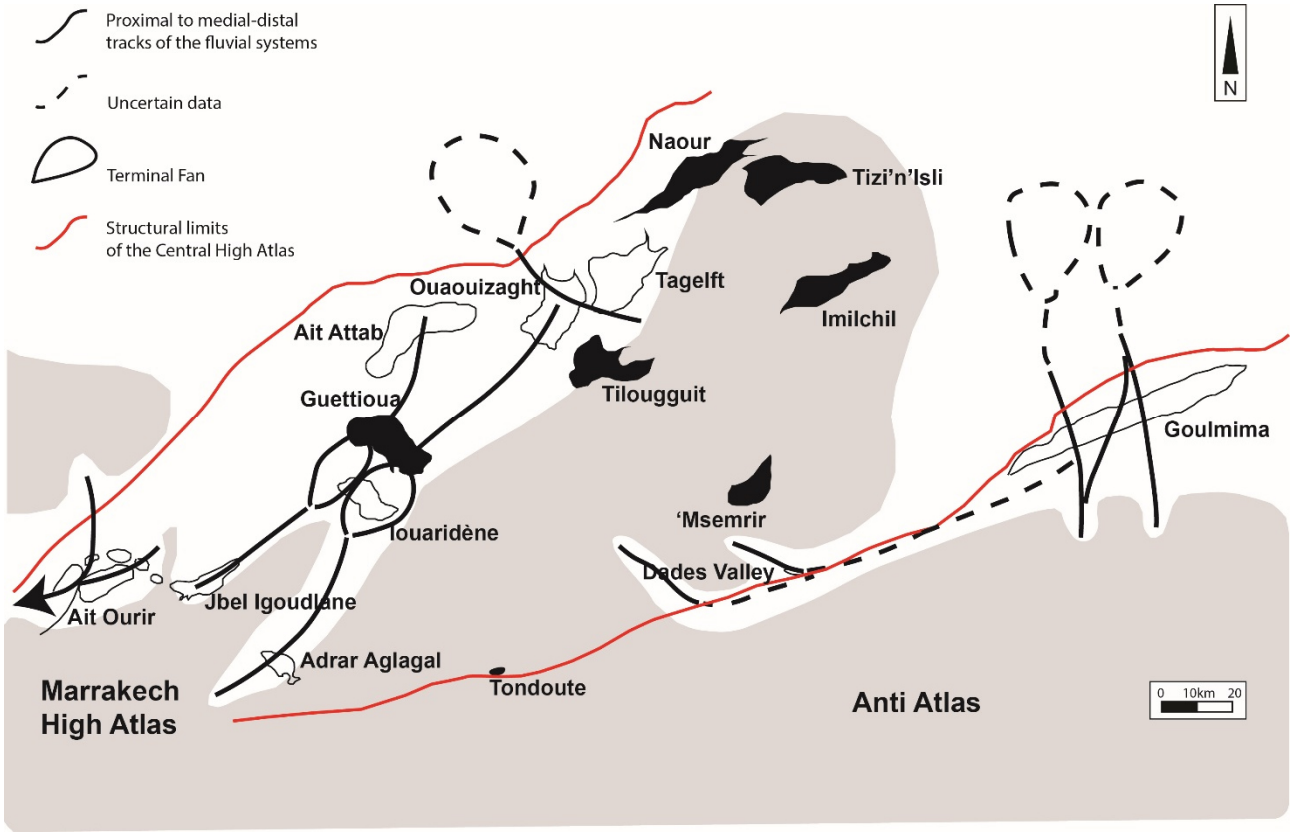

Fig. 20. Paleogeographic reconstruction of the Central High Atlas during the Barremian, based on paleodrainage evidence. In grey the area characterized by a higher elevation. In black the synclines in which the Jbel Sidal Synthem is not recorded.

6.Conclusions

The reconstructed paleogeographic frameworks for the Guettioua and the Jbel Sidal Synthems, contextualized in the Middle Jurassic-Lower Cretaceous deposition, record a dynamic paleo-geography.

During the Bathonian the CHA shows a paleodrainage system subparallel to the chain, with an overall ENE direction, at the northern front, and drainage transversal to the chain at the southern front, outlining a complex paleo-geography and testifying the presence of topographic high in the High Atlas of Marrakech, in the axial portion of the chain and next to the southern structural limit of the chain (the South Atlas Fault). After the deposition of the Guettioua Synthem, only the northern fluvial systems evolved in the lacustrine sedimentation represented by the Iouaridène Formation, testifying the presence of topographic highs separating the Central High Atlas in different sectors. During the Barremian, the paleogeographic framework changed again with the onset of new thresholds in the High Atlas of Marrakech and the development of a WSW oriented paleo-drainage testifying the uplift of the northeastern sector.

The reconstructed scenario, consisting in a dynamic paleogeography in which the paleodrainage appears fragmented in several small basins, could not be explained in a tectonic quiescent context or with generalized regional tilting or tectonic uplift. The development of separate basins in the CHA during the Mesozoic has been tied to either transpressional inversion of preexisting normal/transtensional faults (e.g., Mattauer et al., 1977) or to prolonged salt tectonics evolving from a first active phase to passive diapirism (Vergés et al., 2017). The salt tectonic model (Ettaki et al., 2007; Saura et al., 2014; Ibouh and Chafiki 2017; Moragas, 2017; Vergés et al., 2017; Moragas et al., 2018; Torres-López et al., 2018) that defines the CHA as a major diapiric province during Jurassic times could explain the development of some separate paleodrainage basins. But not all the recognized tresholds corresponds to areas in which the Triassic salts are exposed (cfr El Arabi, 2017). Furthermore, the southern studied areas (Adrar Aglagal, Msemrir, Dades Valley and Goulmima), present evidence of a synsedimentary tectonics that can not be linked to diapirism (Benvenuti et al., 2017; Cavallina et al., 2018; Papini et al., in prep.) and indicate early compressive-transpressive stages of deformation, as already recognized in other parts of the CHA (Laville, 1988, 2002; Laville and Piqué, 1992). Our data point to a dynamic evolution of the paleogeography during this span of time that should be understood in the framework of a regional tectonics in which the Central High Atlas may represent a transfert zone linked to the opening of the Atlantic

system to the west and the Tethys Ocean to the north and east, causing a transtensive to transpressive tectonics, locally mobilizing salt diapirs.

Appendix.: methods

The methodologies adopted in this study refers to standard descriptive approaches to the clastic sedimentary successions.

The continental deposits have been described in terms of sedimentary facies analysis (Bosellini et al., 1989; Nichols, 2009).

- Twelve facies have been distinguished and qualitatively described for their physical characters (lithology, textural features, clast shape, color and sedimentary structures) and interpreted as the record of specific sedimentary processes. The acronyms: UFR (critical to transcritical flow or upper flow regime sedimentary structures), LFR (lower floe regime sedimentary structures) and HDR (High deposition rate sedimentary structures) have been used to describe facies related to a transport by water current.
- The facies described have been grouped in 7 facies associations. Each facies association corresponds to a depositional element of specific systems, Associations 1 and 2 represent floodplain and crevasse splays whereas, Associations 3 to 7 testify to different type of channels, distinguished on the base of their width (W) vs thickness (T) ratio, their gross (broad ribbons, narrow sheets, broad sheets, see Gibling, 2006) and internal (aggradational to low and middle angle accretions sets, see Plink-Björklund, 2015) geometry.
- We subdivided the succession by means of Unconformity Bounded Stratigraphic Units (UBSU; Salvador, 1994), defined on the base of the recognition of erosional and angular unconformities at the base of each unit. The defined UBSU, representing a group of Facies Associations, correspond to the regionally defined units of the *Couches Rouges.*
- The studied successions have been represented through the elaboration of stratigraphic sections in which facies, facies associations, formations, sedimentary structures and paleocurrent plot have been reported (Pan.1, 2, 3 and 4). We described the defined units in terms of: thickness, coarse-grain vs fine-grain abundance in the sedimentary record, amalgamation/thickness of the coarse-grain facies, geometry of the channels, grain of the channel fill, dispersion of the paleocurrent directions, in order to understand the position of the succession in a proximal-distal gradient.

Paleocurrent analysis, aimed at reconstructing the evolution of the paleodrainage through time, has been carried out on the fluvial deposits. We collected most of the measures along the stratigraphic sections, though, we compared them with other paleocurrent measures taken

throughout the studied areas. The measures taken have been processed through the Grapher8 software, getting rose diagrams. Measures have been taken on the lee side of fluvial sedimentary structures as dunes and ripples. We also measured the axes of paleo-channels and paleo-valleys detected in the field. The measurements have been subdivided into different rose diagrams on the base of what kind of sedimentary structure has been taken as paleo-drainage indicator, separating measures taken on high angle planar to trough cross stratified beds, interpreted as the result of dunes or ripple migration in a lower flow regime (here named LFR sedimentary structures) and measures taken on low angle cross stratified beds, interpreted as the result of bed forms migrations in a Froude critical to transcritical flow or upper flow regime (here named UFR sedimentary structures) (Cartigny et al., 2014; Plink-Björklund, 2015). Measures taken on LFR sedimentary structures are considered more reliable, while the measures taken on UFR sedimentary structures could show a high dispersion rate in the flow directions, due to the high turbulence of the flow that also allows up-stream migration. For the tectonic correction of the paleo-drainage measurements, necessary in case of particularly deformed successions, we used an analogical corrector of paleo-currents. This instrument, designed and built as part of this work, consists of two bound rotating plans. The lower plan must be oriented like the layering of the rock in which the measures are taken, the other one must be oriented as the sedimentary structure that we are going to measure as paleo-drainage indicator. Finally, the lower plan must be reported to the horizontal, so that the upper plan would return to the original (pre-deformation) orientation. At this point, it is sufficient to measure, with the geological compass, the upper plan, to obtain the original orientation of the sedimentological structure and, consequently, the direction of the paleo-drainage.

In the Adrar Aglagal syncline we performed a structural analysis of deformations affecting the continental deposits, such as folds and faults. Fault planes sometimes are affected by kinematic indicators such as frictional-wear striae on the rock surface. We elaborated the fault slip data through the inversion method of Angelier and Mechler (1977) to reconstruct the orientation of paleo-stress fields. The orientation of minor fold axes also allowed an estimation of paleo-stress fields. The structural data have been summarized through stereographic projections (lower hemisphere, Schmidt stereonet) obtained with the “Fault” software of Caputo and Caputo (1988) and the “Dips 5.1” software of Rocscience.

References:

Abdullatif, O. M., 1989. Channel-fill and sheet-flood facies sequence in the ephemeral terminal River Gash, Kassala, Sudan. Sedimentary Geology 63, 171-184.

Alexander, J., Bridge, J. S., Cheel, R. J., LeClair, S. F., 2001. Bedforms and associated sedimentary structures formed under supercritical water flows over aggrading sand beds. Sedimentology 48, 133-152.

Allain, R., Aquesbi, N., 2008. Anatomy and phylogenetic relationships of *Tazoudasaurus naimi* (Dinosauria, Sauropoda) from the late Early Jurassic of Morocco. Geodiversitas, 30(2), 345-424.

Allen, J. R. L., 1966. On bedforms and paleocurrents. Sedimentology 6, 153-190.

Allen, J. R. L., 1984. Sedimentary structures. Their character and physical basis. Elsevier, New York (593 pp.)

Allen, J. R. L., Leeder, M. J., 1980. Criteria for the instability of the upper-stage plane beds. Sedimentology 27, 209-217.

Allen, J. P., Fielding, C. R., Gibling, M. R., Rygel, M. C., 2011. Fluvial response to paleo-equatoriaò climate fluctuations during the late Paleozoic ice age. Geological Society of America Bulletin 123, 1524-1538.

Allen, J. P., Fielding, C. R., Rygel, M. C., 2013. Deconvolving signals of tectonic and climatic controls from continental basins: an example from the Late Paleozoic Cumberland Basin, Atlantic Canada. Journal of Sedimentary Research. 83, 847-872.

Allen, J. P., Fielding, C. R., Gibling, M. R., Rygel, M. C., 2014. Recognizing products of paleoclimate fluctuation in the fluvial stratigraphic record: an example from the Pennsylvanian to Lower Permian of Cape Breton Island, Nova Scotia, Sedimentology 61, 1332-1381.

Andreu, B., Colin, J. P., Haddoumi, H., Charrière, A., 2003. Les ostracodes des "Couches Rouges" du synclinal d'Aït Attab, Haut Atlas Central, Maroc: systématique, biostratigraphie, paléoécologie, paléobiogéographie. Revue de micropaléontologie 46, 193-216.

Angelier, J., Mechler, P., 1977. Sur une méthode graphique de recherche des contraines pricipales également utilisable en tectonique et en sismologie: la méthode des dièdres droits. Bulletin de la Société Géologique de France 19, 1309e1318.

Anketell, J. M., Rust, B. R., 1990. Origin of cross-stratal layering in fluvial conglomerates, Devonian Malbaie Formation, Gaspé, Quebec, Canadian Journal of Earth Sciences, 27, 1773-1782.

Bah, T. O., 1993. Le Jurassique du versant nord du Haut-Atlas de Marrakech (Zone des cuvettes d'Ait Ourir): sedimentologie, analyse sequentielle et paleogeographie. These. Université Cady Ayyad, Marrakech.

Beauchamp, W., Allmendinger, R. W., Barazangi, M., Demnati, A., El Alji, M., Dahmani, M., 1999. Inversion tectonics and the evolution of the High Atlas Mountains, Morocco, based on a geological-geophysical transect. Tectonics 18, 163-184.

Bensalah, M. K., Youbi, N., Mata, J., Madeira, J., Martins, L., El Hachimi, H., Bertrand, H., Marzoli, A., Bellieni, G., Doblas, M., Font, E., Medina, F., Mahmoudi, A., Beraâouz, E. H.,

Miranda, R., Verati, C., Be Min, A., Ben Abbou, M., Zayane, R., 2013. The Jurassic-Cretaceous basaltic magmatism of the Oued El-Abid syncline (High Atlas, Morocco): Physical volcanology, geochemistry and geodynamic implications. J Afr Earth Sci 81:60-81.

Benvenuti, M., Martini, I. P., 2002. Analysis of terrestrial hyperconcentrated flows and their deposits. In: Martini, I. P., Garzon, G., Baker, V.R., Flood and megaflood processes and deposits: recent and ancient examples, Oxford, International Association of Sedimentology, Wiley-Blackwell Europe, pp. 167-193

Benvenuti, M., 2009. Missione "Alto Atlas" – Short Term Mobility CNR 2009. Relazione sulle attività svolte. CNR unpublished report, Firenze, December 2009, 45 p.

Benvenuti, M, 2010. Missione "Alto Atlas" – Short Term Mobility CNR 2010. Relazione sulle attività svolte. CNR unpublished report, Firenze, December 2010, 58p.

Benvenuti, M., Moratti, G., Algouti, A., 2017. Stratigraphic and structural revision of the Upper Mesozoic succession of the Dadès Valley, eastern Ouarzazate Basin (Morocco). Journal of African Earth Sciences 135, 54-71.

Bertotti, G., Gouiza, M., 2012. Post-rift vertical movements and horizontal deformations in the eastern margin of the Central Atlantic: Middle Jurassic to Early Cretaceous evolution of Morocco. International Journal of Earth Sciences 101, 2151-2165.

Best, J. L., Bridge, J. S., 1992. The morphology and dynamics of low amplitude bedwaves upon upper stage plane beds and the preservation of planar laminae. Sedimentology 39, 737-752.

Billi, P., 2007. Morphology and sediment dynamics of ephemeral stream terminal distributary systems in the Kobo Basin (northern Welo, Ethiopia). Geomorphology 85, 98-113.

Blackburn, T. J., Olsen, P. E., Bowring, S. A., McLean, N. M., Kent, D. V., Puffer, J., McHone, G., Rasbury, E. T., Et-Touhami, M., 2013. Zircon U-Pb geochronology links the end-

triassic extinction with the Central Atlantic Magmatic Province. Scienze 340(6135):941-945.

Bourcart, J., Roch, E., Ghika-Budesti, S. N., Gubler, J., Clariond, L., Robaux, A., 1942. Carte géologique provisoire des régions d'Ouaouizarht et de Dadès, au 1/200.000. Service Géologique du Maroc.

Bosellini, A., Mutti E., Ricci-Lucchi F., 1989. Rocce e successioni sedimentarie. Scienze della Terra. UTET.

Boutakiout, M., Nouri, J., Diaz-Martinez, I., Pérez-Lorente, F., 2008. Prospecciones paleoicnologicas en el synclinal de Iouaridène (Alto Atlas, Marruecos). Cuantificacion de yacimientos y de icnitas. Geogaceta, 45, 51-54.

Bridge, J. S., 1978. Origin of horizontal lamination under turbulent boundary conditions. Sedimentary Geology 20, 1-16.

Bridge, J. S., 1981. Bed shear stress over subaqueous dunes, and the transition to upper-stage plane beds. Sedimentology 28, 33-36.

Bridge, J. S., Best, J. L., 1988. Flow, sediment transport and bedform dynamics over the transition from dunes to upper-stage plane beds: implications for the formation of planar laminae. Sedimentology 35, 753-763

Brierley, G. J., Fryirs, K. A., 2005. Geomorphology and river management. Applications of the River Styles Framework. Wiley-Blackwell.

Bromley, M. H., 1991. Variations in fluvial style as revealed by architectural elements, Kayenta Formation, Mesa Creek, Colorado, USA: evidence for both ephemeral and perennial fluvial processes. In: MIall, A. D., Tyler, N. (Eds.), The three-dimensional facies architecture

of Terrigenous clastic sediments and its implications for hydrocarbon discovery and recovery. SEPM concepts in sedimentology and paleontology 3, pp. 94-102.

Caputo, M., Caputo, R., 1988. Structural analysis: new analytical approach and applications. Annales Tectonicae 2: 84-89.

Carling, P. A., 1990. Particle over-passing on depth-limited gravel bars, Sedimentology, 37, 345-355.

Cartigny, M. J. B., Ventra, D., Postma, G., Van Den Berg, J. H., 2014. Morphodynamics and sedimentary structures of bedforms under supercritical flow conditions: new insights from flume experiments. Sedimentology 61, 712-748.

Cavallina, C., Benvenuti, M., Papini, M., Moratti, G., 2017. Stratigraphy and paleo-drainage evolution of the Late Mesozoic continental succession in the High Atlas of Marrakach (Ait Ourir, Adrar Aglagal and Jbel Igoudlane successions, Morocco). Journal of Mediterranean Earth Sciences 9, 103-107. Special Section of XIII Geosed Congress.

Cavallina, C., Papini, M., Moratti, G., Benvenuti, M., 2018. The Late Mesozoic evolution of the Central High Atlas domain (Morocco): suggestions from the paleo-drainage record of the Adrar Aglagal syncline. Sedimentary Geology 376, 1-17

Cavin, L., Tong, H., Boudad, L., Meister, C., Piuz, A., Tabouelle, J., Aarab, M., Amiot, R., Buffetaut, E., Dyke, G., Hua, S., Le Loeuff, J., 2010. Vertebrate assemblages from the early Late Cretaceous of southeastern Morocco: An overview. Journal of African Earth Sciences 57, 391-412.

Charrière, A., Haddoumi, H., Mojon, P. O., 2005. Decouverte de Jurassique superieur et d'un niveau marin du Barremien dans les "couches rouges" continentales du Haut Atlas central marocain: implications paleogeographiques et structurales. Comptes Rendus Palevol 4, 385-394.

Charrière, A., Haddoumi, H., 2016. Les “couches rouges” continentals jurassico-crétacées des Atlas marocains (Moyen Atlas, Haut Atlas central et oriental): bilan stratigraphique, paléogéographies successives et cadre géodynamique. Boletín Geológico y Minero, 127 (2/3): 407-430.

Charrière, A., Haddoumi, H., 2017. Dater les couches rouges continentals pour définir la géodynamique atlasique. Géologues 194, 29-32.

Cheel, R. J., 1990. Horizontal lamination and the sequence of bed phases and stratification under upper-flow-regime conditions. Sedimentology 37, 517-529.

Choubert, G., 1959. Carte Géologique du Maroc au 1:500000, feuille Ouarzazate. Service Géologique du Maroc.

Choubert, G., Faure-Muret, A., 1960-1962. Evolution du domaine atlasique marocain depuis les temps paléozoïques. In : Livre à la mémoire du Professeur Paul Fallot (Soc. Géol. Fr., Mem. H.-s.), pp 447-527

Clark, M. K., Schoenbohm, L. M., Royden L. H., Whipple K. X., Burchfiel B. C., Zhang X., Tang W., Wang E., Chen L., 2004. Surface uplift, tectonics, and erosion of eastern Tibet from large-scale drainage patterns. Tectonics 23

Coleman, J. M., 1969. Brahmaputra River: channel processes and sedimentation. Sedimentary Geology 3, 129-239.

Courtinat, B., Algouti, A., 1985. Caractérisation probable du Sinémurian près de Telouat (Haut-Atlas, Maroc): Datation palynologique. Geobios 18, 857-867.

Cox, K. G., 1989. The role of mantle plums in the development of continental drainage patterns. Nature 342, 873-877

Croke, J. C., Magee, J. M., Price, D. M., 1998. Stratigraphy and sedimentology of the lower Neales River, West Lake Eyre, Central Australia: from Palaeocene to Holocene. Palaeogeography, Palaeoclimatology, Palaeoecology 144, 331-350.

Dieguez, C., Peyrot, D., Barron, E., 2010. Floristic and vegetational changes in the Iberian Peninsula during Jurassic and Cretaceous. Review of Palaeobotany and Palynology 162 : 325-340.

Dutuit, J. M., Ouazzou, A., 1980. Decouverte d'une piste de dinosaure sauropode sur le site d'empreintes de Demnat (Haut-Atlas Marocain). Mém. Sóc. Géol. France, N. S., 139 ; 95-102.

El Arabi, E. H., 2007. La serie permienne et triasique du rift haut-atlasique : nouvelles datations ; evolution tectono-sedimentaire. These d'Etat. Univ. Hassan II Casablanca, Fac. Sci. Ain Chok, 225 pp.

Ettachfini, E. M., Andreu, B., 2004. Le Cenomanien et le Turonien de la Plate-forme Preafricaine du Maroc. Cretaceous Research 25, 277-302.

Ettachfini, E. M., Sohuel, A., Andreu, B., Caron M., 2005. La limite Cénomanien-Turonien dans le Haut Atlas Central, Maroc. Geobios 38, 57-68.

Ferrandini, J., Le Marrec. A., 1982. La couverture jurassique est allochtone dans la "zone des cuvettes" d'Ait Ourir (Maroc). C. R. Acad. Sc. Paris, t.295, série II. pp.813-816

Ettaki, M., Ibouh, H., Chellai, E. H., Milhi A., 2007. Les structures "diapiriques" liasiques du Haut-Atlas central, Maroc: exemple de la ride d'Ikerzi. Africa Geoscience Review, Vol. 14, No.1, pp. 79-93.

Fekkak, A., Ouanaimi, H., Michard, A., Soulaimani, A., Ettachfini, E.M., Berrada, I., El Arabi, H., Lagnaoui, A., Saddiqi, O., 2018. Thick-skinned tectonics in a Late Cretaceous-Neogene intracontinental belt (High Atlas Mountains, Morocco): The flat-ramp fault control on basement shortening and cover folding. Journal of African Earth Science 140, 169-188.

Fischer, R. V., 1983. Flow transformations in sediment gravity flows. Geology, v. 11, 273-274.

Foley, M. G., 1978. Scour and fill in steep, sand-bed ephemeral streams. AAPG Bulletin 89, 559-570.

Frizon de Lamotte, D., Saint Bezar, B., Bracene, R., Mercier, E., 2000. The two main steps of the Atlas building and geodynamics of the western Mediterranean. Tectonics 19, 740-761.

Frizon de Lamotte, D., Ziz, M., Missenard,Y., Hafid, M., El Azzouzi, M., Maury, R. C., Charrière, A., Taki, Z., Benammi, M., Michard, A., 2008. The Atlas system. Lecture Notes in Earth Sciences 116, 133-202.

Frizon de Lamotte, D., Leturmy, P., Missenard, Y., Khomsy, S., Tuiz, G., Saddiqi, O., Guillocheau, F., Michard, A., 2009. Mesozoic and Cenozoic vertical movements in the Atlas system (Algeria, Morocco, Tunisia): an overview. Tectonophysics 475: 9-28.

Ghinassi, M., Billi, P., Libsekal, Y., Papini, M., Rook, L., 2013. Inferring fluvial morphodynamics and overbank flow control from 3D outcropsections of a Pleistocene point bar, Dandiero Basin, Eritrea. Journal of Sedimentary Research, v. 83, 1065-1083.

Gibling, M. R., Tandon, S. K., 1997. Erosional marks on consolidated banks and slump blocks in the Rupen River, north-westIndia. Sedimentology 44, 339-348.

Gibling, M. R., 2006. Width and thickness of fluvial channel bodies and valley fills in the geological record: a literature compilation and classification. Journal of sedimentary research 76, 731-770.

Giese, P., Jacobsagen, V.,1992. Inversion tectonics of intra-continental ranges: High and Middle Atlas, Morocco. Geologische Rundschau 81: 249-259.

Gohan, K., Parkash, B., 1990. Morphology of the Kosi megafan. In: Rachocki, A. h., Church, M. (Eds.), Alluvial Fans – a field approach. John Wiley and Sons Ltd., Chichester, UK, pp. 151-178.

Gouiza, M., 2011. Mesozoic Source-to-Sink Systems in NW Africa: Geology of vertical movements during the birth and growth of the Moroccan rifted margin. PhD thesis, Vrije Universiteit, Amsterdam, The Netherlands.

Gradstein, F. M., Ogg, J. G., Smith, A. G., 2004. A geological Time Scale 2004. Cambridge University Press, official website of the International Commission on Stratigraphy (ICS) under www.stratigraphy.org

Hadach, F., Algouti, A., Algouti, A., 2015. Etude sedimentologique du Trias et Jurassique du Haut Atlas de Marrakech, Maroc: contribution a la localization des niveaux favorable a l'exploitation artisanale pur la poterie. European Scientific Journal, vol. 11, No. 21.

Hadach, F., Algouti, A., Algouti, A., 2018. Sédimentologie et paléogéographie du Lias et Dogger de la cuvette d'Ouanina, Haut Atlas Occidental, Maroc. International Journal of innovation and applied studies, No. 1, pp. 31-58.

Haddoumi, H., Charrière, A., Feist, M., Andreu, B., 2002. Nouvelles datations (Hauterivien superieur-Barremien inferieur) dans les "couches rouges" continentales du Haut Atlas central marocain; consequences sur l'âge du magmatisme et des structurations mésozoïques de la chaîne Atlasique. Comptes Rendus Palevol 1, 259-266.

Haddoumi, H., Charrière, A., Mojon, P. O., 2008. Les depots continentaux du Jurassique moyen au Cretace inferieur dans le Haut-Atlas oriental (Maroc): Paleoenvironments successifs et signification paléogéographique. Carnets de Geologie – Notebooks in Geology.

Haddoumi, H., Charrière, A., Mojon, P. O., 2010. Stratigraphie et sédimentologie des

«Couches Rouges» continentals du Jurassique-Crétacé du Haut Atlas Central (Maroc): implications paléogéographiques et géodynamiques. Geobios 43, 433-451.

Hadri, M., Meslouh, S., Morel, J. L., Saint Berzard, B., 2001. Carte Géologique du Maroc, Goulmima. Echelle 1:100000. Notes et Mémoires Service Géologique du Maroc N°432.

Hailwood, E. A., Mitchell, J. G., 1971. Paleomagnetic and radiometric dating results from Jurassic intrusions in South Morocco. Geophys J R Astron Soc 24, 351–364.

Haisheng. Y., Chengshan, W., Zhiqiang, S, Jinhui, L. HU Lidong, Z., 2008. Early Uplift History of the Tibetan Plateau: Records from Paleocurrents and Paleodrainage in the Hoh Xi1 Basin. Acta Geologica Sinica, 82 : 206-213.

Hames, W. E., Renne P. R., Ruppel, C., 2000. New evidence for geologically instantaneous emplacement of the earliest Jurassic Central Atlantic Magmatic Province basalts in the north American margin. Geology 28 :859-862.

Hasiotis, S. T., 2004. Reconnaissance of Upper Jurassic Morrison Formation ichnofossils, Rocky Mountain Region, USA: paleoenvironmental, stratigraphic and paleoclimatic significance of terrestrial and freshwater ichnocoenoses. Sedimentary Geology 167, 177-268.

Howard, A. D., 1967. Drainage analysis in geologic interpretation: a summation. AAPG bulletin 51, 2246-2259.

Hindermeyer, J., Gauthier, H., Destombes, J., Choubert, G., Faure-Muret, A., 1977. Carte geologique du Maroc, Jbel Saghro-Dades (Haut Atlas Central, sillon Sud-Atlasique et Anti-Atlas oriental)-Echelle 1/200000. Notes et Mem Serv Geol Maroc, 161

Ibouh, A., Chafiki, D., 2017. La tectonique de l'Atlas: âge et modalités. Geologues 194, 24-28.

Ielpi, A., Ghinassi, M., 2014. Planform architecture, stratigraphic signature and morphodynamics of an exhumed Jurassic meander plain (Scalby Formation, Yorkshire, UK). Sedimentology.

Iseya, F., Ikeda, H., 1987. Pulsation in bedload transport rates induced by a longitudinal sediment sorting: a flume study using sand and gravel mixtures. Geografiska Annaler 69 A, 15-27

Ishigaki, S., 1989. Footprints of swimming sauropods from Morocco. In: Dinosaurs tracks and traces (Eds. D Gilette & M. G. Lockey). Cambridge University Press, New York, 83-86.

Ishigaki, S., Matsumoto, Y., 2009. "Off-tracking" – like phenomenon observed in the turning sauropod trackway from the upper Jurassic of Morocco. Memoir of the Fukui Prefectural Dinosaur Museum, 8, 1-10.

ISSC – International subcomission on stratigraphic classification, 1994. A Guide to stratigraphic classification, terminology and procedure. 2nd ed., IUGS, Boulder.

Jabour, H., Dakki, M., Nahim, M., Charrat, F., El Alji, M., Hassain, M., Oumalch, F., El Abibi, R., 2004. The Jurassic depositional system of Morocco, geology and play concepts, MAPG Mem. 1. 5-39.

Jackson, M., Hudec, M., 2017. Contractional Salt-Tectonic Systems. In: Jackson, M., Hudec, M. (Eds), Salt Tectonics: Principles and Practice. Cambridge University Press, Cambridge, pp. 304-335.

Jenny, J., Le Marrec, A., Monbaron, M., 1981. Les Couches Rouges du Jurassique moyen du Haut Atlas central (Maroc): correlation lithostratigraphiques, éléments de datations et cadre tectono-sédimentaire. Bulletin de la Société Géologique de France 6, 627-639.

Jenny, J., 1985. Carte géologique du Maroc au 1/100000, feuille Azilal. Notes et Mémoires du Service géologique du Maroc, 339.

Jenny, J., 1988. Mémoire explicatif de la carte géologique du Maroc au 1/100000 (feuille d'Azilal, Haut-Atlas Central). Notes et Mem. Serv. Géol. Rabat, 339 bis, 104.

Kennedy, J. F., 1963. The mechanics of dunes and antidunes in erodible-bed channels. Journal of Fluid Mechanics 16, 521-544.

Knight, K. B., Nomade, S., Renne, P. R., Marzoli, A., Bertrand, H., Youbi, N., 2004. The Central Atlantic Magmatic Province at the Triassic-Jurassic boundary: paleomagnetic and $^{40}Ar/^{39}Ar$ evidence for brief, episodic volcanism. Earth Planet Sci Lett 228:143-160.

Knighton, 1998. Fluvial forms and processes, a new perspective. Taylor & Francis group, London..

Laville, E., 1985. Evolution sédimentaire, tectonique et magmatique du bassin Jurassique du Haut Atlas, Maroc: modéle en relais multiples de décrochements. PhD thesis, Montpellier, France.

Laville, E., 1988. A multiple releasing and restraining stepover model for the Jurassic strike-slip basin of the Central High Atlas (Morocco). In: Manspeizer, W. (Ed), Triassic-Jurassic Rifting: Continental Breakup and the Origin of the Atlantic Ocean and Passive Margins. Developments in Geotectonics, 22, Elsevier, Amsterdam, pp. 499-523.

Laville, E., 2002. Role of the Atlas Mountains (northwest Africa) within the African-Eurasian plate-boundary zone. Comment. Geology 30, 95.

Laville, E., Piqué, A., 1992. Jurassic penetrative deformation and Cenozoic uplift in the Central High Atlas (Morocco) : A tectonic model. Structural and orogenic inversions. Geologische Rundschau 81 : 157-170.

Lazar, R.O., Bohacs, K.M., Macquaker, J.H.S., Schieber, J., Demko, T.M., 2015. Capturing key attributes of fine-grained sedimentary rocks in outcrops, cores, and thin sections: nomenclature and description guidelines. Journal of Sedimentary Research, 2015, v. 85, 230–246

Leier, A. L., DeCelles, P. G., Pelletier, J. D., 2005. Mountains, monsoons, and megafans.

Geology 33, 289-292.

Leopold, L. B., Emmet, W. W., Myrick, R. M., 1966. Channel and hillslope processes in a semiarid area New Mexico. USGS Professional Paper 352-G, 193-253.

Leprêtre, R., Missenard, Y., Barbarand, J., Gautheron, C., Jouvie, I., Saddiqi, O., 2018. Polyphased inversions of an intracontinental rift: case study of the Marrakech High Atlas, Morocco. Tectonics, 37.

Martins, L. T., Madeira, J., Youbi, N., Munha, J., Mata, J., Kerrich, R., 2008. Rift-related magmatism of the Central Atlantic Magmatic Province in Algarve, Southern Portugal. Lithos 101 :102-124.

Martins, L., Miranda, R., Alves, C., Mata, J., Madeira, J., Munhá, J., Terrinha, P., Youbi, N., Bensalah, K. H., 2010. Mesozoic magmatism at the West Iberian Margins : timing and geochemistry. In : II Central and North Atlantic conjugate margins conference, Lisbon 2010. Re-discovering the Atlantic, new winds for an old sea. Extended abstracts, pp. 172-175.

Marzoli, S., Renne, P. R., Piccirillo, E. M., Ernesto, M., Bellieni, G., De Min, A., 1999. Extensive 200-million-year-old continental flood basalts of the Central Atlantic Magmatic Province. Science 284 :616-618.

Marzoli, A., Bertrand, H., Knight, K. B., Cirilli, S., Buratti, N., Verati, C., Nomade, S., Renne, P. R., Youbi, N., Martini, R., Allenbakh, K., Neuwerth, R., Rapaille, C., Zaninetti, L., Bellieni, G., 2004. Syn-chronism of the Central Atlantic Magmatic Province and the Triassic-Jurassic boundary climatic and biotic crisis. Geology 32 :973-976.

Marzoli, A. F., Jourdan, J. H., Puffer, T., Cuppone, L. H., Tanner, R. E., Weems, H., Bertrand, S., Cirilli, G., Bellieni, G., De Min, A., 2011. Timing and duration of the Central Atlantic Magmatic Province in the New-ark and Culpeper basins, eastern USA. Lithos 122 (3-4) :175-188.

Mattauer, M., Tapponier, P., Proust, F., 1977. Sur le meanismes de formation des chaines

intracontinentales. L'exemple des chaines atlasiques du Maroc. Bulletin de la Société Geologique de France 77 : 521-526

Matton, G., Jébrak, M., 2009. The Cretaceous Peri-Atlantic Alkaline Pulse (PAAP): Deep mantle plume origin or shallow lithospheric break-up? Tectonophysics 469:1-12.

McBride, E. F., Shepherd, R. G., Crawley, R. A., 1975. Origin of parallel near-horizontal laminae by migration of bed forms in a small flume. Journal of Sedimentary Petrology 45, 132-139.

McHone, J. G., 2003. Volatile emissions from Central Atlantic Magmatic Province basalts: mass assumptions and environmental consequences. In: Hames, W. E., McHone, J. G., Renne, P. R., Ruppel, C. (eds). The Central Atlantic Magmatic Province: Insights from fragments of Pangea. AGU Geophys Mon 136:241-254.

McKee, E. D., Crosby, E. J., Berryhill, M. L., 1967. Flood deposits, Bijou Creek, Colorado. June 1965. Journal of sedimentary petrology 37, 829-851.

Merle, R., Marzoli, A., Bertrand, H., Reisberg, L., Verati, C., Zimmermann, C., Chiaradia, M., Bellieni, G., Ernesto, M., 2011. $^{40}Ar/^{39}Ar$ ages and Sr-Nd-Pb-Os geochemistry of CAMP tholeiites from Western Maranhao basin (NE Brazil). Lithos 122(3-4): 137-151.

Miall, A. D., 1978. Fluvial sedimentology. Canadian Society of Petroleum Geologists, Calagary, Canada.

Miall, A. D., 2010. Alluvial deposits. In: N. P. James and R. W. Dalrymple (eds), Facies Model 4. 105-138, Geological Association of Canada.

Middleton, G.V., 1965. Antidune cross-bedding in a large flume. Journal of Sedimentary Petrology 35, 922-927.

Middleton, G. V., Southard, J. B., 1984. Mechanics of sediment movement. SEPM Short Course 3 (Tulsa, OK).

Milhi, A., Alaoui Mdaghri, D., Guerraoui, A., Bensaïd, M., Dahmani, M., 1993. Carte Géologique du Maroc. Tinehrir. Echelle 1:1000000. Notes et Mémoires Service Géologique du Maroc N° 377.

Mojon, P. O., Haddoumi, H., Charrière, A., 2009. Nouvelles données sur les Charophytes et ostracodes du Jurassique moyen-supérieur – Crétacé inférieur de l'Atlas marocain. Carnets de Géologie – Notebooks on Geology, Mémoire 2009/03, 38 p.

Monbaron, M., 1981. Sédimentation, tectonique synsédimentaire et magmatisme basique: l'évolution paléogéographique et structurale de l'Atlas de Beni Mellal (Maroc) au cours du Mésozoïque; ses incidences sur la tectonique tertiaire. Eclogae Geologicae Helvetiae 74, 625-638.

Monbaron, M., 1982. Précisions sur la chronologie de la tectogenèse atlasique: exemple du domaine atlasique mésogéen du Maroc. Comptes Rendus de l'Academie des Sciences de Paris 294, 883-886.

Monbaron, M., Russell, D. A., Taquet, P., 1999. *Atlasaurus imelakei* n.g., n.sp., a brachiosaurid-like sauropod from the Middle Jurassic of Morocco. Comptes Rendus de l'Académie des Sciences – Series IIA – Earth and Planetary Science, 329, 519-526.

Montenat, C., Monbaron, M., Allain, R., Aquesbi, N., Dejax, J., Hernandez, J., Russel, D., Taquet, P., 2005. Stratigraphie et paléoenvironnement des dépôts volcano-détritiques à dinosauriens du Jurassique inférieur de Toundout (Province de Ouarzazate, Haut-Atlas, Maroc). Eclogae geol. Helv. 98, 261-270.

Moragas, M., 2017. Multidisciplinary characterization of diapiric basins integrating field examples, numerical and analogue modelling : Central High Atlas (Morocco). PhD thesis. Universitat de Barcelona.

Moragas, M., Vergés, J., Saura, E., Martín-Martín, J. D., Messager, G., Merino-Tomé. O., Suarez-Ruiz, I., Razin, P., Grélaud, C., Malaval, M., Joussiaume, R., Hunt, D. W., 2018. Jurassic rifting to post-rift subsidence analysis in the Central High Atlas and its relation to salt diapirism. Basin Research 30(suppl. 1), 336-362.

Moratti, G., Benvenuti, M., Santo, A. P., Laurenzi, M. A., Braschi, E., Tommasini, S., 2018. New ^{40}Ar-^{39}Ar dating of Lower Cretaceous basalts at the southern front of the Central High Atlas, Morocco: insights on Late Mesozoic tectonics, sedimentation and magmatism. International Journal of Earth Sciences, 107, 2491-2515.

Najman, Y., Garzanti, E., Pringle, M., Bickle, M., Stix, J., Khan, I., 2003. Early-Middle Miocene paleodrainage and tectonics in the Pakistan Himalaya. Geol. SOC. Am. Bull., 115: 1265-1277.

Nichols, G. J., 2009. Sedimentology and stratigraphy 2nd edition. Wiley-Blackwell.

Nichols, G. J., Fisher, J. A., 2007. Processes, facies and architecture of fluvial distributary systems deposits. Sedimentary Geology 195, 75-90.

North, C. P., Taylor, K. S., 1996. Ephemeral-fluvial deposits: integrated outcrop and simulation studies reveal complexity. AAPG Bulletin 80, 811-830.

Nouri, J., Pérez-Lorente, Y., Boutakiout, M., 2001. Descubrimiento de una pista semiplantígrada de dinosaurio en el yacimiento de Tirika (Demnat. Alto Atlas Central marroquí). Geogaceta, 29, 83-86.

Picard, M. D., High, L. R., 1973. Seimentary structures of ephemeral streams. Developments in sedimentology 17, Elsevier, Amsterdam (233 pp.). and High, 1973

Piqué, A., Ait Brahim, L., Ait Ouali, R., Amrhar, M., Charroud, M., Gourmelen, C., Laville, E., Rekhiss, F., Tricart, P., 1998. Evolution structural des domains atlasiques du Maghreb au Méso-Cénozoïque; le rôle des structures héritées dans la deformation du domaine atlasique de

l'Afrique du Nord. Bulletin de la Société Géologique de France 169, 797-810.

Plink-Björklund, P., Birgenheier, L., 2013. Highly seasonal ancient monsoonal river systems: depositional style, allogenic and aoutogenic controls. 10th International Conference on Fluvial Sedimentology. Leeds, pp. 206-207 (Extended Abstract).

Plink-Björklund, P., Wang, J., Belobraydic, M., McDowell, B., Don, J., Jaikla, J., Shi, G., 2014. Distributive fluvial systems, fluvial megafans, terminal fans – Stratigrapher's nightmare? AAPG Search and Discovery

Plink-Björklund, P., 2015. Morphodynamics of rivers strongly affected by monsoon precipitation: review of depositional style and forcing factors. Sedimentary Geology 323, 110-147.

Plink-Bjorklund, P., 2015. Effects of strongly seasonal and yearly variable precipitation patterns on fluvial facies: Tropics and Subtropics. AAPG Search and Discovery

Rust, B. R., 1984. Proximal braid plain in the Middle Devonian Malbaie Formation of Eastern Gaspé, Quebec, Canada, Sedimentology, 31, 675-695.

Saadi, M., Bensaïd, M., Dahmani, M., 1985. Carte Géologique du Maroc, Azilal. Echelle 1:100000. Notes et Mémoires Service Géologique du Maroc N°339.

Saadi, M., Bensaïd, M., Dahmani, M., 1985. Carte Géologique du Maroc, Beni Mellal. Echelle 1:100000. Notes et Mémoires Service Géologique du Maroc N°341.

Saadi, M., Bensaïd, M., Dahmani, M., 1985. Carte Géologique du Maroc, Demnat. Echelle 1:100000. Notes et Mémoires Service Géologique du Maroc N°338.

Saadi, M., Hilali, E., Bensaid, M., Boudda, A., Dahmani, M., 1985. Carte Géologique du

Maroc. Echelle 1:1000000. Notes et Mémoires Service Géologique du Maroc N° 260.

Saadi, M., Hilali, E., Bensaid, 1975. Carte Géologique du Maroc. Jbel Saghro-Dadès (Haut Atlas central, sillon Sud-Atlasique et Anti-Atlas oriental). Echelle 1:1000000. Notes et Mémoires Service Géologique du Maroc N° 161.

Saez, A., Anadon, P., Herrero, M. J., Moscariello, A., 2007. Variable style of transition between Paleogene fluvial fan and lacustrine systems, southern Pyrenean foreland, NESpain. Sedimentology 54, 367-390.

Salvador, A., 1994. International Stratigraphic Guide, 2nd ed. International Subcommission on Stratigrphic Classification. International Union of Geological Sciences Trondheim and Geological Society of America, Boulder, Co.

Saura, E., Vergés, J., Martín, J. D., Messager, G., Moragas, M., Razin, P., Grélaud, C., Joussiaume R., Malaval, M., Homke, S., Hunt, D. W., 2014. Journal of the Geological Society, London. 171, 97-105

Schieber, J., 2016. Mud re-distribution in epicontinental basins e Exploring likely processes. Marine and Petroleum Geology 71, 119-133

Scotese, C. R., 2014a. Atlas of Middle & Late Permian and Triassic Paleogeographic Maps, maps 43-48 from Volume 3 of the PALEOMAP Atlas for ArcGIS (Jurassic and Triassic) and maps 49-52 from Volume 4 of the PALEOMAP PaleoAtlas for ArcGIS (Late Paleozoic), Mollweide Projection, PALEOMAP Project, Evanston, IL.

Scotese, C. R., 2014a. Atlas of Jurassic Paleogeographic Maps, PALEOMAP Atlas for ArcGIS, volume 4, The Jurassic and Triassic, Maps 32-42, Mollweide Projection, PALEOMAP Project, Evanston, IL.

Scotese, C. R., 2014b. Atlas of Early Cretaceous Paleogeographic Maps, PALEOMAP Atlas for ArcGIS, volume 2, The Cretaceous, Maps 23-31, Mollweide Projection, PALEOMAP Project, Evanston, IL.

Scotese, C. R., 2014c. Atlas of Late Cretaceous Paleogeographic Maps, PALEOMAP Atlas for ArcGIS, volume 2, The Cretaceous, Maps 16-22, Mollweide Projection, PALEOMAP Project, Evanston, IL.

Sereno, P. C., Dutheil, D. B., Iarochene, M., Larsson, H. C. E., Lyon, G. H., Magwene, P. M., Sidor, C. A., Varricchio, D. J., Wilson, J. A., 1996. Predatory dinosaurs from the Sahara and Late Cretaceous faunal differentiation. Science 272, 986-991.

Seward, A. C., 1894-1895. The Weakden Flora: Catalogue of the Mesozoic plants in the department of geology British Museum (Natural History), London British Museum 1894, 2 volumes.

Shukla, U. K., Singh, I. B., Sharma, M., Sharma, S., 2001. A model of alluvial megafan sedimentation: Ganga megafan. Sedimentary Geology 144, 243-262.

Simons, D. B., Richardson, E. V., Nordin Jr., C.F., 1965. Sedimentary structures generated by flow in alluvial channels. In: Middleton, G. V. (Ed.), Primary sedimentary structures and their hydrodynamic interpretation. SEPM Special Publication 12, pp. 34-52.

Simons, D.B. and Richardson, E.V. (1963) Forms of bed roughness in alluvial channels. A.S.C.E. Transactions, 128-I, 248-302.

Singh, A., Bhardwaj, B. D., 1991. Fluvial facies model of the Ganga River sediments, India. Sedimentary Geology 72, 135-146.

Singh, H., Parkash, B., Gohain, K., 1993. Facies analysis of the Kosi megafan deposits. Sedimentary Geology 85, 87-113.

Smith, N. D., 1972. Some sedimentological aspects of planar cross-stratification in a sandy braided river. Journal of sedimentology and petrology, 42, 3, 624-634.

Smith, N. D., 1974. Sedimentology and bar formation in the Upper Kicking Horse River, a braide outwash stream, Journal of Geology, 82, 205-223.

Smith, R. L., Pozzobon, J.C., 1979. The Imiter gabbroic complex, High Atlas Mountains, Morocco. Journal of Geology, 87, 317–324.

Souhel, A., 1987. Dynamique sédimentaire des couches rouges intercalcaires (Bathonien-Cénomanien) dans l'Atlas de Beni Mellal (Haut Atlas central, Maroc). Master's thesis, Université Paul Sabatier, Toulouse, France.

Souhel, A., 1996. Le Mesozoïque dans le Haut-Atlas de Beni-Mellal (Maroc). Stratigraphie, sédimentologie et évolution géodynamique. PhD thesis, Marrakech.

Stear, W. M., 1985. Comparison of the bedform distribution and dynamics of modern and ancient sandy ephemeral flood deposits in the southwestern Karoo region, South Africa. Sedimentary Geology 45, 209-230.

Steel, R. J., Thompson, D. B., 1983. Structures and textures in Triassic braided stream conglomerates ("Bunter" Pebble Beds) in the Sherwood Sandstone Group, North Staffordshire, England, Sedimentology, 30, 341-367.

Steiger, R. H., Jäger, E., 1977. Subcommission on geoghronology : convention on the use of decay constants in geo- and cosmochronology. Earth Planet Sci Lett 36 :359-362.

Studer, M., du Dresnay, R., 1980. Déformations synsédimentaires en compression pendant le Lias supérieur et le Dogger, au Tizi n'Irhil (Haut-Atlas central de Midelt, Maroc). Bulletin de la Société géologique de France 7, 391-397.

Teixell, A., Arboleya, M. L., Julivert, M., Charroud, M., 2003. Tectonic shortening and topography in the central High Atlas (Morocco). Tectonics 22, 1051, doi:10.1029/2002TC001460.

Termier, H., 1941. Carte geologique provisoire des regions de Demnat et de Telouet. Service des Mines et de la Carte geologique. Cartes geologiques provisoires. Notes et memoires de Service geologique NM ; no.55

Tesón, E., Teixell, A., 2008. Sequence of thrusting and syntectonic sedimentation in the eastern Sub-Atlas thrust belt (Dadès and Mgoun valleys, Morocco). International Journal of Earth Sciences, 97, 103-113.

Torres-López, S., Casas, A. M., Villalaín, J. J., Moussaid, B., Ruiz Martínez, V. C., El-Ouardi, H., 2018. Evolution of the Ridges of Midelt-Errachidia section in the High Atlas revealed by Paleomagnetic data. Tectonics, 37, 3018–3040.

Tunbridge, I. P., 1981. Sandy high-energy flood sedimentation – some criteria for recognition, with an example from the Devonian of SW England. Sedimentary Geology 28, 79-95.

Uba, C. E., Heubeck, C., Hulka, C., 2005. Facies analyses and basin architecture of the Neogene Subandean synorogenic wedge, southern Bolivia. Sedimentary Geology 180, 91-123.

Verati, C., Rapaille, C., Féraud, G., Marzoli, A., Marzoli, H., Bertrand, H., Youbi, N., 2007. Ar-Ar ages and duration of the Central Atlantic Magmatic Province volcanism in Morocco and Portugal and its relation to the Triassic-Jurassic boundary. Paleogeogr Paleoclim Paleoecol 244 :308-325.

Vergés, J., Moraga, M., Martín Martiín, J. D., Saura. E., Casciello. E., Hunti, D. W., 2017. Permo-Triassic Salt Provinces of Europe, North Africa and the Atlantic Margins, Tectonics and Hydrocarbon Potential: 563-579. Elsevier.

Vergés, J., Moragas, M., Martín-Martín, J.D., Saura, E., Casciello, E., Razin, Ph., Grelaud, C.,

Malaval, M., Joussiame, R., Messager, G., Sharp, I., Hunt, D.W., 2017. Salt Tectonics in the Atlas Mountains of Morocco. In: Soto, J.I., Flinch, J.F., Tari, G. (Eds), Permo-Triassic Salt Provinces of Europe, North Africa and the Atlantic Margins, Elsevier, pp. 563-579.

Vezzoli, G., Garzanti, E., 2009. Tracking paleo-drainage in Pleistocene foreland basins. The journal of geology 117, 445-454.

Waheed, A., Wells, N.A., 1990. Changes in paleocurrents during the development of an obliquely convergent plate boundary (Sulaiman fold-belt, southwestern Himalayas, westcentral Pakistan). Sedimentary Geol., 67: 237-261.

Whalen, L., Gazel, E., Vidito, C., Puffer, J., Bizimis, M., Henika, W., Caddick, M. J., 2015. Supercontinental inheritance and its influence on supercontinental breakup: the Central Atlantic Magmatic Province and the breakup of Pangea. Geochem Geophys Geosyst 16: 3532-3554

Westphal, M., Montigny, R., Thuizat, R., Bardon, C., Bossert, A., Hamzeh, R., Rolley, J., 1979. Paléomagnétisme et datation du volcanisme permien, triasique et crétacé du Maroc. Can J Earth Sci 16:2150-2164.

Williams, G. E., 1971. Flood deposits of sand-bed ephemeral streams of Central Australia. Sedimentology 17, 1-40.

Zavala, C., Otharán, G., Arcuri M., 2017. The importance of fluid mud flows in the accumulation of thick mudstone successions: Examples from the Jurassic – Cretaceous Vaca Muerta Formation, Neuquén Basin, Argentina. Schlumberger Geology Community Webinar

Zouibaa, A., 2003. Carte Géologique du Maroc. Imilchil. Echelle 1:1000000. Notes et Mémoires Service Géologique du Maroc N° 397.